A Low Complexity Method of Resource Allocation in Up-link Macrodiversity Systems Using Long-Term Power

Yu-An Chen

Department of Electrical and Computer Engineering

A thesis presented for the degree of
Master of Engineering

University of Canterbury
Christchurch, New Zealand
18th December 2013

To my dearest parents

Abstract

Macrodiversity systems have many promising features that can improve system performance from a network perspective, such as improving the weak signals of users affected by shadow fading, or users at the cell-edge. They also allow multiple users to share the same resource in time and frequency, improving the overall user capacity.

Traditionally, evaluating the link quality of resource-sharing users requires instantaneous channel state information (CSI). However, finding compatible users to share resource in macrodiversity systems is a challenging task. For macrodiversity systems, instantaneous CSI could be passed to the backhaul processing unit (BPU) through the network backhaul. This creates a delay in the signal, and makes instantaneous CSI a less accurate reflection of the channel environment at the time. Passing instantaneous CSI of all users also creates a significant amount of network overheads, reducing the overall efficiency of the network. Compared to MIMO systems with co-located antennas, macrodiversity systems cover a larger geographical area and more users. For this reason, the number of user selection combinations can become extremely large, making scheduling decisions in real time an even more challenging task. These problems limit the realisation of the user capacity potential of macrodiversity systems.

This thesis presents a low complexity method of resource allocation for up-link macrodiversity systems. In particular, it uses long-term power to estimate the link quality of resource-sharing users. Using long-term power bypasses the issue of channel estimation error introduced by the network delay, and it also reduces the communication overhead on the network backhaul. In this thesis, we use *Symbol-Error Rate* (SER) as the measure for link quality. Using the method developed by Basnayaka [1], we are able to estimate SER of resource-sharing users using long-term power. Using the SER estimation method, we further proposed a user compatibility check (UCC), which evaluates the compatibility of users sharing the same resource. Users are only considered compatible with each other if all of them meet a pre-defined SER threshold.

We attempt to reduce the complexity of user selection by using heuristic solution-finding methods. In our research, we found that greedy algorithms have the least complexity. We propose four low-complexity user selection algorithms based on a greedy algorithm. These algorithms are simulated under different environment parameters. We evaluate the system performance in terms of utilisation and complexity. Utilisation refers to the percentage of

allocated users compared to the theoretical user capacity. Complexity refers to the number of SER calculations required to find a resource allocation solution. From the simulation results, we observed that with the proposed user selection algorithms, we can achieve moderately high utilisation with much lower complexity, compared to finding user selections via an exhaustive search method. Out of the proposed user selection algorithms, the Priority Order with Sequential Removal (PO+SR) and the First-Fit (FF) algorithm have the best overall performance, in terms of the trade-off between utilisation performance, and complexity performance. The final choice of the algorithm will depend on the processing power and the system performance requirement of the macrodiversity system.

Acknowledgements

I started my masters since the beginning of 2009, as an engineer aspired to develop his technical competency through the pursuit of higher knowledge. It has been a long journey, along the way, there had been challenges, but also supports from people around me.

First and foremost I would like to thank my supervisors, Professor Peter Smith and Dr. Graeme Woodward, for their constant guidance, and encouragement throughout the project. Their time and effort in providing me with insights and directions, have been invaluable. I especially want to thank both supervisors for their patience in me, not being put-off or being judgemental by my constant stream of questions, even they may seem trivial at times.

I would also like to thank Tait Communication Ltd, especially Dr. Clive Horn, who supported me with this amazing thesis topic, allows me to grow professionally in the field of wireless communication. Also thanks to my colleagues at Tait, especially Hannes Prinsloo, Quang Ta, and Nicholas Dollin, for encouraging me pursuit of the masters, and becoming better in my professional career.

Next, I would like to thank all my past and present colleagues in the Wireless Research Centre, especially Fred Samandari and Jill Bond who make the environment a warm and friendly place to study, and making the enduring thesis writing much more bearable. Special thanks to Dr. Nicholas Pau for his helpful inputs and enlightening advice. He has been an invaluable friend to me, spending countless hours of his own time, helping me refine details of the theory and simulation, which is essential to the success of this project.

I should also mention Dr. William Lee, and Judy Zhou, they are my aspiration for my postgraduate study, and a special thank to Ysabel Legaspi, and Andrew Collin, being a long-time friend in my life. Making good times better and hard times easier.

Most importantly, I am deeply indebted to my parents for their endless love, support and encouragement. Especially my father, who passed away in 2011. You are an inspiration of my life, and will always live in my heart.

Thank you everyone, for being part of this journey with me.

Yu-An Chen

23rd September 2013

Contents

List of Figures

List of Tables

Abbreviation and Acronyms

AFR	Adaptive Frequency Reuse
BER	Bit Error Rate
BF	Best-Fit Algorithm
BLER	Block Error Rate
BPU	Backhaul Processing Unit
BS	Base-Station
BSG	Base-Sation Group
CDMA	Code-Division Multiple Access
CO	Convex Optimisation Algorithm
CoMP	Coordinated Multi-Point
CSI	Channel State Information
CSMA	Carrier-Sense Multiple Access
DAB	Digital Audio Broadcasting
DVB-T	Digital Video Broadcasting-Terrestrial
ECC	Error Control Coding
EDF	Earliest Deadline First
ES	Exhaustive Search Algorithm
FDMA	Frequency-Division Multiple Access
FFR	Fractional Frequency Reuse
FF	First-Fit Algorithm
GA	Genetic Algorithm
GD	Greedy Algorithm
ICI	Inter-Cell Interference
IGI	Inter-Group Interference
LTE	Long-Term Evolution
MCI	Maximum Channel to Interference Ratio
MCS	Modulation Coding Scheme
MDHO	Macro-Diversity Hand-Over

ML	Maximum Likelihood
MIMO	Multiple-Input Multiple-Output
MMSE	Minimum Mean-Squre-Error
MU-MIMO	Multi-User MIMO
PDF	Probability Density Function
PLE	Path Loss Exponent
PF	Proportional Fair
QoS	Quality of Service
QPSK	Quadrature Phase-Shift-Keying
RB	Resource Block (Resource)
SCC	Spatial Compatibility Check
SDMA	Space-Division Multiple Access
SER	Symbol Error Rate
SF	Shadow Fading
SFN	Single Frequency Network
SFR	Soft Frequency Reuse
SNR	Signal-to-Noise Ratio
SINR	Signal-to-Interference and Noise Ratio
SU-MIMO	Single-User MIMO
SVD	Single Value Decomposition
TDMA	Time-Division Multiple Access
TS	Tree Structure Algorithm
UCC	User Compatibility Check
UE	User Equipment (User)
UMTS	Universal Mobile Telecommunications System
ZF	Zero-Forcing

List of Symbols

Symbol	Description
k	Number of resources (Literature Review)
l	Number of groups in the TS algorithm (Literature Review)
n	Number of users (Literature Review)
r	Number of antennas (Literature Review)
A	Power Scaling Factor
K	Minimum number of antennas in the system (Literature Review)
N	Number of users
N_{BS}	Number of base stations
N_{comb}	Number of user combinations (Literature Review)
N_g	Number of generations (Literature Review)
N_{P}	Number of partitions
N_p	Number of individuals in a population (Literature Review)
N_{RB}	Number of resources
N_{SER}	Number of SER calculations
N_{UCC}	Number of UCCs (Literature Review)
R	Maximum number of resource-sharing (Literature Review)
γ	Path loss exponent
σ_{SF}	Standard deviation for shadow fading

Chapter 1

Introduction

The ever-increasing demand for high-speed mobile broadband any time, anywhere, drives the development of different channel access methods and network architectures so that more user services and data throughput can be achieved within the same network and bandwidth. The changing wireless channel condition due to multi-path, fading and interference is a major challenge to maintaining the signal quality for mobile users. Some channel effects can be addressed by advanced signal processing techniques such as equalisation, using multiple-input multiple-output (MIMO) communication, or different error control coding (ECC) schemes. Another approach is by addressing the problem from the network level [1, 2].

Macrodiversity is an emerging network technology that enables greater system performance. It is an extension of MIMO communication techniques in which base stations (BSs) form the distributed nodes of a MIMO transmitter (or receiver). For the case of an up-link system, signals received from the cooperative BSs are centrally processed by a backhaul processing unit (BPU). Macrodiversity can achieve greater signal strength by combining the received power of the distributed nodes, and can overcome the effects of large-scale shadow fading by providing alternative signal paths between the user and the BSs. Another feature of macrodiversity is that it increases user capacity by allowing multiple users sharing the same the channel resource. By exploiting the spatial separation between users in the network, the system can allocate the same resource to different users simultaneously. In general, macrodiversity improves signal quality at the cell edge, as well as the user capacity of the system [3], [4]. In the literature, there are similar ideas such as *network MIMO*, *Coordinated Multi-point (CoMP)*, or *massive MIMO* [5, 6, 7].

The wireless channel can be divided into multiple orthogonal time-frequency resource blocks. The process of allocating resources to users is known as *resource allocation*. For resource allocation that involves multiple users sharing the same resource, such as in multi-user MIMO (MU-MIMO) systems, it is referred to as *multi-user resource allocation* [8, 9], or *joint resource allocation* [10]. Multi-user resource allocation consists of two parts: *User se-*

lection, which chooses candidate users for resource-sharing; and *a user compatibility check* (UCC), which evaluates the compatibility between the resource-sharing users. These tasks are executed by a scheduler inside the BPU. For every time slot, it produces a *resource schedule*, which contains information about resource allocation to users. Figure 1.1 shows an example of an up-link macrodiversity system. Signals received by the BSs are jointly processed at the BPU, and resource allocation decisions are made by the scheduler inside the BPU, before passing them back to the BSs.

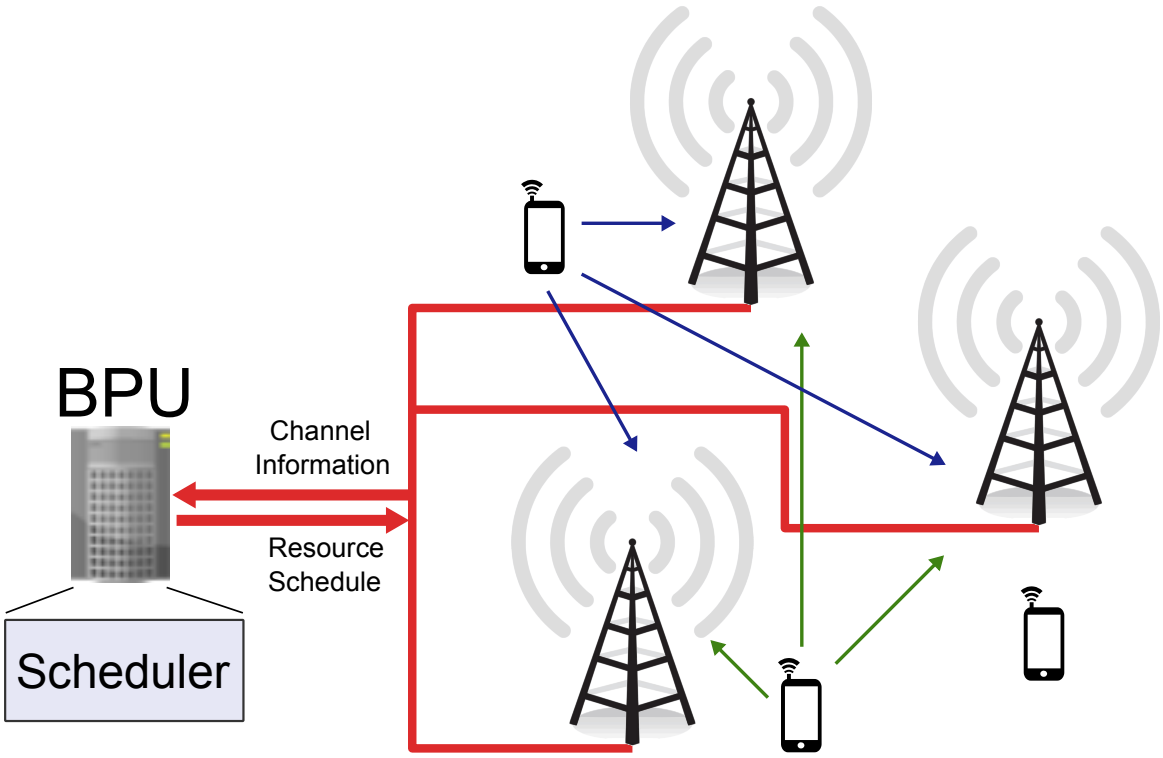

Figure 1.1: Resource allocation in a macrodiversity system.

Selecting appropriate users for resource-sharing is a combinatorial problem that already exists in MU-MIMO systems in traditional single-cell networks [11]. The complexity of the combinations depends on the number of users, antennas, and available RBs in the system. Finding the optimal user selection for multi-user resource allocation is a challenging task which requires evaluating the user compatibility of many different combinations. The problem often becomes too difficult to solve for large systems [12]. Computation time also adds a delay in the decision making, resulting in the resource schedule lagging behind the prevailing channel conditions. Heuristic solutions to the user selection problem have been studied in the past for MU-MIMO systems with co-located antennas [13, 8, 14, 15, 16]. However, often they are based on an assumption of there being zero network delay, and on the availability of complete and accurate information on the instantaneous channel state information (CSI), which is often not applicable in real communication systems.

The compatibility between resource-sharing users is often evaluated by system perform-

ance metrics, such as the sum capacity or outage error probability, which is calculated using the available instantaneous CSI at the time. Estimating instantaneous CSI is a process that is prone to estimation error. In macrodiversity systems, the geographical separation between BSs introduces latency in the system, which exacerbates channel estimation errors, and degrades the effectiveness of the UCC [17]. The cooperative BSs encompass a larger geographical area and more users, which up-scales the problem of user selection, and the computational complexity of user selection limits the scalability of the system. Another challenge with multi-user resource allocation in a macrodiversity system is the increased overhead on the network backhaul. Performing instantaneous channel estimation for all potential users in the network and passing this information to the BPU creates a lot of overhead on the network backhaul, which reduces the efficiency of the network. Challenges in user selection complexity, network delays, and overheads limit the performance benefits of multi-user resource allocation in macrodiversity systems.

These unique problems in macrodiversity systems motivate studies into resource allocation methods with reduced complexity and resilience to channel estimation error. One approach is to calculate user compatibility using long-term power. The benefit of the long-term power approach is that it eliminates the dependency on making resource allocation decision using instantaneous CSI, and consequently avoids delay-induced channel estimation error. Long-term power of the channel resources are the same, for each communication link there only needs one long-term power estimation. Therefore it also requires much less overhead than the instantaneous CSI approach.

1.1 Research Contributions

In this thesis, we present a low-complexity method of resource allocation for up-link macrodiversity systems using long-term power. The research contributions are:

- *Development of user selection algorithms with reduced complexity.*
  In this research we proposed four different user selection algorithms with the goals of maximising the system user capacity potential, and minimising the computational complexity. Different user selection algorithms were investigated, ranging from the most extensive search algorithm, where the compatibility of all user combinations are checked and the best performing combination is used, to the most basic algorithm, where the user combination is a simple grouping based on the priority order of the users. We also tried assigning users and resources into smaller partitions to further minimise complexity.

- *Implementation of a user compatibility check (UCC) using long-term power.*
  The compatibility of resource-sharing users is evaluated based on the link quality of each user. In this research we used the equations developed by Basnayaka [18], and implemented a method of checking user compatibility by estimating the SER of the resource-sharing users in a macrodiversity system using long-term power. UCC

estimates the SER of all users sharing the same resource, and is considered "passed" if the target user and all other users meet the SER threshold. When combined with the user selection algorithms we consider here, this forms a complete method of resource allocation for up-link macrodiversity systems.

- *Evaluating system performance over different environmental parameters.*
  System performance is evaluated in terms of *utilisation* and *complexity*. Utilisation refers to the percentage of users being allocated with a resource, relative to the system user capacity. Allocation of resource depends on the user passing the UCC. Complexity refers to the complexity of the user selection algorithms. It is generally evaluated by the number of UCCs required to reach a resource allocation solution. For the simulations in this research, we measure complexity by the number of SER calculations performed on individual users. Four different parameters relating to resource allocation in a macrodiversity system were investigated: system dimensions, user distributions, propagation parameters, and different link quality requirements. These are followed by an analysis of the observed effects.

In this research, we assume a small up-link macrodiversity system with a single antenna on each BS and on each users, with no interference from outside the cooperative BS group. The goal of this research is to obtain greater understanding of the user selection algorithms, and the effectiveness of the overall resource allocation method in practical scenarios.

1.2 Thesis Outline

Chapter 2 provides a background study on the topic of resource allocation. It examines the challenges with regards to resource-sharing in macrodiversity systems, and how this problem manifests itself in the CoMP systems of LTE. Chapter 3 describes the simulation model in which the performance of the resource allocation is evaluated. This includes network layouts, user distributions, and a model for the wireless channel. It also explains how utilisation and complexity in greater details. Chapter 4 describes the operation of the resource allocation methods. It explains the mechanism of the user selection algorithms, and the calculation of the long-term SER. It also proposes two additional strategies that could further reduce the complexity of user selection. Chapter 5 presents the simulation results and the analyses, and Chapter 6 offers some concluding remarks about these findings.

Chapter 2

Literature Review

2.1 Managing the Wireless Channel

The wireless channel has always been a scarce resource in wireless communication. In the early days of wireless communication, when multiple users shared the same radio resource, users used either a broadcast system with a simple listen-before-talking protocol, or a control channel to establish a working channel with the recipient before talking (circa. 1950) [19, 20]. These approaches were simple, but not efficient, users often needed to "take-turns" accessing the channel [19]. As a result, the number of users in the system was limited to a small size.

As the wireless channel was becoming increasingly crowded, different channel access methods were developed to accommodate more users in the system. The access methods can be channel-based or packet-based. Channel-based access methods allow multiple users to co-exist with each other by exploiting the physical properties of the wireless channel such as time, frequency, code, and space. This led to the development of respective multiple-access technologies such as Time-Division Multiple Access (TDMA), Frequency-Division Multiple Access (FDMA), Code-Division Multiple Access (CDMA), and Space-Division Multiple Access (SDMA) [21, 22, 23]. This is common in systems where there are multiple radio resources available, such as cellular networks. Packet-based access methods create rules that minimise collision between transmitting packets, allowing systems to achieve good channel efficiency. This is often seen in systems where multiple users need to share the same radio resource in different time slots. Examples of packet-based access method includes ALOHA, slotted-ALOHA, and Carrier-Sense Multiple Access (CSMA) systems [24, 25, 26]. Applications of packet-based access methods can be found in *ad hoc* networks and shared-media Ethernet.

In channel-based multiple access methods, the wireless channel is divided into independent resources. Users who access different resources can enjoy the communication channel without interference. For centrally controlled networks such as cellular networks, chan-

nel efficiency can be further improved by better resource allocation. Resource allocation involves considerations in multiple dimensions. The frequency dimension represents the spectrum resources available in the system, the space dimension represents spatial separation between the antennas of users and BSs, and the time dimension represents the queuing order of users accessing the resource, if there are more users than the resources available. Figure 2.1 shows a very simplistic relationship between frequency, space, and time of the radio resource, and some strategies for optimising channel efficiency with active management of resources.

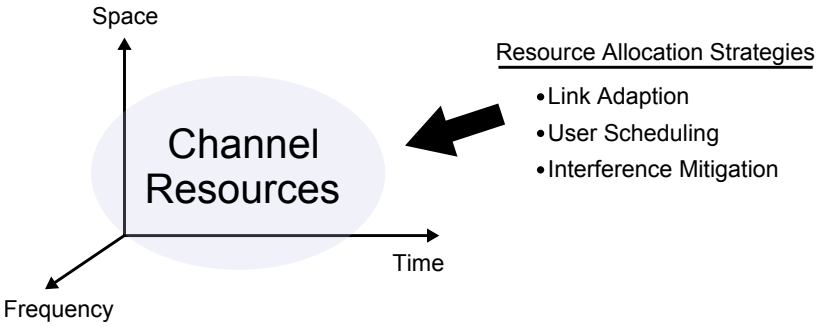

Figure 2.1: Considerations for resource allocation and some common strategies.

Generally, a wider available bandwidth in a system indicates greater channel capacity. Often the availability of channel bandwidth is pre-determined by the government regulations or the spectrum ownership. To increase data rate within the bandwidth, systems could allocate more power to the channel, and use a higher order modulation scheme. These techniques are known as *link adaptation* [27, 28, 29, 30]. Knopp [27] proposed allocating more power to weaker user-channels to obtain consistent link quality for all users. Chung [31] examined the effects of adaptive modulation schemes in improving channel efficiency and showed that rate control is more efficient than changing the power level of the channel [32].

Prioritising users for the available resources in a system is commonly known as *user scheduling*. At any time instance, when the number of available resources is known, the scheduler decides the set of users that should be served at the time. Hassel [33] provided a good overview of different user scheduling algorithms used in wireless networks. These methods are mostly gradient-based algorithms where each user is assigned a utility function based on network parameters such as delay and throughput, and scheduling decisions are made based on the system objective. Common scheduling algorithms include Maximum Channel to Interference ratio (MCI) scheduling, Proportional Fair (PF) scheduling, and Earliest Deadline First (EDF) scheduling [34, 35, 36, 37].

Managing radio resources to reduce interference between users is known as *interference mitigation*. In cellular networks, interference occurs when users from nearby cells are accessing the same channel. This is known as *inter-cell interference* (ICI). Many studies have been made on ICI mitigation. One way to reduce ICI is by careful frequency planning. Frequency planning defines a pattern of how radio resources should be allocated between

cells, and reuses the frequency spectrum where users are least likely to interfere with each other, hence achieving better frequency reuse. Kwan [38] gave a good overview of different methods of frequency reuse including Fractional Frequency Reuse (FFR), Soft Frequency Reuse (SFR), and Adaptive Frequency Reuse (AFR), *etc*. Other methods of interference mitigation that utilise the spatial aspects of radio propagation include relaying, sectoring, and heterogeneous networks such as femto-cells. Sectoring achieves higher cell density by using directional antennas that divide cells into smaller sectors. One practical benefit of sectoring is that the antennas can be placed at the same location, which simplifies the cell-site design because access to additional cell-sites is not always possible. Femto-cells achieve a higher spectral efficiency by having smaller cell area, which increases the density of frequency reuse. A more distributed network also means more consistent power distribution over the deployed areas.

These strategies address different aspects of resource allocation. They are often implemented in conjunction with one another to achieve the optimal channel utilisation.

2.2 Multi-User Resource Allocation

In traditional cellular systems, there is only one antenna on each BS, and each radio resource can support only one user. For this type of system, optimisation of spectral efficiency is limited to prioritising user services according to the channel conditions, and frequency planning to avoid interference from the neighbouring cells. The development of MIMO communication allows the same resource to be shared by multiple users, this is known as a MU-MIMO system (as oppose to single-user MIMO systems: SU-MIMO). MU-MIMO can be regarded as a form of SDMA, where resource-sharing is achieved by exploiting spatial diversity in the MIMO systems. When signals from different sources are received by multiple antennas; although they interfere with each other, the spatial diversity will often allow the signals to be separated, hence achieving a higher spectral efficiency [11, 39].

Multi-user resource allocation involves selecting users for resource-sharing, and evaluating the compatibility between the selected users. The following describes some popular strategies for user selection and compatibility evaluation. The symbols described in this section applies only to this Chapter. The symbols used in the remaining of this thesis are defined in Chapter 3.

2.2.1 User Selection

Selecting compatible users for resource-sharing is known as *user selection*, or *user grouping*. Users who share the same resource is referred to as a *user group*. To check the compatibility of the resource-sharing users, a UCC is used to evaluate the fitness of each user group in relation to the system objective. The general goal of user selection is finding appropriate user groups so the system throughput or the overall link quality is maximised. Finding

the optimal user selection is a combinatorial problem in which a huge number of grouping combinations exists even for a small number of users and resources. An exhaustive search of all combinations is not practical, and it is often impossible to execute in real life [12]. The following are some common user selection strategies that have been proposed in the past:

No Resource-Sharing:

In resource allocation with no resource-sharing, users who are allocated with a resource have the exclusive right to access it. If users are ranked according to a system objective and assigned with a priority order, then the resources are typically allocated to the first k users on the priority order. Because all resources are independent, therefore the order of the k selected users is not important. Hence, there is no need to search for different user combinations, or check user compatibilities for this setup.

Figure 2.2 shows a resource allocation scenario where there is no resource-sharing. To simplify the notation, in the figures, resources are referred to as RB (*Resource Block*), and users are referred to as UE (*user equipment*). In this example, there are k available resources and n users. Here, we refer to the first k users as *primary users*, all other users are referred to as *secondary users*. The primary users have exclusive access to the resources, however, the overall user capacity is low because each resource is only being used once.

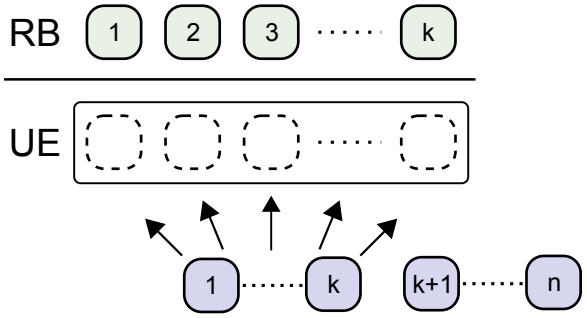

Figure 2.2: Resource allocation with no resource-sharing. The first k users are allocated with a resource. The remaining users are unallocated.

Exhaustive Search (ES):

Figure 2.3 shows the same scenario with resource-sharing. Resource allocation is done in such a way that the primary users are served first, before the secondary users are considered. Within the same resource, the link quality of an additional user is dependent on the existing user who has been allocated the same resource. In this case, the order of the selected users is important for all other users beyond the first row.

Here, we consider the exhaustive search (ES) algorithm, where all combinations of the secondary users are considered. This combinatorial behaviour can be evaluated using *permutations*, ${}^{n}P_{k}$, where n is the number of users, k is the number of resources available in the system.

Assuming fixed allocation for the primary users, the number of combinations, N_{comb}, can be described by

$$N_{\text{comb}} = \prod_{i=1}^{R=\min(\lfloor n/k \rfloor, r)} {}^{n-ik}P_k. \tag{2.1}$$

Here, r is the total number of antennas of the BSs[1], and R is the maximum number of users sharing the same resource. If $n < k \times r$, then $R = \lfloor n/k \rfloor$; if $n > k \times r$, then $R = r$. Given that the UCC is performed on each user group independently, the complexity of user selection can be described by the number of UCCs, N_{UCC}:

$$N_{\text{UCC}} = kN_{\text{comb}} = k \prod_{i=1}^{R=\min(\lfloor n/k \rfloor, r)} {}^{n-ik}P_k. \tag{2.2}$$

For the special case where n is a multiple of R, (2.2) has a simplified expression:

$$N_{\text{UCC}} = k\frac{(n-k)!}{(n-2k)!}\frac{(n-2k)!}{(n-3k)!}\cdots\frac{(n-(R-1)k)!}{(n-Rk)!} = k\frac{(n-k)!}{(n-Rk)!}. \tag{2.3}$$

From (2.2) and (2.3), the complexity of the algorithm grows exponentially as the number of users increases. This is similar to the well-known knapsack problem and it is $\mathcal{NP}$-complete [15]. It is computationally intensive for any practical system, and for this reason, people have been searching for heuristic solutions to address the problem.

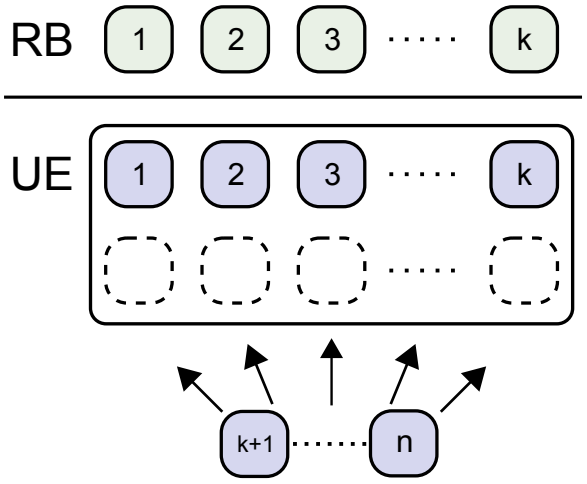

Figure 2.3: Resource allocation in a MU-MIMO system using ES method.

Greedy (GD):

One of the most common solutions is the use of greedy algorithms. Greedy algorithms accept the first solution that passes UCC [13, 40, 15, 9, 16, 41]. Based on a greedy algorithm, Shad [13] proposed two user selection methods for each additional user in the user group: one chooses the first candidate user that meets the compatibility criteria (First Fit - FF);

[1]Since we assume each BS only has one antenna, r is also the number of BSs.

the other one chooses the best performing candidate user (Best Fit - BF). These methods are "greedy" in the sense that once a candidate user is selected, it is removed from the user selection pool, hence removing the possibility of the selected users being in a different group.

Figure 2.4 shows an example of user selection by a greedy algorithm. The compatibility of each additional user is tested in a sequential manner assuming fixed allocation for the primary users. In each iterative search, one suitable candidate is added into the user group (hence removed from the user selection pool). N_{UCC} can be described by

$$N_{\mathrm{UCC}} = \sum_{i=k}^{\min(n-1,rk)} (n-i). \tag{2.4}$$

For the FF algorithm, this is the upper bound of the search complexity; for the BF algorithm, this is the minimum search complexity.

If the channel condition is such that there is no compatible user for resource-sharing, then N_{UCC} can be described by

$$N_{\mathrm{UCC}} = \sum_{i=1}^{k} (n-k), \tag{2.5}$$

where the algorithm terminates after the first round of search for resource-sharing users.

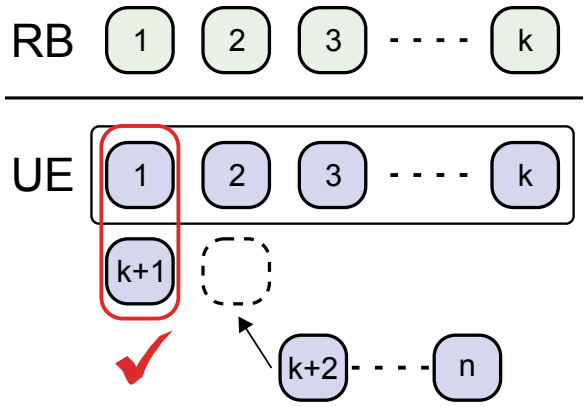

Figure 2.4: User selection by the greedy algorithm. Unallocated users are tested sequentially according to the priority order. Each time a compatible user is identified, it is added to the user group and removed from the user selection pool.

In [13], Shad also argued that by allocating the same resource to users with similar uplink power levels, it is less likely that the stronger interferers will corrupt the weaker transmissions. Shad proposed sorting users in ascending power order before starting the user allocation process.

Tree Structure (TS):

Similar to the greedy algorithm, Fuchs [14] extended the idea to a tree-based structure where users are merged or divided into groups, depending on whether the tree is constructed following a *top-down* or a *bottom-up* approach. Figure 2.5 is an excerpt from the paper, showing the grouping process. Here, l, is the number of groups. For a bottom-up structure, an additional user is merged into a group if the candidate user meets the compatibility criteria. Ideally, the number of groups should be less than or equal to the number of resources. If the number of groups is greater than the number of resources, either the users with higher priority order (priority-oriented), or groups with a higher number of users (capacity-oriented) should be granted the resource. N_{UCC} can be described by

$$N_{\mathrm{UCC}} = \sum_{i=1}^{l-k} {}^{l-i}C_2 = \sum_{i=1}^{l-k} \frac{(l-i)!}{2(l-i-2)!}. \tag{2.6}$$

One benefit of this algorithm is that it retains memory from the last resource allocation. Between different time instances, it only needs to make modifications to the existing schedule to accommodate the change. The algorithm does not need to start from $l = n$ or $l = 1$. This is a useful feature in networks where past user behaviour has a high correlation with the future user behaviour.

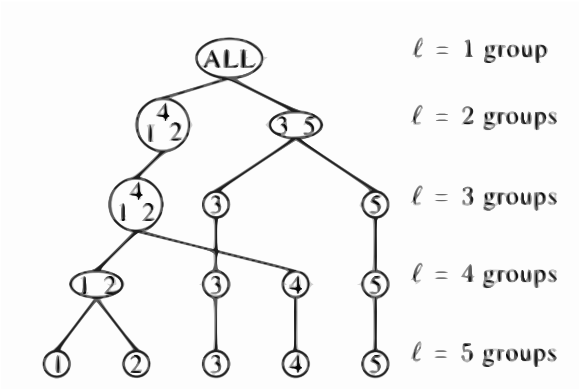

Figure 2.5: Tree-based user selection. (From [14].)

Genetic Algorithm (GA):

Wang [10] applied genetic algorithms to the user selection problem. In his method, a resource schedule is an *individual* in an evolutionary population. Each individual has a *chromosome* that contains k gene vectors. In this case, k, is the number of resources. As shown in Figure 2.6, each gene vector (row) contains a binary representation of the user selection for one resource and the bit loading schemes for the users in the group.

Chromosomes are evaluated by a fitness function. In the case of Wang, he looked at the transmission rate of users who vary their transmission rate according to the channel condition. The two fittest individuals are selected as parents, who breed offspring by genetic operators such as crossover and mutation. In each generation, the pair of parents breed N_p individuals to replace the old population. Over generations, the chromosomes eventually

converge on the system objective. The complexity of user selection can be calculated as

$$N_{\mathrm{UCC}} = kN_pN_g. \tag{2.7}$$

N_p, is the population of individuals in the current generation, and, N_g, is the number of generations. Both N_p and N_g can be arbitrarily defined, where the larger the number, the higher likelihood of convergence.

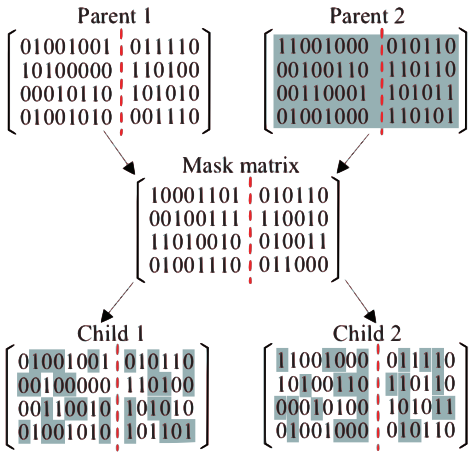

Figure 2.6: An example of a genetic crossover operation with 8 users, 4 resources, and a frequency re-use factor of 3. (From [10].)

Convex Optimisation (CO):

In [42], Maciel formulated the user selection problem into a convex optimisation problem. In this method, user selection is presented in the form of a binary selection vector. The goal is to find a selection combination where the channel correlation between users is minimal. By allowing values in the selection vector to be continuous, the task is turned into a convex quadratic problem with linear constraints. The solution can be found without exhaustively searching through all combinations, hence reducing the search complexity. Assuming the worst case scenario where the CO algorithm goes through the combination iteratively, the upper bound of N_{UCC} can be described as

$$N_{\mathrm{UCC}} \leq \sum_{i=1}^{k} {}^{n-ir}C_R = \sum_{i=1}^{k} \frac{(n-iR)!}{R!(n-(i+1)R)!},\ R = \min(\lfloor n/k \rfloor, r). \tag{2.8}$$

Here, R, has the same definition as in (2.1). In theory, convex optimisation provides a means of finding the user selection without an exhaustive search, however, the complexity involved in solving the convex optimisation problem means that the overall complexity of the algorithm is still high. The trade-off between the user selection complexity and solving the convex quadratic problem may not be beneficial for the overall efficiency.

Summary:

Figure 2.7 compares the selection complexity of the algorithms over different numbers of users. From the figure, we can see that the complexity of the ES algorithm becomes exponentially higher than all other algorithms as the number of users grows large. The GD algorithms have the least complexity: In this figure, we assume that a suitable candidate is added into the user groups in each round of search. FF has less complexity than BF, because it accepts the first candidate that meets the compatibility criteria. The TS algorithm has slightly a higher complexity than the GD algorithms. Unlike the GD algorithms, where each row has to be filled before moving onto the next row, the TS algorithm has no constraint on the group size, resulting in more possible grouping combinations. For GA, the complexity depends on the number of individuals in the population (N_p), and the number of generations (N_g). These numbers are arbitrarily defined but they need to be of a sensible size for the result to converge. As a result, GA has a higher complexity in systems with a small number of users, but it is more efficient in systems with a larger number of users. For the CO algorithm, we provide only an upper bound on the complexity. In this case, the CO algorithm has a similar complexity to the GD algorithms. The complexity of CO surpasses GD, TS and GA, when the number of users becomes large. In practice, the CO algorithm is likely to be much less complex than the estimated upper bound.

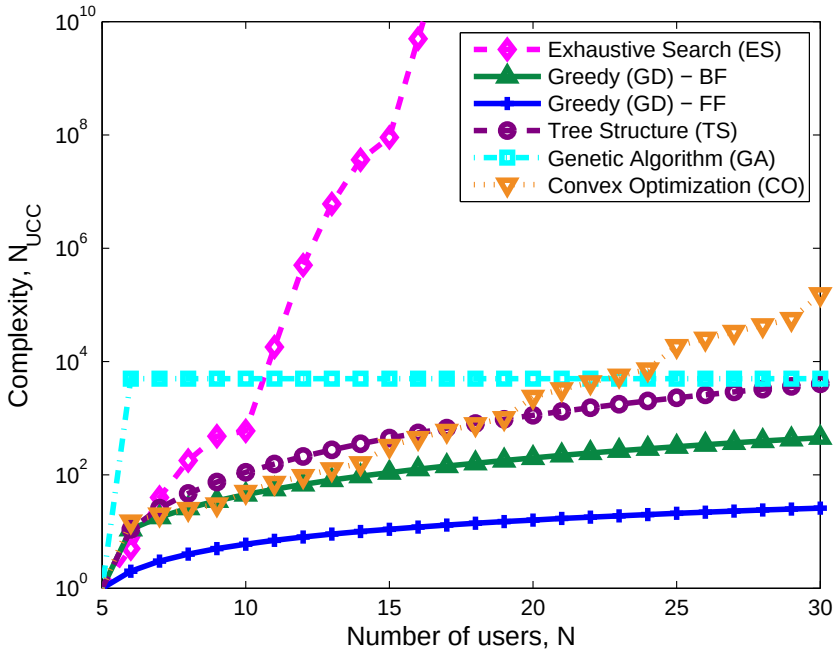

Figure 2.7: Complexity of user selection measured in N_{UCC}. In this example, $k = 5$, and $r = \lceil n/k \rceil$. For the TS algorithm $l = n$. For the GA algorithm, $N_p = 20$, and $N_g = 50$.

Table 2.1 shows an example of the maximum N_{UCC} required for each class of user selection algorithm. From Figure 2.7 and Table 2.1, the GD algorithm has the least user selection complexity. The simplicity and low complexity characteristics make the GD algorithm an attractive option for systems with a large number of users.

Table 2.1: Estimated complexity for the user selection algorithms.

User Selection	**Number of UCCs**
Exhaustive Search (ES)	$k\prod_{i=1}^{R} {}^{n-ik}P_k$
Greedy (GD)	$\sum_{i=k}^{\min(n-1,rk)} n-i$
Tree Structure (TS)	$\sum_{i=1}^{l-k} \frac{(l-i)!}{2(l-i-2)!}$
Genetic Algorithm (GA)	kN_pN_g
Convex Optimisation (CO)	$\sum_{i=1}^{k} \frac{(n-iR)!}{R!(n-(i+1)R)!}$

2.2.2 Compatibility Evaluation

When there are multiple users in the user group, it is inevitable that some mutual interference will occur, resulting in poorer link quality for all users in the group sharing the same resource. It is possible to reduce the interference using MIMO detection techniques such as zero-forcing (ZF), minimum mean-square-error (MMSE), or maximum likelihood (ML) detection. UCC provide a means of evaluating the compatibility of the resource-sharing users. In general, UCC evaluates the link quality of the users. The following are some common approaches for evaluating link quality:

Sum Capacity:

Fundamentally, multi-user resource allocation is often about achieving higher user capacity or system throughput. Therefore, many resource allocation algorithms use *sum capacity* (or *sum rate*) for evaluating user compatibility. For SU-MIMO systems, channel capacity can be described by [39], where

$$C = \max_{\mathbf{Q}:\mathrm{tr}(\mathbf{Q})=P} \log_2 \det(\mathbf{I}_K + \mathbf{HQH}^\dagger). \tag{2.9}$$

C is the channel capacity measured in *bits per second*. $\mathbf{I}_K$ is an identity matrix with size $K \times K$, where K is the minimum number of antennas between the transmitter and the receiver. $\mathbf{H}$ is the instantaneous channel matrix, $\mathbf{H}^\dagger$ is the conjugate transpose of $\mathbf{H}$, and $\mathbf{Q}$ is the covariance matrix of the transmitted symbols. For MU-MIMO channels, the channel capacity of an individual user depends on the channel capacity of the other user. The sum capacity is described by

$$C = \max_{\mathbf{Q}_1,\ldots,\mathbf{Q}_n} \log_2 \det(\mathbf{I}_M + \sum_{i=1}^{n} \mathbf{H}_i\mathbf{Q}_i\mathbf{H}_i^\dagger). \tag{2.10}$$

Here, C is the sum capacity of all users, n refers to the number of resource-sharing users and i is the index of the individual user. M is the number of antennas of the individual users. Examples of compatibility evaluation using sum capacity can be found in [40, 14, 42, 43, 10, 44].

Sum capacity gives an indication of the potential rates available on the user channels, but this is only the sum rate of a particular user group, not the rate or the link quality of individuals in the group.

Quality of Service (QoS):

As an alternative approach, link quality may be defined such that a minimum Quality of Service (QoS) for each user is guaranteed. QoS can be measured by the error probability of the link. Ideally, QoS should reflect the *block-error rate* (BLER) of the user channel. However, BLER depends on many factors such as the ECC scheme and the Modulation Coding Scheme (MCS), which may vary from user to user. Very often, *bit-error rate* (BER) or SER is used for measuring QoS instead, and these values can be converted to BLER using standard lookup tables.

There is a technical problem in using long-term power to evaluate error rates. Since the channel matrix in macrodiversity systems does not follow a Wishart form, it is difficult to characterise the SNR/SINR distribution using long-term power. We can not derive error rates without understanding of the characteristic function of SNR. Basnayaka [45] derived a method of calculating the exact and approximate SER of users for macrodiversity systems using long-term power. From Basnayaka's work [18, 45], the exact SER in macrodiversity system can be calculated in scenarios where there is only one user using the frequency resource. However, the same argument can not be extended to multiple users sharing the same resource. For the multi-user scenario, the characteristic function of SNR can be estimated by the use of the Laplace approximation, and an estimated SER can be calculated if the MCS is known. In Basnayaka's paper, he used QPSK modulation schemes as an example. These equations provide a simple, closed-form method for estimating the link-quality of resource-sharing users in macrodiversity systems. Similar work appears in Zhang [46], where the BER is part of the objective function for user compatibility.

SINR:

In conventional cellular systems, the instantaneous *signal-to-interference-and-noise ratio* (SINR) is often used as an indicator for link quality. This is because SINR can be easily derived from the instantaneous CSI, and there is a high correlation between SINR, channel capacity, error rates, and QoS.

In [13], Shad proposed that for a down-link MU-MIMO system, the average SINR after

beam-forming, can be described by

$$\gamma = \frac{\mathrm{E}[|\mathbf{w}^T \mathbf{x}_d|^2]}{\mathrm{E}[|\mathbf{w}^T \mathbf{x}_u|^2]}. \tag{2.11}$$

In (2.11), γ is the average SINR, $\mathbf{w}$ is the beam-forming weighting vector, $\mathbf{x}_d$ is the desired signal, and $\mathbf{x}_u$ is the undesired signal, consisting of the noise and the interfering signals. The author further proposed that a minimum SINR requirement be adopted as the compatibility criteria.

In MU-MIMO systems, the link quality of user channels does not follow a direct relationship with SINR. For MU-MIMO systems, the SINR varies depending on the channel characteristics of the resource-sharing users. This is therefore a less commonly used method for compatibility evaluation.

Channel Correlation Matrix:

The less correlation between the user channels, the higher the likelihood of users being compatible for resource-sharing. In [8], Spencer proposed a scaled Frobenius norm as a measure of user compatibility. The metric estimates the total correlation between two users' channels, and produces a single constant, in which a set of user groups is selected so the overall channel correlation is minimised. The limitation of this metric is that it can only evaluate channel correlation between two users. Zhang [46] proposed a method that groups the most correlated users together as a single group. Within the group, each user is allocated an independent resource so users do not interfere with each other. Users in different groups are allowed to share the same resource so that spectral efficiency can be utilised. Tolli [40] proposed that for MU-MIMO systems with block diagonalisation pre-coding, the maximum sum channel gain can be obtained by selecting the users with the highest eigenvalues. The eigenvalues correspond to the beam-forming vectors of the channel, which are obtained by Single Value Decomposition (SVD) of the channel matrix. In this case, only the channel energy is taken into account. In [15, 47], Maciel proposed a Spatial Compatibility Check (SCC), that looks at the average correlations among all channels. This metric has a weighting which favours groups with a larger number of users.

These methods are relatively simple to compute, however, they are loose indicators of the link quality. If we can not ascertain an accurate link quality for the users, it is difficult to estimate whether the performance trade-off is acceptable between user link quality and higher user capacity. As a result, the system can not fully realise its capacity potential.

Summary:

The above metrics provide a means of evaluating link quality for the resource-sharing users with varying degrees of accuracy and complexity. Most of the metrics use instantaneous

CSI to generate the compatibility result. Instantaneous CSI is prone to channel estimation errors, and the problem is exacerbated in macrodiversity systems, where there often is a significant delay between the channel estimation and the actual data transmission. Estimating instantaneous CSI for all users at all resources also creates a large amount of overhead, reducing the overall efficiency of the wireless channel and the supporting backhaul. For these reasons, it is worth exploring UCCs that do not use instantaneous CSI. In this study, we focus on estimating SER using long-term power.

2.3 Resource Allocation in Macrodiversity Systems

MU-MIMO systems have two configurations: *microdiversity* or *macrodiversity*. Most current MU-MIMO systems are "micro-diversity", where separation of the antennas in the antenna array is a few wavelengths apart, generally co-located at the same geographical point [48]. "Macro-diversity" refers to the antennas in the antenna array being geographically separated with distances between BSs in the order of hundreds of metres or kilometres [49, 50, 51, 52]. Macrodiversity systems treat BSs as distributed nodes of a MIMO receiver and require simultaneous control of all the BSs within the network group. The concept of macrodiversity has already been applied in existing technologies such as the soft-handover in CDMA and Universal Mobile Telecommunications System (UMTS) networks [53, 54, 55, 56], and macro-diversity handover (MDHO) in WiMax [57, 58, 59]. Single frequency networks (SFN), such as Digital Video Broadcasting-Terrestrial (DVB-T) and Digital Audio Broadcasting (DAB) in broadcasting networks, are also a form of macrodiversity system [60]. The advantage of macrodiversity is that it can provide diversity gain in areas where microdiversity could not, such as in areas experiencing large-scale shadowing effects, and at the cell edge [61]. This is attributed to the geographical separation between antennas, where each antenna has different path loss and shadowing characteristics. In general, macrodiversity improves signal performance at the cell edge and increases user capacity within the cell group [3], [4]. Microdiversity and macrodiversity systems can be implemented independently, or combined.

One of the challenges with macrodiversity systems is the inherent delay in the network. This has a significant impact on resource allocation in macrodiversity systems. Most resource allocation algorithms rely on the availability of instantaneous CSI [13, 8, 14, 40]. However, passing instantaneous CSI over the network backhaul creates large network overheads, and the inherent network delay also makes the received information unreliable as fast fading means that channel conditions can change in the order of microseconds (μs) [62, 63]. Diehm [64] showed that the effectiveness of instantaneous CSI decreases significantly if the delay is longer than $10ms$, and up to 50% degradation in channel capacity (bits per channel use) can be observed if the user is moving faster than $10km/h$.

One way of avoiding the effect of network delay is by using long-term power for UCC. In 2007, Bandemer proposed a method of evaluating user compatibility for MU-MIMO systems using long-term power [43]. In his work, user compatibility is evaluated based on the

channel capacity (ergodic sum capacity) of users in the system. Bandemer's work is confined to up-link MIMO systems with co-located antennas, where the received signal power of the BS is constant for each user. In 2012, Basnayaka and Smith extended Bandemer's work into macrodiversity systems. Basnayaka presented a series of studies on evaluating link qualities of resource-sharing users in up-link macrodiversity systems using long-term power [18, 44, 65, 66, 1, 67, 45, 68]. The author developed closed-form equations for the ergodic sum capacity [44], calculations of the exact symbol-error rate (SER) for single and dual user macrodiversity scenarios [65, 66], and a calculation of the approximate SER for general multi-user macrodiversity scenarios [1] for different receiver detection techniques such as maximumal ratio (MRC) combining, Zero-Forcing (ZF), Minimum Mean Square Error (MMSE) and maximum likelihood (ML) detection using an extended Laplace approximation. Basnayaka provided a comprehensive framework for evaluating link quality based on long-term power in macrodiversity systems. This work is useful as part of the UCC. However, reducing user selection complexity remains a challenging task. For practical implementation of multi-user resource allocation in macrodiversity systems, the user selection complexity needs to be further reduced.

2.4 Application: LTE CoMP Systems

In LTE release 11 (LTE-advanced), a version of macrodiversity is supported, known as Coordinated Multi-Point (CoMP) [3, 69]. In the 3GPP technical report, it is shown that CoMP schemes can potentially improve cell edge performance by up to 40% (no resource-sharing), without the need for a major infrastructure change.

CoMP in LTE uses Orthogonal Frequency Division Multiplexing (OFDM) in its radio access. OFDM divides radio resources into time and frequency resource blocks (RBs) and dynamically allocates RBs to UEs by the radio resource control (RRC) scheduler [70, 71]. Like other macrodiversity systems, CoMP also suffers from delays in the network, resulting in degradation of performance [72, 73]. Passing instantaneous CSI through the network backhaul also creates significant strain on the network, limiting the potential of macrodiversity to provide system performance improvement. Currently there is no standardised resource allocation method for CoMP in LTE. An investigation of resource allocation using long-term power could improve the performance of CoMP and potentially make the system deployable on a larger scale than before.

2.5 Summary

This chapter described the role of resource allocation in improving the utilisation of wireless channels. It showed that in MIMO systems, the same frequency resource can be shared by multiple users by exploiting spatial diversity in the system. A macrodiversity system is a sub-class of MIMO systems where the antenna arrays are located at BSs that are geographically separated from each other. This presents a challenging problem as the delay

inherent in the network makes instantaneous CSI ineffective, and system performance suffers as a consequence. Basnayaka [18] proposed various metrics for user compatibility in macrodiversity systems using long-term power, enabling the development of resource allocation methods for macrodiversity systems that are resilient to network delay. Research into this resource allocation method has applications to the CoMP system in the LTE standard, potentially increases cell-edge throughput, and can lead to a general improvement in signal quality and user capacity.

Chapter 3

System Model

To evaluate performance of multi-user resource allocation in macrodiversity systems, a simple model is constructed to represent the real-life macrodiversity system, and resource allocation is simulated under different system parameters. This chapter defines the network laytouts of the macrodiversity system model, the user distributions, the wireless channel model, and the method in which link quality and system performance are evaluated. For individual user channels, link quality is evaluated by the analytical SER, calculated using long-term power. Users are considered meeting the link quality requirement if the SER passes the SER threshold, and resources are only allocated to the users if they meet the link quality requirement. From the system perspective, we are interested in how much the user capacity can be realised in macrodiversity systems with resource-sharing. This is measured by the percentage of allocated users over the theoretical user capacity. We are also interested in the complexity of the user selection algorithms. In the simulation, complexity is defined as the number of analytical SER calculations required for the user selection algorithm to find a resource schedule.

3.1 Network Layouts

In conventional cellular systems, users connect only to one cell at a time - often the BS with the strongest received signal strength to each user. Such a configuration often means that the users have poor link quality at the cell edge as neither cell experiences good received signal strength. Macrodiversity systems overcome this problem as the users are supported by multiple BSs simultaneously. Within the coverage area, the signal transmitted by a user is received by every BS within the macrodiversity group, and the received signal is combined to achieve greater overall signal strength. Another benefit of macrodiversity is that it can also support multiple users simultaneously on the same frequency channel because the signals can be separated out using detection techniques such as ZF or MMSE.

Figure 3.1 illustrates the difference between a conventional cellular system and a macrodi-

versity system. In the figure, cells are centre-excited with no sectoring involved. In macrodiversity systems, the BSs are joined together and centrally controlled by the BPU. The BPU combines the information received from the BSs in the group, and allocates resources to users according to a resource allocation algorithm. As shown in the Appendix A1 of [3], there are many different network layouts for macrodiversity systems. In this thesis, only homogeneous networks are considered, and the total coverage area of the macrodiversity system is the combined area of all cooperating BSs.

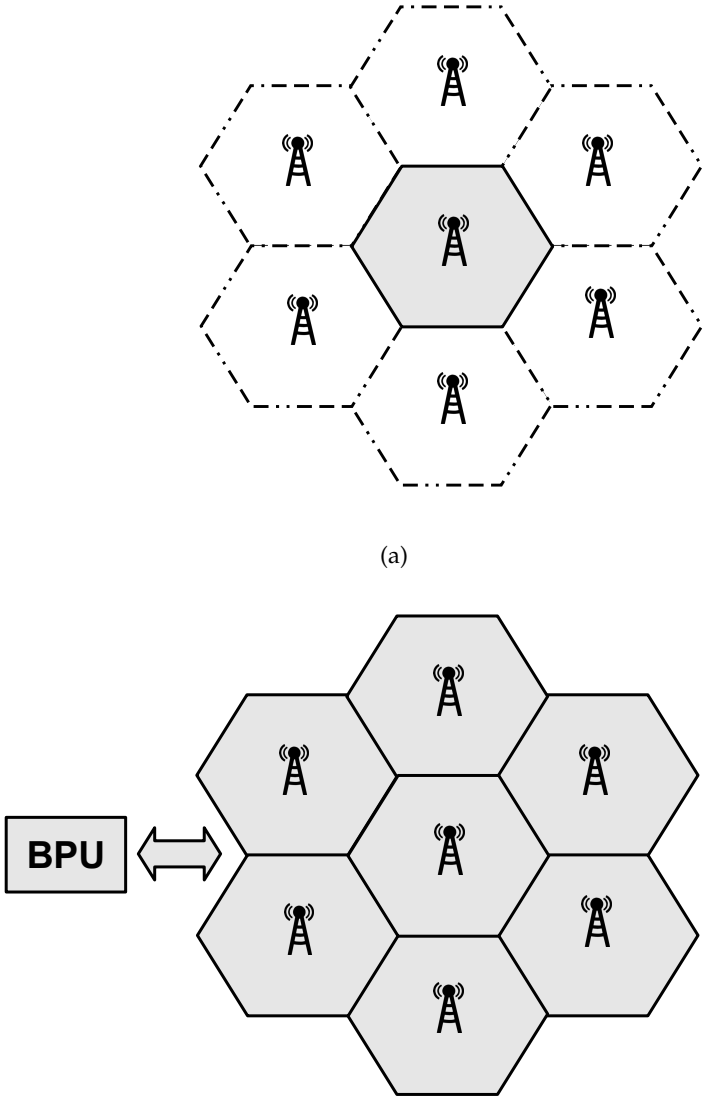

Figure 3.1: (a) A conventional cellular system: the cell shaded in gray operates independently of the surrounding cells. (b) A macrodiversity system: the group of 7 cells co-operate via a BPU, covering the area of all 7 cells.

There can be multiple cooperating BS groups within a macrodiversity system. We define a set of cooperating BSs as a base station group (BSG) [1]. With more BSs in a BSG, the network can support more users in the system, but the user selection complexity can also become very large. One way to break the problem down is to have multiple smaller BSGs. Figure 3.2 shows a macrodiversity system with multiple BSGs. Each group has a BPU and resource allocation decisions are made within the BSG.

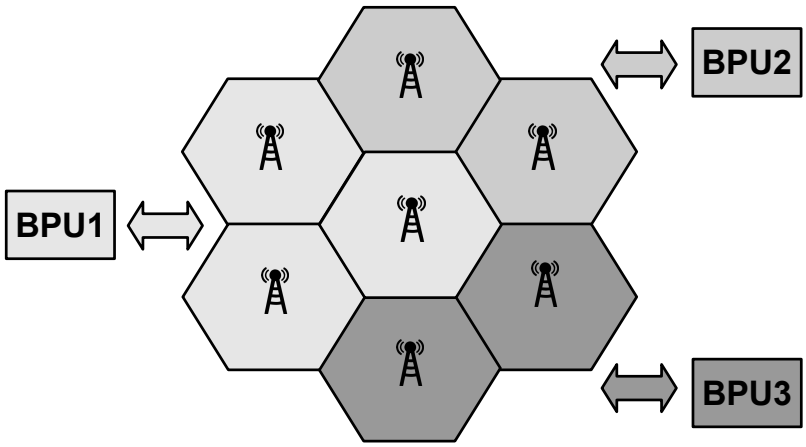

Figure 3.2: Macrodiversity with multiple BSGs.

As shown in Figure 3.3, when two BSGs are next to each other, a transmitting user can potentially interfere with neighbouring BSGs, similar to inter-cell interference (ICI) in conventional cellular systems. Mitigating Inter-Group Interference (IGI) is a complex field of study on its own, so this is not in the scope of this research. The focus of this research is on reducing user selection complexity of a single macrodiversity system.

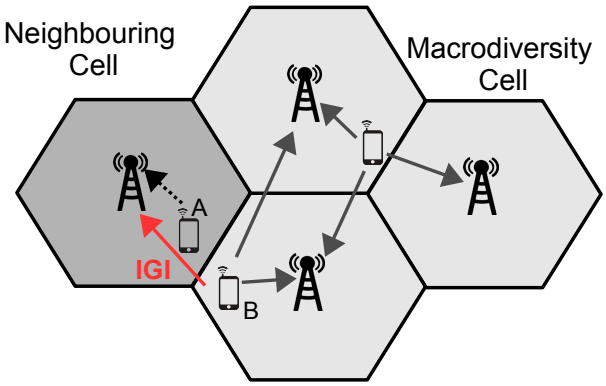

Figure 3.3: IGI: User B is interfering with the neighbouring BSG.

[1] In LTE-Advanced, a group of cooperating cells is called a CoMP Cooperating Set [3]

3.2 User Distribution

There are two types of user distributions considered in the simulation: a random uniform distribution and a random clustered distribution. A uniform distribution reflects a general system scenario where users tend to be evenly spread, and a clustered distribution simulates scenarios where there is a sudden increase of data demand in a focused spot such as a disaster event.

Figure 3.4 shows examples of two user distributions with 3 BSs. Here, we define the radius of the BSs as 1, which is the distance of the BSs away from the centre of the map. Figure 3.4a shows a uniform user distribution: users are in the vicinity of the BSG, which is described by a circle positioned at the centre of the BSG. In this case the radius of the circle is 1.5 times the radius of the BSs. Figure 3.4b shows a clustered user distribution: in the simulation, we describe the user cluster as a Gaussian distribution, and the centre of the cluster could be at the centre of the BSG or at the cell-edge, depending on what distribution scenarios we intend to create. In this case, the variance of the cluster is 0.375 of the radius of the BSs. These two user distribution models are the primary scenarios we considered in our simulations in Chapter 5. In the figures, we plot 500 users on the map to give readers a stronger sense of user distribution; in the simulation in Chapter 5, we only consider a small number of users, to keep the simulation manageable.

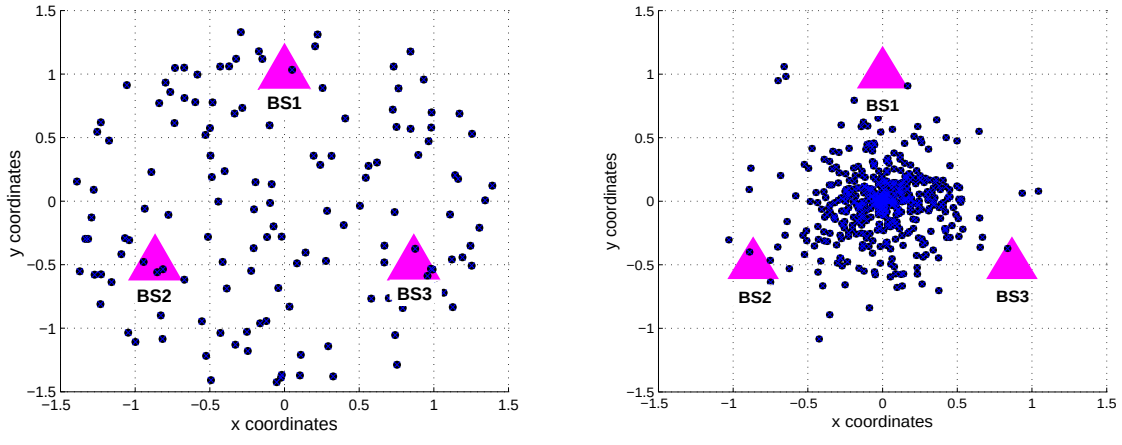

(a) (b)

Figure 3.4: (a) Uniform distribution: Centred at $(x, y) = (0, 0)$, with radius = 1.5.
(b) Gaussian distribution: Centred at $(x, y) = (0, 0)$, with variance $\sigma^2 = 0.375$.

3.3 Channel Model

As explained in Chapter 2, it is difficult to accurately estimate instantaneous CSI of all users in macrodiversity systems simultaneously, because of delays and overheads in the network. Therefore, in this research, we use long-term power for evaluating link-quality, and only consider long-term channel effects such as path loss and shadowing in the channel model. To maintain generality of the analysis, the channel model is based on a generic *log-distance path loss model* [23]. Application specific models such as Hata-Okumura or ITU models [74, 75, 76] are omitted in this research. This section first describes the channel model in a simple point-to-point link, then extends the model to the macrodiversity system with multiple users and multiple BSs. In the model, we assume that each user and BS has only one antenna.

3.3.1 Point-to-Point Links

Long-term channel effects include distance-based path loss and shadowing. Distance-based path loss is the effect of signal attenuation due to the distance separation between the transmit and the receive antennas. In free space, the signal attenuation can be described by the free space path loss model, where signal strength is inversely proportional to the square of distance [23]. In real life, radio propagation goes through obstructions such as buildings and foliage, hence attenuation tends to be greater than the free space path loss. We describe the rate of attenuation by the path loss exponent, γ, which is the rate of path loss over distance. In free space, $\gamma = 2$; in environments with obstructions, γ ranges between 3 and 6 [23].

Shadowing describes the effect of the average signal attenuation due to signal diffractions and reflection from large obstacles. The effect of shadow fading is described by Ψ. It is a random variable often modelled a log-normal distribution [23, 77].

For a simple system with only one transmit antenna and one receive antenna, the receive power P is

$$P = \overline{P}(d_0) \times \underline{d}^{-\gamma} \times \Psi. \tag{3.1}$$

Here, d_0 refers to a reference distance for which a reference measurement close to the transmitter is made. $\overline{P}(d_0)$ refers to the ensemble average of all possible received power measured at the reference distance d_0. $\underline{d}$ is the distance between the transmit and the receive antenna; it is a unit-less value where distance is a factor of the reference distance d_0. For the actual distance,

$$d = \underline{d} \times d_0. \tag{3.2}$$

Ψ is the shadowing fading factor,

$$\Psi = 10^{x_\sigma/10}, \tag{3.3}$$

where x_σ is a zero-mean Gaussian random variable with standard deviation, σ_{SF}.

3.3.2 Macrodiversity Links

For macrodiversity systems, there are multiple users transmitting, and multiple BSs receiving, hence multiple channel paths exist. Assume element-wise multiplication and exponentiation, the channel model in (3.1) becomes

$$\mathbf{P} = \overline{P}(d_0) \circ \underline{\mathbf{d}}^{-\gamma} \circ \mathbf{\Psi}. \tag{3.4}$$

$\circ$ is Hadamard product representing element-wise multiplication. $\mathbf{P}$, $\underline{\mathbf{d}}$, and $\mathbf{\Psi}$ are $N_{\text{BS}} \times N$ matrices. N_{BS} is the number of receiving BS antennas and N is the number of users in the system. The receive power matrix for the macrodiversity system is

$$\mathbf{P} = \begin{pmatrix} P_{1,1} & P_{1,2} & \cdots & P_{1,N} \\ P_{2,1} & P_{2,2} & \cdots & P_{2,N} \\ \vdots & \vdots & \ddots & \vdots \\ P_{N_{BS},1} & P_{N_{BS},2} & \cdots & P_{N_{BS},N} \end{pmatrix}. \tag{3.5}$$

Here, $P_{i,j}$ is the received power of individual paths, where i is the index of the BSs, and j is the index of the users. We also define *spatial dimension* of a channel matrix as the number of independent paths a user is being supported by the BSG. In this research, the spatial dimension is N_{BS}.

3.3.3 Power Scaling

Section 3.3.1 and Section 3.3.2, describe the effect of path loss and shadowing on the channel model, however, we have to define the appropriate level for $\overline{P}(d_0)$. Here, we simplify (3.4) to

$$\mathbf{P} = A \times \underline{\mathbf{d}}^{-\gamma} \times \mathbf{\Psi}, \tag{3.6}$$

and A is the power scaling factor which defines the relative transmit power of each user.

In the simulations, we expect all entries of the received power $\mathbf{P}$ to be such that:

> *Statistically, 95% of the users must have sufficient power to meet the target SER threshold, when they are considered independently in a traditional cellular system.*

In traditional cellular systems, *95%* is the typical connectivity requirement for commercial networks. By setting the power level so the connectivity requirement aligns with the traditional cellular systems, it allows us to compare results directly with the current system. In our model, we define the link quality requirement for the user connection by the target SER threshold.

We calculate A using the following steps:

1. Simulate 10,000 users around the BSG. Users are in a uniform distribution as defined in Figure 3.4a.
2. Find $\mathbf{P}$ using (3.6), assuming $A = 1$.
3. Each column represents the power received by all BSs from one user. For each column, find the strongest power. The row index i of this power is the BS which the user will be connecting to in traditional cellular systems (assume no interference).
4. Rank all users in terms of the power received by the connecting BS, from the lowest to the highest.
5. From the ranking, find the power of the 500^{th} user, $P_{500\text{th}}$. Statistically, this is the 5% user margin.
6. Find the minimum power requirement to achieve the SER threshold, P_{th}. Assuming traditional cellular system, where users have only single connection to the nearest BS.
7. Scale the power so the 500^{th} user meets the minimum power requirement. Hence, $A = P_{\text{th}} / P_{500\text{th}}$.

Table 3.1 shows a summary of key channel parameters and their values in the simulation. These are the baseline parameters used in the simulations, but different values are also considered.

Table 3.1: Summary of key channel parameters.

System Parameters	Symbol	Value
Path Loss Exponent	γ	3.5
Shadow Fading Factor	X_σ	8 dB
Power Scaling Factor	A	$200 \sim 300$

3.4 Analytical SER Prediction

The calculation of the analytical SER is considered a way of predicting future link quality when users are transmitting according to the resource schedule. As shown in Chapter 2, we can calculate the exact SER using long-term power with a relatively simple expression if the resource is allocated to a single user. If the resource is allocated to multiple users, only an approximate SER can be found, and the calculation is more complex. In the proposed SER calculation, user up-links can be classified into two types of scenarios: *No resource-sharing*, which refers to the resource being allocated to only a single user; and *with resource-sharing*,

which refers to the resource being allocated to multiple users. Although the focus of this research is on systems with resource-sharing, there are times where none of the available users are compatible. In this case, we still need a way to calculate SER. For this reason, when predicting SERs of users, the scheduler applies different calculation methods depending on the specific scenario. SER calculation for no resource-sharing scenarios allows us to estimate SER of the user with high accuracy in a relatively low computation time.

3.4.1 No Resource-Sharing

For scenarios with no resource-sharing, the exact long-term SER can be expressed as an integral of probability error functions in a quadratic form, which is reduced into a relatively simple algebraic expression involving the long-term powers. Equation (3.7) shows the algebraic expression of the exact SER for an arbitrary user, labelled user 1.

$$SER = \sum_{i=1}^{N_R} \frac{P_{i,1}}{2}^{(N_R-1)} \prod_{i\neq j}^{N_R} 2\left(P_{i,1} - P_{j,1}\right)^{-1} \left(\frac{3}{4} - \frac{1}{\sqrt{\frac{2\sigma^2}{P_{i,1}}+1}}\left(1 - \frac{1}{\pi}\arctan\left(\sqrt{\frac{2\sigma^2}{P_{i,1}}+1}\right)\right)\right), \tag{3.7}$$

where N_R, is the number of receiving BSs. $P_{i,1}$, is the long-term power of each up-link from the transmitting user to the i^{th} receiving BS, and σ^2 is the noise variance. In this research we consider noise has a normal distribution, which σ^2 is also the average noise power. A detailed derivation of the equation can be found in Appendix A.1.

3.4.2 With Resource-Sharing

For scenarios with resource-sharing, there is no simple analytical solution for calculating the exact SER. In [66, 67], the authors showed that the exact SER can be calculated if there are two users in the group ($N = 2$). However, this does not extend to the general multi-user case ($N \geq 2$), and the exact SER expression for the dual-user case requires numerical integration, which is not preferable in real-time, delay-sensitive operations. In [1], the authors showed that an approximate SER is available for the general multi-user case. For a macrodiversity system with M-PSK modulation and ZF detection, the approximate SER of the target user is

$$\text{SER} = \tilde{K}_0\, \tilde{\mathcal{I}}\, \bar{\gamma}^{-G_d}. \tag{3.8}$$

Here, $\tilde{K}_0$ is a constant depending only on the long-term powers, and it is given by

$$\tilde{K}_0 \simeq \frac{\text{Perm}(\mathbf{Q}_n)}{|\mathbf{P}_n|\text{Perm}({\mathbf{P}_n}^{-1}\mathbf{Q}_n)}. \tag{3.9}$$

$\mathbf{P}_n$ is the diagonal matrix of the power vector of the target user from the main power matrix, $\mathbf{P}$ from (3.6). $\mathbf{Q}_n$ is a matrix containing the column vectors of the other resource-sharing users. $\text{Perm}(.)$ is the *permanent* of a rectangular matrix as defined in [78].

For example, consider a macrodiversity system where

$$\mathbf{P} = \begin{pmatrix} P_{1,1} & P_{1,2} & \cdots & P_{1,N} \\ P_{2,1} & P_{2,2} & \cdots & P_{2,N} \\ \vdots & \vdots & \ddots & \vdots \\ P_{N_R,1} & P_{N_R,2} & \cdots & P_{N_R,N} \end{pmatrix}. \tag{3.10}$$

Consider a user group where users 1, 3, and 5 share the same resource, and user 1 is the target user of this calculation.

$$\mathbf{P}_n = \mathbf{P}_1 = \operatorname{diag}(\mathbf{P}(:,1)) = \begin{pmatrix} P_{1,1} & & & \\ & P_{2,1} & & \\ & & \ddots & \\ & & & P_{N_R,1} \end{pmatrix}, \tag{3.11}$$

and

$$\mathbf{Q}_n = \mathbf{Q}_1 = \begin{pmatrix} P_{1,3} & P_{1,5} \\ P_{2,3} & P_{2,5} \\ \vdots & \vdots \\ P_{N_R,3} & P_{N_R,5} \end{pmatrix}. \tag{3.12}$$

The remaining part of (3.8) is given by

$$\begin{aligned} \tilde{\mathcal{I}} &= \frac{1}{\pi \sin\left(\frac{\pi}{\mathrm{M}}\right)^{2G_d}} \int_0^{(M-1)\frac{\pi}{M}} \sin(\theta)^{2G_d}\, d\theta, \\ \bar{\gamma} &= \frac{1}{\sigma^2}, \\ G_d &= N_R - N + 1. \end{aligned} \tag{3.13}$$

A closed-form expression for $\tilde{\mathcal{I}}$ is available, using Equation (2.513.1) in [79].

$$\tilde{\mathcal{I}} = \frac{1}{\pi \sin\left(\frac{\pi}{\mathrm{M}}\right)^{2G_d}} \left(\frac{1}{2^{2G_d}} \binom{2G_d}{G_d} \theta + \frac{(-1)^{G_d}}{2^{2G_d-1}} \sum_{k=0}^{G_d-1} (-1)^k \binom{2G_d}{k} \frac{\sin\left((2G_d - 2k)\theta\right)}{2G_d - 2k} \right), \tag{3.14}$$

where $\theta = (M-1)\frac{\pi}{M}$. M us the moment of the MCS.

The calculation of the approximate SER involves the computation of the two permanents in (3.9). Computing the permanent is a #P-complete problem [80], which means that the computational complexity of calculating the approximate SER can be very high if the number of users and BSs in the BSG is large. The fastest known exact algorithm for computing the permanent is the Ryser Formula [81]. Using the Ryser Formula, the permanent of a matrix with dimension $n \times n$ can be computed with $\mathcal{O}(n^2 2^n)$ arithmetic operations. Hence, com-

puting SER for resource-sharing users can be a complex process if the number of cooperative BSs is large. Therefore, in this research, we are mostly interested in macrodiversity systems with a small number of cooperative BSs. This is realistic for many systems, but for distributed massive MIMO systems in the future, it may become too complex. In these cases, further work will be required. Note that although the permanent is computationally intensive for large systems, it is trivial for small systems with 2 to 5 BSs.

3.4.3 Accuracy of the SER Prediction

To evaluate the accuracy of the analytical SER predictions, we compare the SER results of both using the analytical methods and the Monte Carlo method. In this investigation, a power matrix, $\mathbf{P}$, is created according to Section 3.3; however, instead of using the power scaling method in Section 3.3.3, the channel power is then scaled to 1, where

$$\sum_{i=1}^{N_{\mathrm{R}}} P_{i,j} = 1. \tag{3.15}$$

By scaling the combined power of all users to unity, we can control the ratio between signal and noise, and observe how SER changes in relation to noise power. Here we define the SNR as $\bar{\gamma}$ in (3.13); it is a function of the average noise power, σ^2.

Figure 3.5 shows the results between the analytical calculations and the Monte Carlo simulations. In Figure 3.5a, a macrodiversity system with 3 cooperative BSs ($N_{\mathrm{BS}} = 3$) is serving 3 randomly located users in the vicinity ($N = 3$). The SER of each user is calculated by both the exact calculation (no resource-sharing) and the approximate calculation (with resource-sharing). In the Monte Carlo simulation, SER is obtained by repetitively sending symbols through independently generated transmission channels 10^6 times, and checking the probability of error occurrence. From Figure 3.5a, we can see a close resemblance between the exact SER and the simulated results.

Figure 3.5b shows the results of a macrodiversity system where $N = 4, N_{\mathrm{R}} = 6$. The results are obtained from [1], where in the legend, "Simulation" refers to the SER result obtained by using the Monte Carlo method, and "High SNR approx." refers to the SER result obtained by using the approximation method. From the figure, the approximate SER deviates from the simulated result in low SNR condition. In low SNR condition, the approximate SER is worse than the simulated SER. This indicates that the actual SER is likely to be lower than the predicted SER, which is preferable when making resource allocation decisions.

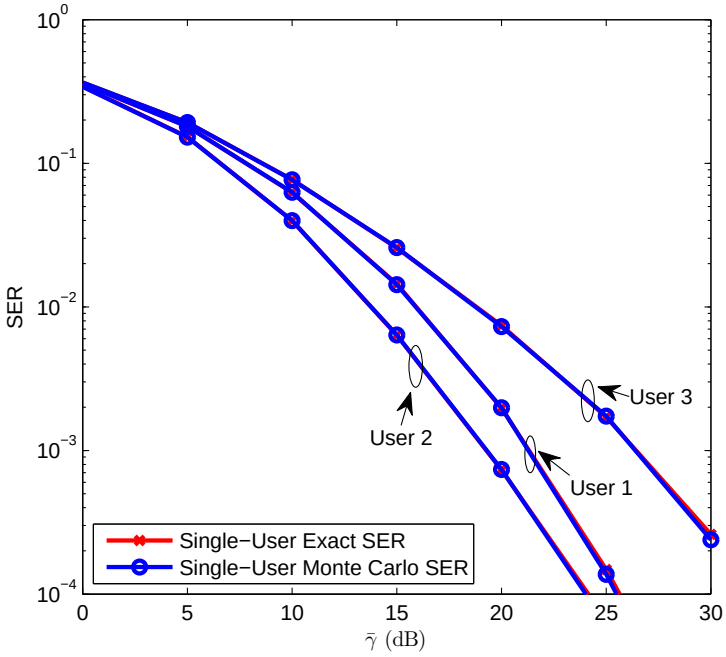

(a)

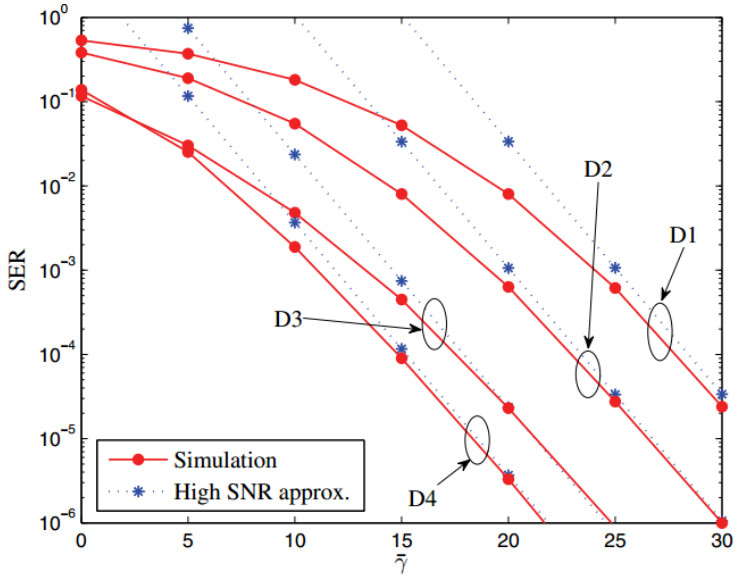

(b)

Figure 3.5: Comparison between analytical SER results and Monte Carlo simulations, in a macrodiversity system assuming QPSK modulation and ZF detection. The SNR, $\bar{\gamma}$ is in dB. (a) No Resource-Sharing: each user is assigned with an independent resource. (b) With Resource-Sharing: all three users share the same resource.

Figure 3.6 shows the process flowchart for calculating the long-term SER. The resource sharing decision is made based on the SER prediction result. The scheduler allows resource-sharing if all users in the user group pass the SER threshold.

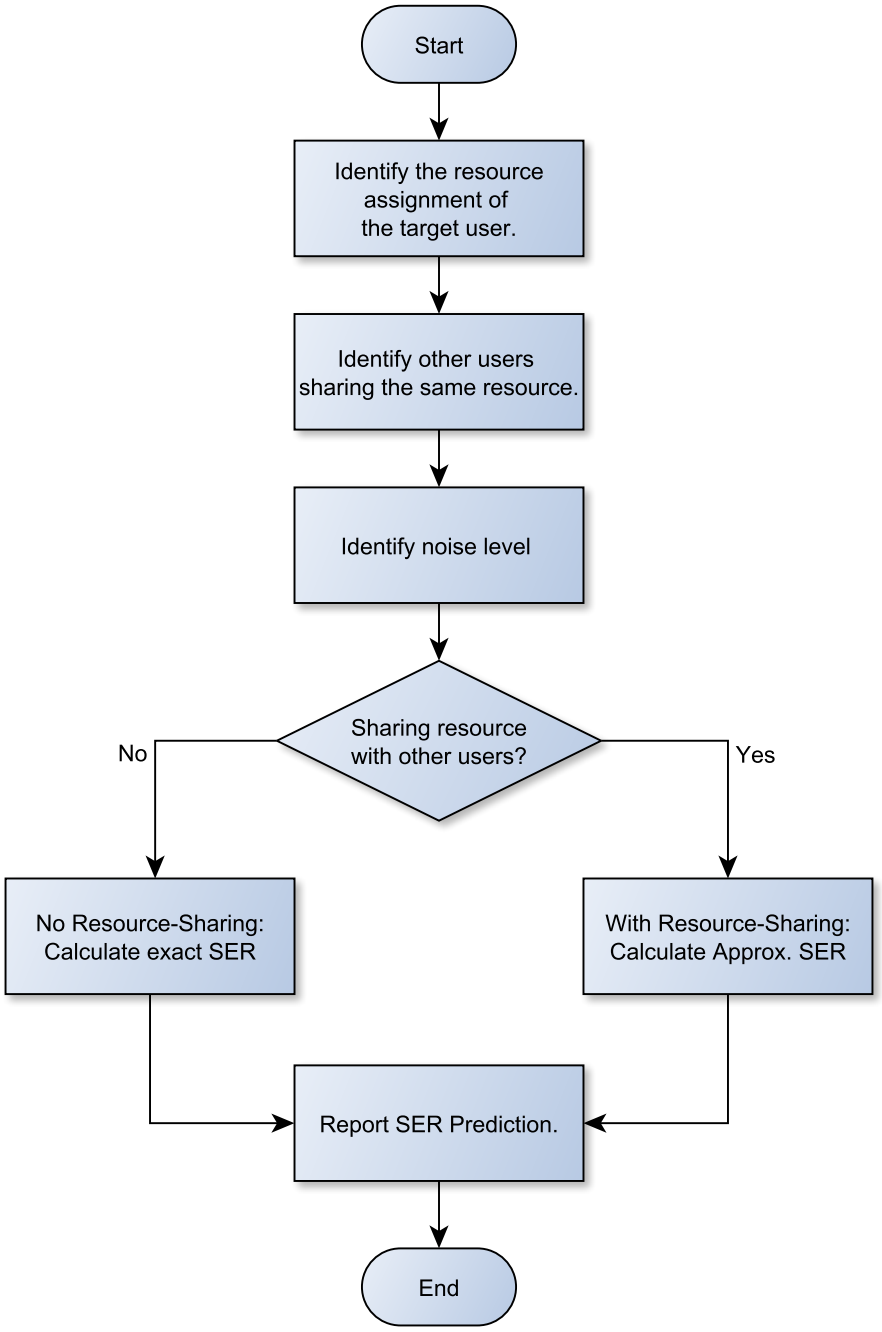

Figure 3.6: SER calculation flowchart.

3.5 Performance Evaluation

As explained in Chapter 2, we can increase the user capacity of a single BSG by the number of co-operating BSs N_{BS} if we allow resource-sharing between users. However, this does not translate to the actual increase in user services unless we can identify compatible users in an effective manner. This problem of user selection is a part of the resource allocation problem. In this thesis, we have developed multiple user selection algorithms, and we want to evaluate the effectiveness of the algorithms by how much can they utilise the increased user capacity with resource-sharing, and at what cost in terms of complexity of the algorithm.

We measure the effectiveness of the capacity utilisation by *utilisation*, which is defined as

> *The percentage of users being allocated with a resource, over the system user capacity.*

Mathematically, this can be described as

$$\text{Utilisation} = \frac{N_{\text{alloc}}}{N_{\text{max}}} \ (\%). \tag{3.16}$$

Here, N_{alloc} is the number of the allocated users. Allocated users refer to the users that has been allocated with resources. N_{max} is the system user capacity, which theoretically, is the maximum number of users that could be allocated with a resource at the same time. With resource-sharing, N_{max} is

$$N_{\text{max}} = N_{\text{BS}} \times N_{\text{RB}}, \tag{3.17}$$

where N_{BS} is the number of BSs, and N_{RB} is the number of resources in the system.

We consider the number of users in the system as N. In real systems, we have no control over N. A system is considered *lightly-loaded* if N is much less than N_{max}. A system is considered *heavily-loaded* if N is close or equal to N_{max}. A system is considered *over-loaded* if N is greater than N_{max}. To keep the argument simple, we consider only cases where $N \leq N_{\text{max}}$; for over-loaded scenarios, where N is greater than N_{max}, we assume that the scheduler disregards the extra users.

From a users perspective, the user is more interested in the probability of being granted with a resource when a request for service is sent. For this reason, we define *allocation rate* is defined as

> *The percentage of users being allocated with a resource, over the number of users in the system.*

Mathematically, this can be described as

$$\text{Allocation Rate} = \frac{N_{\text{alloc}}}{N} \ (\%). \tag{3.18}$$

In general, we expect the allocation rate close to 100% in a lightly loaded system, and less than 100% in a heavily loaded system. This is because in a lightly loaded system, users can be separated into small user groups. In a smaller user group, the number of users is less than the spatial dimension of the channel matrix, and hence it is easier for the receiver to separate out the signals. When a system is heavily loaded, i.e. number of users near the maximum capacity, it is more difficult to separate the users into different user groups. Because with the number of users close to the spatial dimension of the channel matrix, it is more difficult for the receiver to separate out the signals.

Theoretically, if the user selection algorithm is able to identify user groups such that all users are allocated with a resource, then utilisation is maximised for the N number of users in the system. Thus, we define *maximum utilisation (max. utilisation)* as

> *The percentage of users being allocated with a resource, over the system user capacity. If the allocation rate is 100%.*

Mathematically, this can be described as

$$\text{Maximum Utilisation} = \frac{N}{N_{\max}} \ (\%). \tag{3.19}$$

Figure 3.7 below shows a difference between macrodiversity systems with resource-sharing and without resource-sharing. With resource-sharing, the maximum number of user allocation becomes a fluid concept, which depends on the availability of compatible users for resource-sharing.

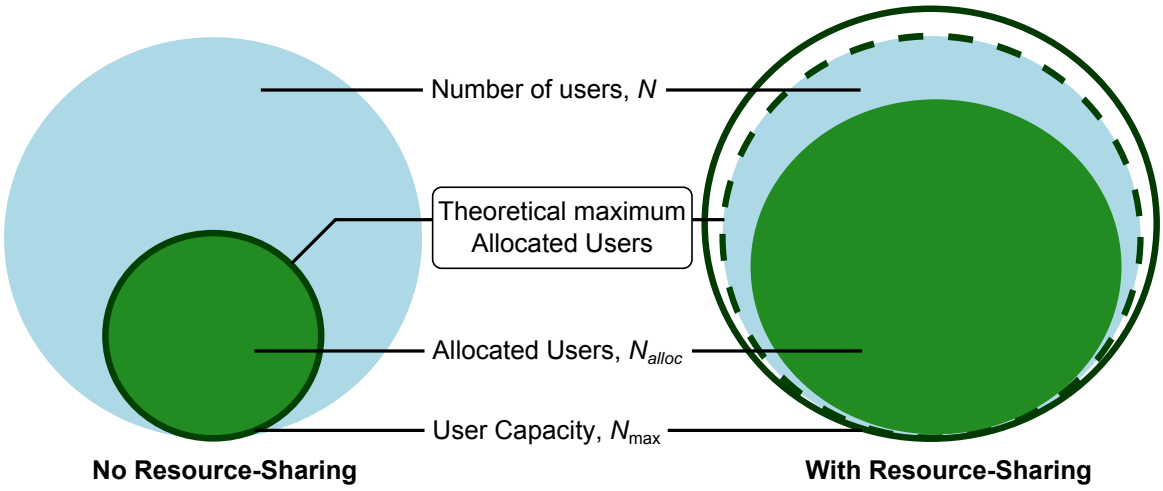

Figure 3.7: A comparison of user capacity for macrodiversity systems with resource-sharing and without resource-sharing.

The full complexity of a resource allocation method includes both the complexity of the UCC and the complexity of the user selection algorithm. In Chapter 2, we have shown

that we can reduce the network overhead of resource allocation by using long-term power. In Section 3.4, we have also shown that we can estimate SER by using analytical calculation, which is effective for the purpose of evaluating link quality. Under this premise, we established that the analytical SER is an efficient way of measuring user compatibility, in terms of low network overhead, and low complexity compared to simulating SER using the Monte Carlo method. We define UCC such that all resource-sharing users must meet the SER threshold. Because the SER calculation is the basis of UCC, and it is used in all the user selection algorithms, for the simulation we define *complexity* as

> *The number of SER calculations (N_{SER}) required for the user selection algorithm to find a solution.*

Both utilisation and complexity depend on the power profile of users in the system, and it varies according to the user distribution and the channel fading effects. To obtain statistically meaningful performance results, we create multiple samples with users located in different places according to the distribution model, and generate the channel power according to the user distribution. The utilisation and the complexity are the averaged results of different samples.

The specific steps of performance evaluation are:

1. Identify the system parameters: the network layout, propagation parameters, N_{BS}, N_{RB}, and N.
2. Generate randomly distributed users around the BSG, according to the user distribution model.
3. Based on the user location and the propagation parameters, generate the power matrix of the system.
4. Allocate resource to users according to the user selection algorithm.
5. Record the utilisation and complexity results of this particular sample scenario.
6. Repeat the process 100 times, and find the mean utilisation and the mean complexity results.

3.6 Summary

The system model developed in this chapter provides a platform which allows us to demonstrate the argument and gain insights on how to realise the user capacity potential with minimum complexity. In this chapter, we have defined the network layout, the user distribution, and the channel model of a macrodiversity system. We have also decided on using long-term SER to predict the link quality of users with dedicated resource and shared resource, and shown that although the analytical SER prediction is not accurate in low SNR

conditions, it is consistently lower than the results from the Monte Carlo method. This suggests that the analytical SER prediction is a conservative link quality indicator. The actual long-term SER is always going to be better than the estimated result. Under this premise, we argued that the analytical SER is a sufficient measure of the link quality, and proposed that the performance of user selection in multi-user resource allocation can be evaluated by the percentage of users meeting the target SER threshold, based on the analytical SER prediction.

Another benefit of the analytical SER prediction is that it is much quicker to calculate than the Monte Carlo method. In our simulation, the system performance is a statistical average of multiple randomly generated samples. Calculating the SER using the Monte Carlo method is a computation-intensive task. It is even more challenging, as performance evaluation requires calculating SER of all users in all sample scenarios. For example, to observe SER with accuracy down to SER $= 10^{-6}$, we need to simulate the transmission for significantly more than 10^6 times. If we extend this to 100 different sample scenarios, each scenario has 10 users, we would need to simulate the users transmissions for at least 10^9 times. For the same situation, using the analytical method, we only need to calculate SER 10^3 times. Thus, the analytical SER calculation enables us to evaluate the system performance in a much shorter time-frame.

Overall, this chapter outlines the platform for evaluating resource allocation performance in macrodiversity systems.

Chapter 4

Resource Allocation Algorithms

A good resource allocation scheme should maximise the utilisation of a macrodiversity system. In systems with resource-sharing, resource allocation consists of two functional parts: user selection, and compatibility evaluation of the resource-sharing users (i.e. UCC). A good scheduler not only consistently makes good resource allocation decisions, it also does this quickly so that the schedule remains relevant to the transmission environment at the time. In Chapter 2, we investigated the state of the art of the scheduler in terms of the user selection and the compatibility evaluation methods for macrodiversity systems. In this research, we focus on making resource allocation decisions using long-term power. This chapter shows our own implementation of user selection algorithms and UCC. It explains the design principle behind the algorithms, and the mechanism of their operations.

4.1 User Selection

In resource allocation schemes with no resource-sharing, resources are generally allocated to the highest priority users. User priority can be defined by many different criteria: it can be by the nature of the content (e.g. voice v.s. data), by the queuing order (e.g. first-in-first-served), by the link quality (e.g. SNR) of the users, or by the identity or type of users (e.g. public safety v.s. general users). The study of how to prioritise users for the limited resources is commonly known as *user scheduling*, and it has been covered in Chapter 2. In resource allocation schemes with resource-sharing, user capacity increases because the same resource can be allocated to multiple users. In this mode, the scheduler has an additional objective: to maximise the number of resource-sharing users in the system. For the user selection algorithms, the goal is finding compatible users for resource-sharing in an effective and low complexity manner. To simplify the argument, in this research we have made the following assumptions:

- *User numbering is the user priority order.*
  We consider resource allocation and user scheduling as two separate topics. Because

our focus is on the capacity utilisation of radio resources with resource-sharing, we assume the user priority is defined elsewhere (e.g. a higher layer loop), and provided to the scheduler as an input. There in the simulation, we assume that the numbering of the users is the priority order of the users. User priority is in descending order: for example, user 1 has the highest priority, user 2 has the second-highest priority, and so on.

- *All primary users should be served.*
  Resource-sharing should improve the overall utilisation of the system user capacity without jeopardizing the primary user services. As defined in Chapter 2, the primary users are the higher priority users. Therefore, all the algorithms discussed in this chapter ensure that the primary users are first served with the available resources. This condition also reduces the number of user combinations in user selection. Ensuring the primary user service is especially important in public safety networks for example. This way we can ensure the priority users have guaranteed services[1].

- *All users in the user group should meet the link quality requirement.*
  If the allocated user does not meet the link quality requirement, it may as well be considered as an invalid link. Allocating a resource to users who do not meet the link quality requirement is a waste of resource. The same resource could be allocated to other users who meet the requirement, or if the resource is shared by fewer users, they could enjoy a better overall link quality. For this reason, in the resource allocation algorithm, only users who meet the link quality requirement are allocated a resource. In this research, we estimate link quality by the predicted SER as defined in Chapter 3.

In Chapter 2, we showed that the greedy algorithm has the least user selection complexity - hence, we developed our own user selection algorithms based on a modified greedy algorithm. In this chapter, we propose four different heuristic user selection algorithms and the exhaustive search (ES) algorithm. This chapter explains the operation of each user selection algorithm, as well as the formation of user groups, and the mechanism of rejecting bad allocations. A macrodiversity system with 3 BSs, 15 users, and 5 resources is used as an example for explaining the algorithms. When describing figures and equations, users are referred to as UEs (user equipment), and resources are referred to as RBs (resource blocks), to keep the notation simple and less cluttered.

4.1.1 Priority Order (PO)

This is the most basic algorithm proposed in the study. It groups users based on their numbering. The steps of the algorithm can be explained as follows:

Selection Steps:

[1] In this thesis, we scale the power level so that 95% of users meet the SER threshold as if in the single-cell system. With macrodiversity, we should expect the SER to be even lower.

1. Allocate available resources to all the primary users, i.e. the first N_{RB} users with the highest priority (Figure 4.1).

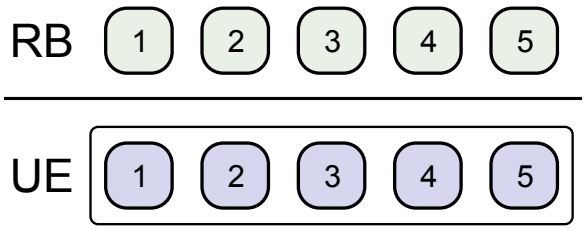

Figure 4.1: Allocate resources to all the primary users. The primary users are framed inside a rounded box to distinguish the difference between the primary users and the secondary users. In this example, the primary users are user 1 to user 5.

2. Fill up the remaining slots with secondary users according to the priority order.

   In Figure 4.2, there are 3 BSs, so the maximum number of users which a resource can be shared to is 3. As shown in the figure, RB1 is allocated to UE1, UE6, and UE11, RB2 is allocated to UE2, UE7, and UE12, and so on. We call the group that shares RB1 user group 1, the group that shares RB2 user group 2, and so on.

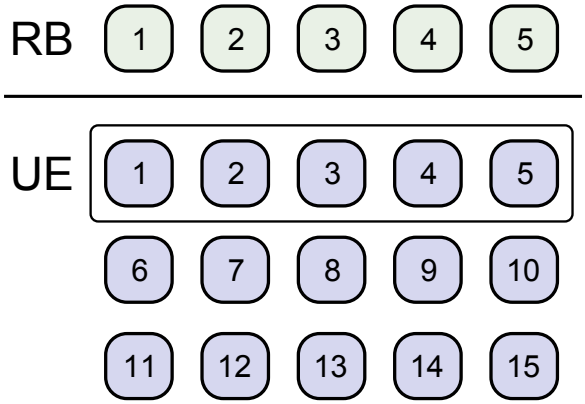

Figure 4.2: Fill up the remaining slots with secondary users. In this example, the secondary users are user 6 to user 15.

3. Check the predicted SER of all users in the system.

4. For each user group:

   - If all users meet the SER threshold, do nothing.
   - If the primary user fails to meet the SER threshold, remove all secondary users who share the same resource.
   - If secondary users fail the to meet the SER threshold, remove the failed user(s) from the resource schedule.

   Figure 4.3 shows an example of user removal in this algorithm. In this example, all users in user group 1 meet the SER threshold, and no users are removed from the

resource schedule. In user groups 2 and 3, because the primary users fail to meet the SER threshold, all secondary users in the respective user groups are removed. In user groups 4 and 5, only the secondary users that fail to meet the SER threshold are removed.

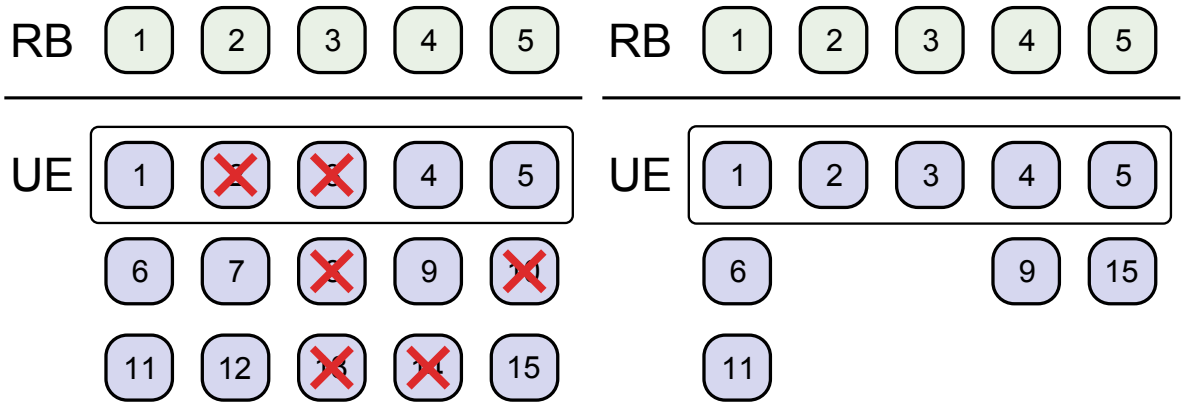

Figure 4.3: (a) Resource schedule indicating some users fail to meet the SER threshold. (b) Resource schedule after selective removal of users.

Here, the SER of all users needs only be checked once, making the complexity of the algorithm very low. However, due to the aggressive user removal strategy, we also expect the utilisation of this algorithm to be low, especially when the same resource is shared by many users. Figure 4.4 shows the flowchart of the PO algorithm:

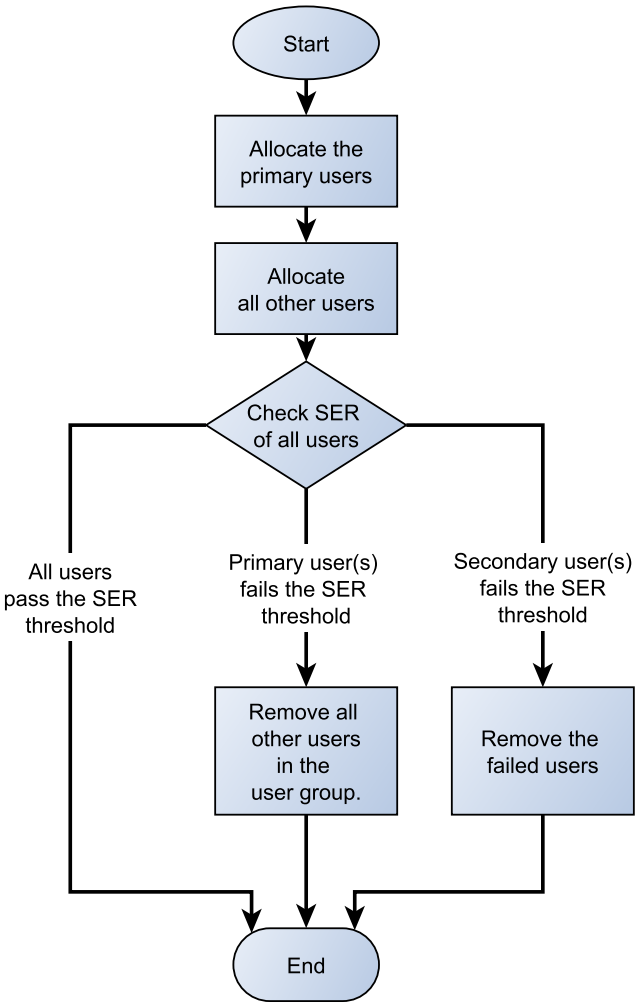

Figure 4.4: Flow-chart for the PO algorithm.

4.1.2 Priority Order + Sequential Removal (PO+SR)

This algorithm is essentially the same as the PO algorithm, except that after the pre-allocation, it removes the users one by one. Each time it removes one user, it checks the SER of the remaining users in the user group. If all remaining users meet the SER threshold, it stops removing users from the group.

Selection Steps:

1. Allocate the available resources to all the primary users.
2. Fill up the remaining slots with secondary users according to the priority order.
3. Calculate the predicted SER of all users in the system.
4. For each user group:

- If all users meet the SER threshold, do nothing.
- If the primary user fails to meet the SER threshold, remove the secondary user with the lowest priority. Calculate SER of the user group again.
- If only secondary users fail the to meet the SER threshold, remove the failed user with the lowest priority. Calculate SER of the user group again.

5. Repeat Step 4 until all users pass the SER threshold.

Figure 4.5 shows the flowchart of the PO+SR algorithm:

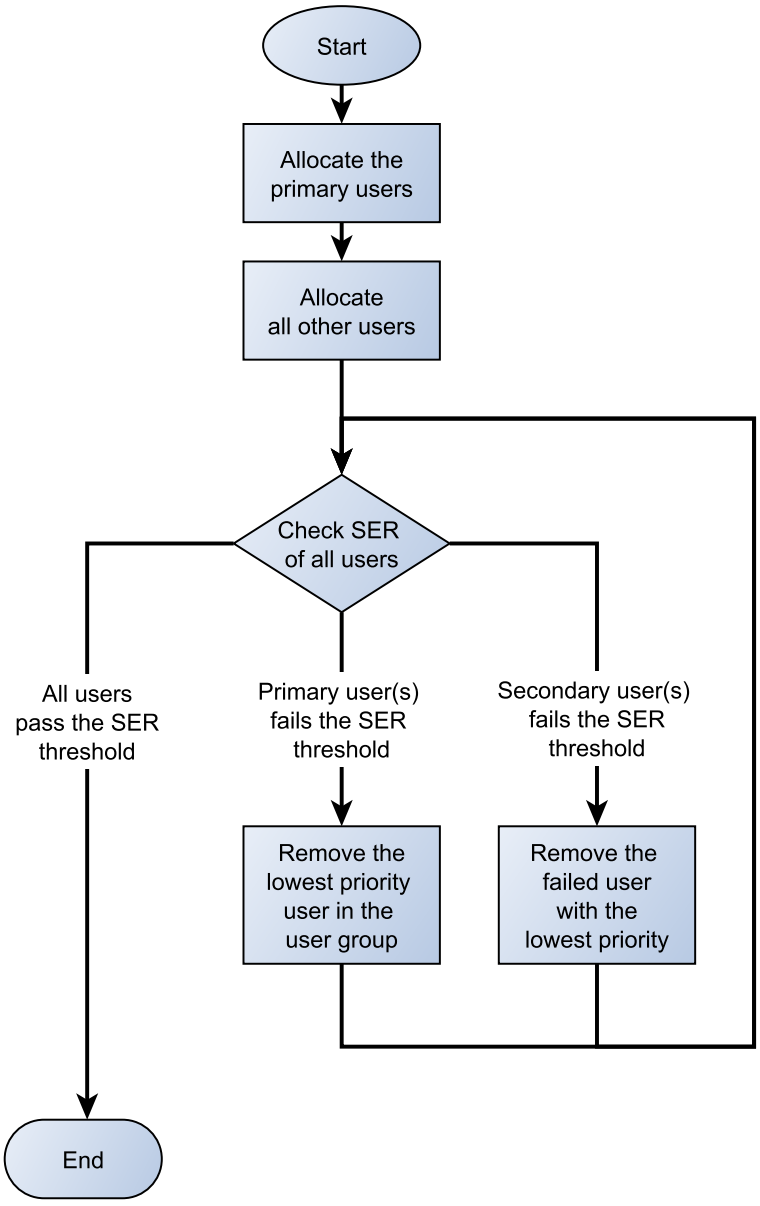

Figure 4.5: Flow-chart for the PO+SR algorithm.

4.1.3 First-Fit (FF)

This algorithm utilises user capacity by sequentially adding secondary users into each user group. Each time an additional user is added to the group, the scheduler checks the SER of all users in the group. The compatibility requirement is that all users in the user group must meet the SER threshold. The first additional user that meets the compatibility requirement is kept for the resource schedule.

Selection Steps:

1. Allocate available resources to all the primary users.
2. Check if there is any available free resource slots (each row must be filled first before progressing onto the next row).
3. If there is an available free slot, try adding one user to the next available free slot in the user group.
4. An UCC is performed on the user group every time a new user is added.
5. Accept the first combination where all users meet the SER threshold .
6. Repeat Step 2 through Step 5 until no more users can be added to the resource slots (or no more suitable slots available).

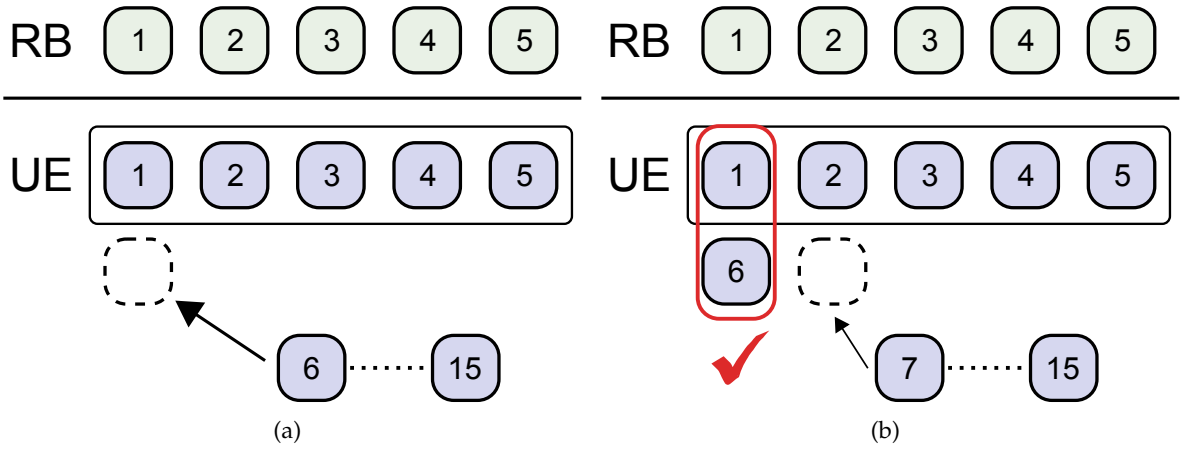

Figure 4.6: (a) Adding users to the resource group.
(b) Check user compatibility and accept the first user that passes the UCC.

As an example, suppose we are to find the first compatible user to share the resource with UE1 in the user group 1. We pair UE1 with all the remaining users from UE6 to UE15, and check the user compatibility of the pairs one by one: UE1-UE6, UE1-UE7..., and so on.

We accept the first user combination that passes the UCC, and we do not further check the compatibility of the remaining users. If the first compatible pair is UE1-UE7, we do not check UE8 to UE15.

This algorithm makes sure that the new user does not jeopardise the link quality of the allocated users. However, this is not optimal as it accepts only the first combination that passes the compatibility requirement, which may reduce the possibility of a better user combination that is behind the queue. Figure 4.7 shows the flowchart of the algorithm:

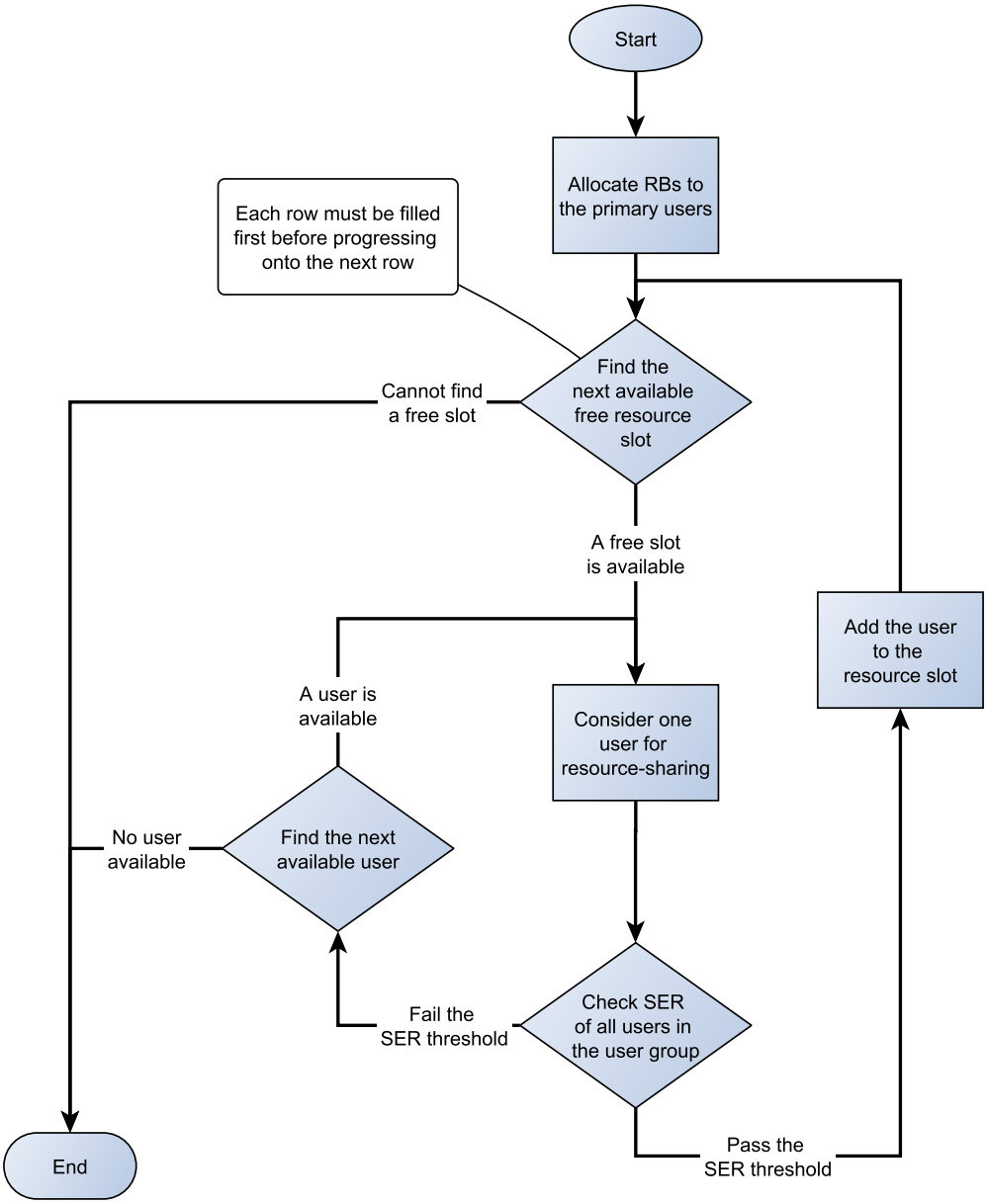

Figure 4.7: Flow-chart for the FF algorithm.

4.1.4 Best-Fit (BF)

The Best-Fit (BF) algorithm is virtually the same as the FF algorithm, except that it checks through all the user selection combinations within each user group and choose the combination where the users in the user group has the best overall performance. In terms of the complexity, for BF, it is a fixed number, whereas for FF it is a soft bound. Thus most of the time, BF has a higher complexity than FF. In scenarios where no compatible user can be found, FF would have the same complexity as BF.

Selection Steps:

1. Allocate available resources to all the primary users.
2. Check if there is any available free resource slots (each row must be filled first before progressing onto the next row).
3. If there is an available free slot, try adding one user to the next available free slot in the user group.
4. An UCC is performed on the user group every time a new user is added.
5. Accept the best user combination is such that the worst performing user in the user group has lowest SER, compared to other user combinations.
6. Repeat Step 2 through Step 5 until no more users can be added to the resource slots (or no more suitable slots available).

As an example, suppose we are to find the most compatible user to share the resource with UE1 in user group 1. We group UE1 with all the remaining users from UE6 to UE15: UE1-UE6, UE1-UE7..., and so on; we then check the user compatibility of all combinations by checking the SER of all users in the user group. Table 4.1 shows the predicted SER results of the user pairs. Consider an SER threshold of 0.01, only user pairs with UE6, UE7, UE8, UE9, UE11, and UE12 meet the SER threshold. The worst performing UE of these pairs are UE1: 0.01 (UE1-UE6); UE7: 0.009 (UE1-UE7); UE1: 0.006 (UE1-UE8); UE1: 0.0008 (UE1-UE9); UE11: 0.006 (UE1-UE11); and UE1: 0.007 (UE1-UE12). We see that UE1-UE9 has the lowest SER out of these choices, so in this algorithm we consider UE1-UE9 the best-fit solution.

Table 4.1: SERs of users pairing with UE1 - an example.

SER	**UE6**	**UE7**	**UE8**	**UE9**	**UE10**	**UE11**	**UE12**	**UE13**	**UE14**	**UE15**
UE1	0.01	0.005	0.006	0.0008	0.05	0.0002	0.007	0.0001	0.008	0.0009
Additional UE	0.003	0.009	0.001	0.0005	0.1	0.006	0.004	0.03	0.6	1

This algorithms tries to select user that will produce the best overall link quality for the user group. The "best-fit" here refers to the overall link quality. It does not mean the best utilisation. Utilisation is not optimal as once the "best-user" is removed from the pool of unallocated users, we cannot consider the combinations where with the users that has already been selected. Figure 4.8 shows the flowchart of the BF algorithm:

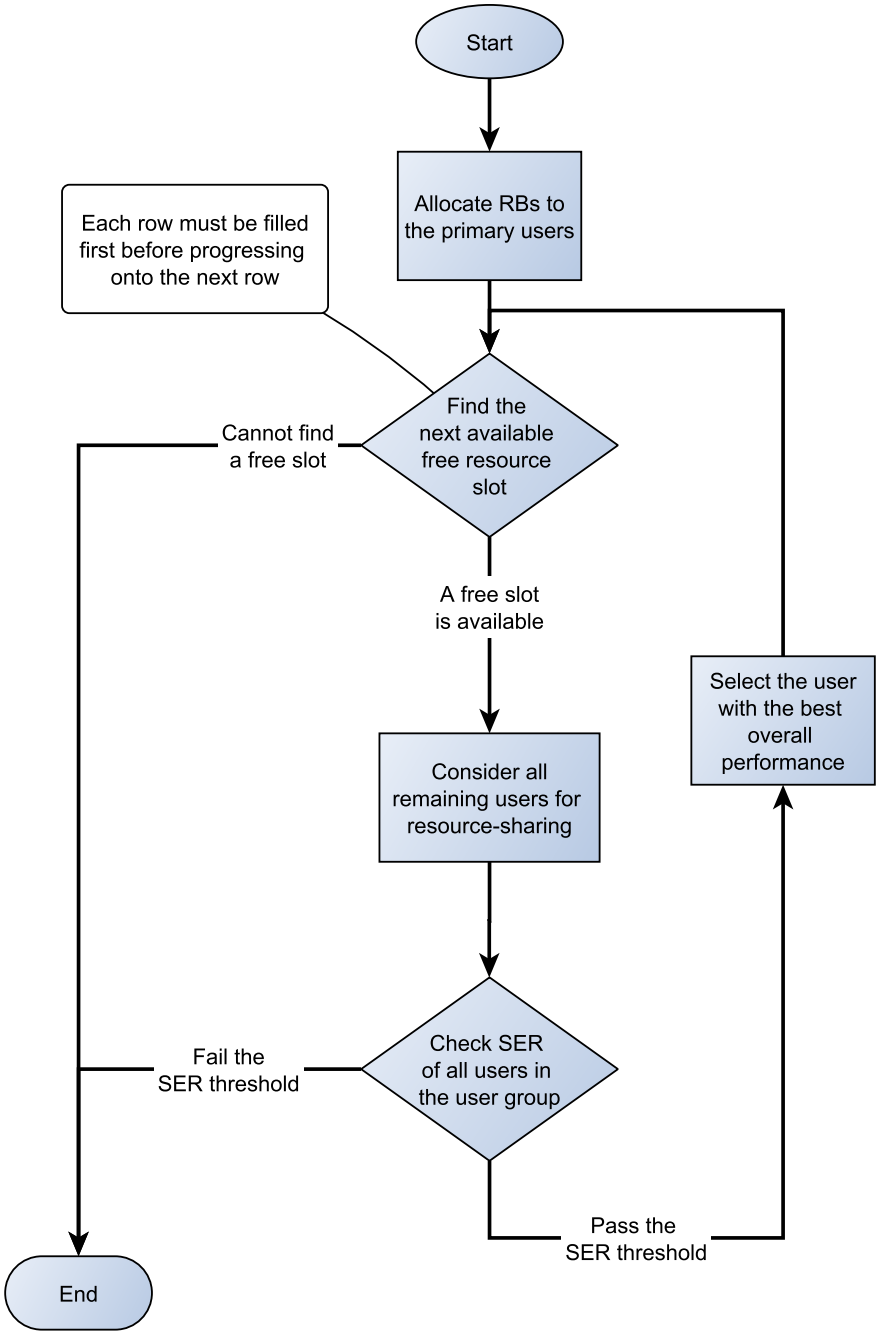

Figure 4.8: Flow-chart for the BF algorithm.

4.1.5 Exhaustive Search (ES)

This algorithm finds out all possible combinations for the resource schedule under the given assumptions listed at the beginning of this section. It checks the SER of all users across all combinations, and keeps the one that has the best utilisation result.

Selection Steps:

1. Allocate available resources to all the primary users.
2. Find out all possible user combinations for the resource schedule.
3. For each combination, An UCC is performed on all user groups in the combination. The combination is rejected if any user fails to meet the UCC.
4. If the combination passes the UCC, then the it is recorded as a candidate resource schedule, and the scheduler moves on to the next combination (Figure 4.9).
5. Repeat Step 3 and Step 4 until all combinations have been tried. During the repetition phase, if utilisation of the new combination is better the previous combination, then the new combination replaces the old one for the candidate resource schedule.
6. Use the resource schedule that has the highest utilisation result.

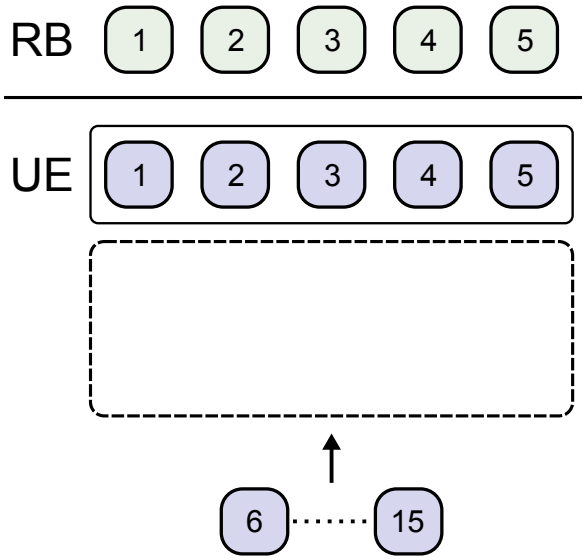

Figure 4.9: For 3 BSs and 5 RBs, there are 10 available resource slots, and the resources need to be shared with the primary users, so the order of filling these slots is important. The ES algorithm tries all combinations of user selections and choose the one that gives the best utilisation result.

With ES, it finds the resource schedule that has the maximum maximum utilisation. However, it can become very time consuming for large system dimensions. As shown in Figure 2.7, in a small system with 3 BSs, 5 RBs, and 15 UEs, the complexity of user selection

is in the order of 10^{10} combinations. The algorithm is not suitable for practical implementations, but is useful for benchmarking other heuristic solutions. Figure 4.10 shows the flowchart of the ES algorithm:

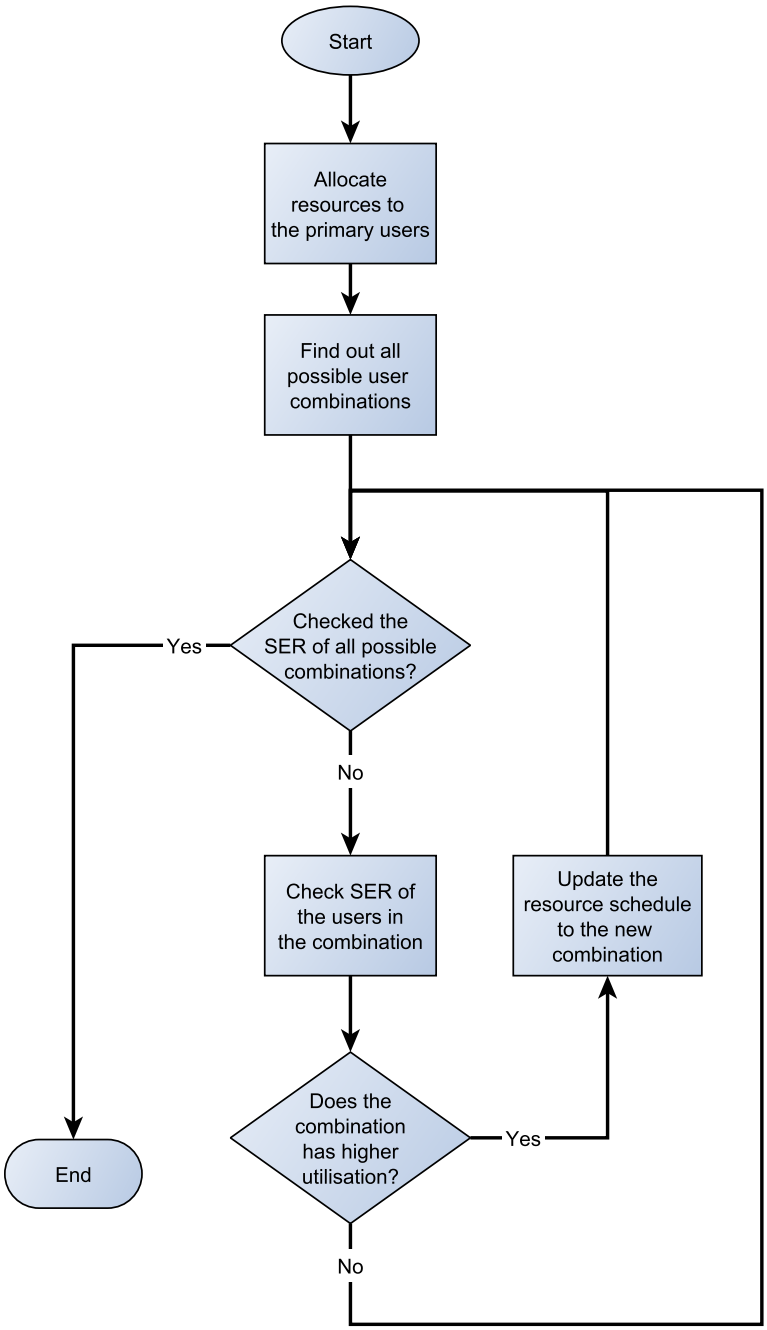

Figure 4.10: Flow-chart for the ES algorithm.

4.2 User Partitions

One premise in user selection is that the more users and resources are available in the selection pool, the higher the likelihood will be of finding compatible users for resource-sharing. However, with a larger system dimension, this also means the complexity of user selection is higher. The improvement in utilisation may not justify the complexity involved in finding the solution. This leads to the question of how many users and resources we really need, in order to achieve good utilisation.

One approach to further reduce computational complexity is to limit the size of the user selection pool through assigning users and resources into smaller partitions and executing user selection algorithms within individual partitions. Figure 4.11 shows how user partitions could be applied in user selection. The example in the figure has 25 resources[2]. Consider there are 3 BSs, with resource-sharing, the user capacity of the system is 75. Consider a case with 75 users in the system, the primary users are still being served first before adding the secondary users. With user partitions, we can consider them as 5 independent partitions, each one has 5 resources and 15 users. The number of combinations is smaller in smaller systems; it is also possible to process the partitions in parallel, further reducing the processing time.

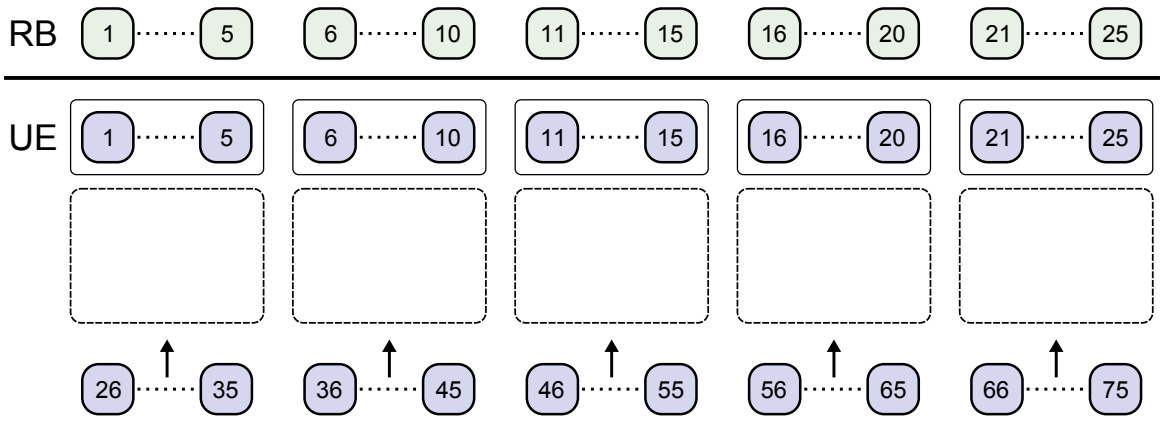

Figure 4.11: An example of user partitions. $N_{\text{BS}} = 3$ and $N_{\text{RB}} = 25$.

4.2.1 Power Ranking:

In Figure 4.11, users are partitioned according to their numbers. In this work, we assume the power profiles of users in each partition are independent. We may be able to further improve the success rate of user selection in each partition if we can apply some intelligence in the way users are assigned into different partitions. The method of intelligent user partitioning should be very simple, otherwise it defies the purpose of complexity reduction. One way is by looking at the power profile between users. Figure 4.12 shows

[2]25 is a common value for the number of available resources in a typical LTE system.

three common scenarios for user power profile, and how the power profile may affect the link quality of other resource-sharing users.

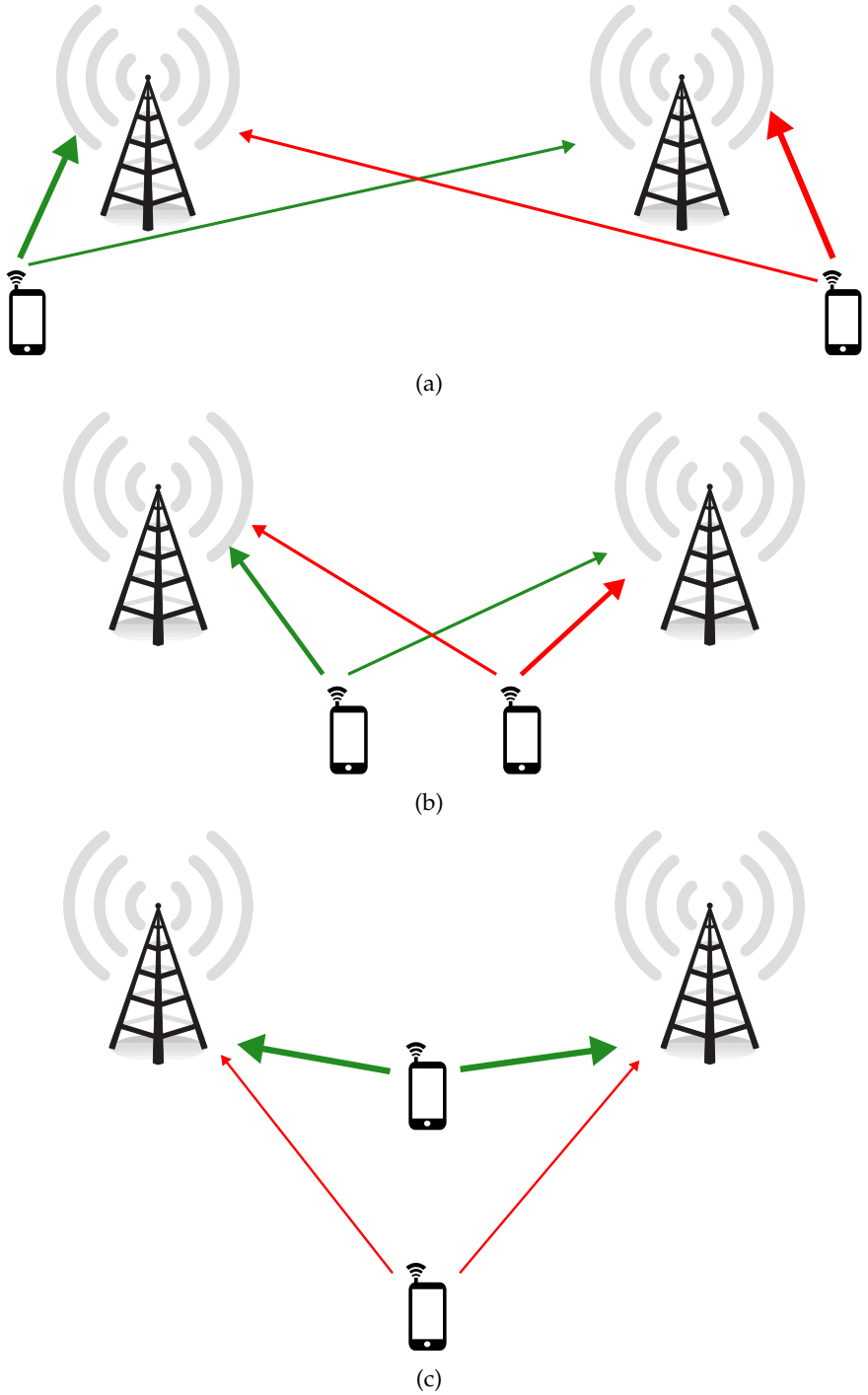

Figure 4.12: Distance-based link power of two users at different locations in reference to two BSs (a) Users close to one local BS but far away from each other, with similar total link power. (b) Users between two BSs, with similar total link power. (c) Users between two BSs, with different total link power.

A macrodiversity system is more likely to separate out signals from different users if they have orthogonal or semi-orthogonal channel characteristics. In Figure 4.12, scenario (a) has the highest likelihood of successful resource-sharing. Scenario (b) may or may not be suitable for resource-sharing depending on the degree of correlation between the user channels. In scenario (c), users have similar power profile but one has a much stronger overall power than the other. In this case, the user with stronger overall power tends to dominate the communication channel, resulting in poor link quality for the user with weaker overall power.

In this work, we proposed that by ranking users according to their combined channel power and assigning users with similar power rankings into the same partition, we could minimise the possibility of poor link performance due to one user dominating the other user channel(s). The steps for power ranking are the following:

1. Rank primary users in terms of the total channel power received by the BSs. Group them in respective partitions according to their power, and allocate one resource to each primary user.
2. Rank secondary users in the same manner. Divide the total number of secondary users with the total number of partitions, so each partition has similar share of secondary users. Assign them into respective partitions according to their powers.
3. Find compatible resource groups in each partition as per user selection process.

Figure 4.13 shows how a user partitioning system with power ranking is different from user partitioning with no power ranking. In the figure, users with stronger combined power are in the darker shades of red. Users with similar power levels are grouped into the same partition. Note that each partition needs at least 2 resources to provide user selection.

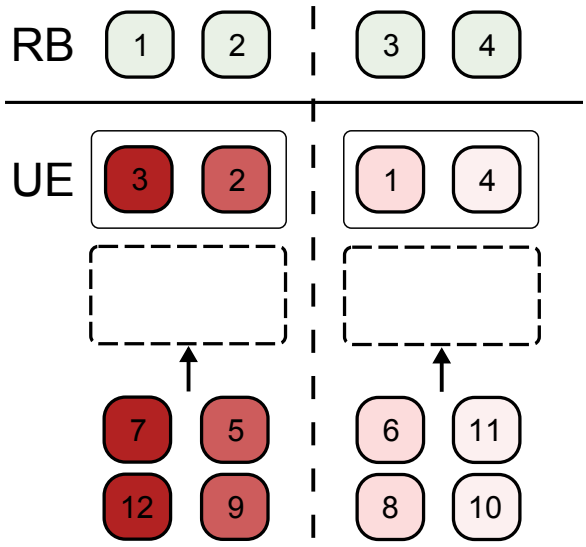

Figure 4.13: An example of user partition with power ranking.

4.3 User Compatibility Check (UCC)

A UCC is a crucial part of resource allocation. Every time there is a change in the resource schedule, the modified user group need to be checked by the UCC: The goal of UCC is ensuring the link quality of all resource-sharing users meets the link quality requirement. In Chapter 2, we have explained the function of the UCC, and in this research we decided to measure the link quality by the SER of resource-sharing users, uses long-term power, and we define the compatibility criteria such that all resource-sharing users must pass a pre-defined SER threshold. The specific steps of the UCC are defined as the following:

1. Identify the target user of interest, and the corresponding user group.
2. Identify other users in the group, sharing the same resource.
3. Calculate the SERs of all users in the user group.
4. If the SER of all users meets the SER threshold, the user group passes the UCC; If one or more users fail to meet the SER threshold, then the user group does not pass the UCC.

Figure 4.14 shows the flowchart of the UCC:

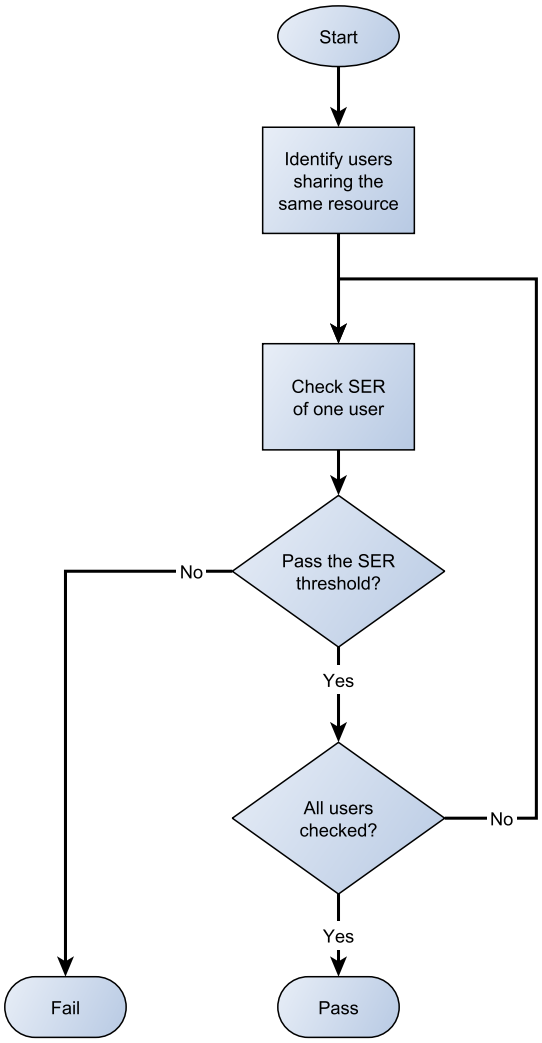

Figure 4.14: Flow-chart for the UCC.

4.3.1 Alternative Metrics for UCC

The analytical SER calculation provides a relatively simple metric for measuring link quality. However, in the user selection stage, the scheduler needs to consider multiple user combinations, The accumulative effect of calculating the SER of multiple users adds up the total processing complexity. In this research, we have also considered alternative metrics to replace the SER calculation in the UCC. The motivation is to find a metric that can be used for UCC, but with lower complexity.

In our investigation, we could not find any meaningful correlation between the proposed alternative metrics and the analytical SER calculation, therefore, none of the metrics are used in the simulation. For this reason, the results are not included in the main body of research. They can be found in Appendix B instead.

4.4 Summary

In this chapter we explained the operations of the different user selection algorithms, and we proposed a user partitioning method which could further reduce the complexity of user selection. The partitioning of users can be ranked by their channel power, which may increase the likelihood of successful user allocation. We also explained the operation of the UCC. In the next chapter, we evaluate the performance of the proposed user selection algorithms.

Chapter 5

Simulation Results

In general, the effectiveness of resource allocation depends on the performance of both the user selection algorithm and the user compatibility check (UCC). In the earlier chapters, we have explained the benefits of making scheduling decisions using long-term power, and shown that the proposed UCC is an effective metric for evaluating the compatibility. In this research, our primary focus is developing a resource allocation method using long-term power. Therefore, in this chapter we assume that the proposed UCC is the preferred method of evaluating user compatibility, and we do not further evaluate the UCC in the scope of this analysis. Under this premise, the prime focus is evaluating the performance of user selection algorithms in different environments.

The performance of the user selection algorithms is evaluated in two parts: *utilisation* and *complexity*. As defined in Chapter 3, utilisation refers to the percentage of the theoretical user capacity of the system that is utilised by the user selection algorithm. Complexity is evaluated by the number of SER calculations required to reach the resource allocation solution. Using the system model proposed in Chapter 3, we consider four environmental parameters that may affect the system performance. First, we look at the user capacity of the system with different numbers of resources and BSs, and how complexity changes as a result. With a larger system dimension, we also look at how user partitions can reduce the complexity. Secondly, we look at the performance under a clustered user distribution, and how utilisation varies if the cluster is at a different location. Thirdly, we look at the performance under different propagation parameters, considering different path-loss exponents (PLE) and shadow fading factors (SF). Lastly, we looked at the performance with a higher link quality requirement. These scenarios aim to represent a range of real life environments, and the simulation results help us better understand the system behaviour in different environments. Collectively, this represents the overall performance of the proposed resource allocation method.

5.1 System Dimensions

One of the major challenges of resource allocation in macrodiversity systems is the complexity of user selection, which increases with system dimension. Here, the system dimension refers to the number of resources and the number of cooperating BSs in the system. As described in (3.17), the more resources and BSs in the system, the greater the user capacity. This also means more possible user selection combinations. Heuristic solutions that can find an appropriate user selection without an excessive number of SER calculations make resource allocation for larger system dimension possible, thereby realising a greater user capacity potential.

The following subsections look at the performance of two macrodiversity systems. One is a BSG with 3 BSs, another is a BSG with 7 BSs. Within each system, the performance is evaluated in terms of the utilisation of the system under different levels of user loading, and the number of SER calculations required to find the solution. The performance of the BSGs are also evaluated with more resources. We also look at the reduction in complexity when user partitions is applied to the system. Table 5.1 shows a summary of the environment settings used in the simulations.

Table 5.1: The environment settings for different system dimensions.

System Parameters	Symbol	Value
Number of BSs	N_{BS}	3, 7
Number of Resources	N_{RB}	5, 20
Number of Partitions	N_{P}	1, 2, 4
Number of Users	N	$0 \sim 100\%$ User Capacity
User Distribution	-	Uniform
Modulation Scheme	-	QPSK
SER Threshold	-	10^{-2}
Path Loss Exponent	γ	3.5
Shadow Fading s.d.	σ_{SF}	8
Power Scaling Factor	A	Adaptive

5.1.1 Small BSG Size: 3 BSs

To keep the analysis simple, a small BSG with 3 BSs is used as the default network layout for most simulations. Under the standard setup, $N_{\text{RB}} = 5$, and the user capacity of the system is 15 ($N_{\max} = 15$). In most cases, a uniform user distribution and standard propagation parameters are assumed. Figure 5.1 shows the network layout of the BSG with users

randomly located in a uniform distribution around the BSs.

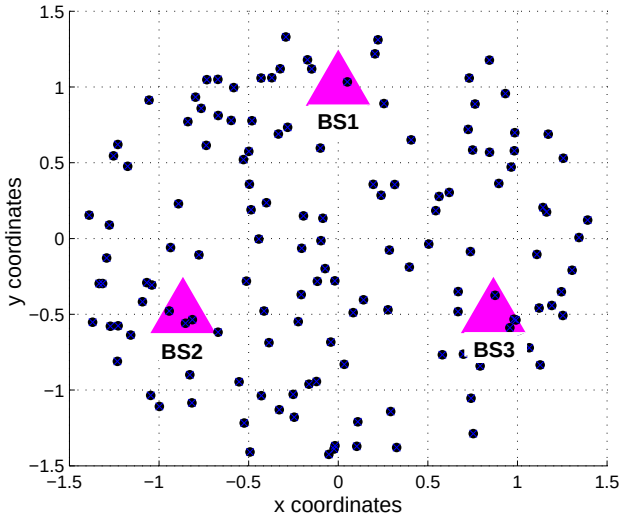

Figure 5.1: BSG layout with 3 BSs. $N = 200$.

Figure 5.2 shows the system performance with different levels of user loading. As defined in Chapter 3, *maximum utilisation* refers to the maximum capacity utilisation for the given number of users; this is also the percentage of user loading of the system. Theoretically, the ES algorithm finds the best possible resource allocation solution for the any scenarios. In the case of Figure 5.2, the ES algorithm has a utilisation performance equal to the maximum utilisation. However, ES also has the highest complexity. When the number of users is equal to the full capacity ($N = 15$), the number of SER calculations approaches 10^8. The FF and BF algorithms have a similar utilisation performance, the PO+SR has a moderate performance, and the PO algorithm has the worst result. PO, PO+SR, FF, and BF algorithms are relatively low complexity compared to the ES algorithm.

Figure 5.3 shows the system performance with $N_{\text{RB}} = 20$. Here, the user capacity is increased to 60. With the increased number of users, the complexity also increases. At this point, we are not able to simulate the ES algorithm, so it is omitted from the results. The complexity of the BF algorithm has increased significantly to the order of 10^3, and the FF algorithm has also increased to the order of 10^2. The utilisation of BF and FF algorithms in Figure 5.2 is slightly better compared to the results in Figure 5.2. This is because the availability of additional resources has increased the degrees of freedom for the user selection.

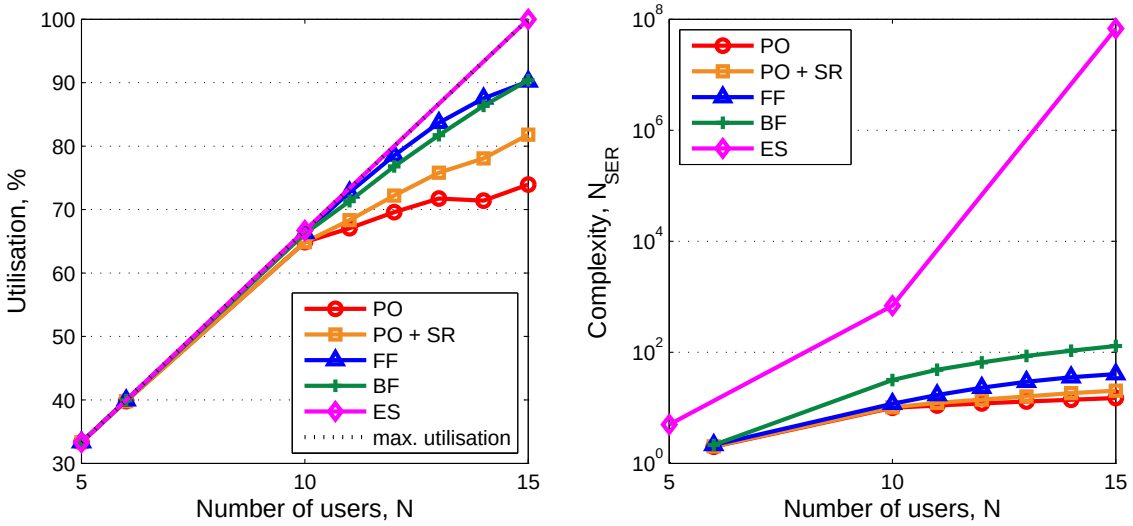

Figure 5.2: Performance of user selection with $N_{\text{BS}} = 3$ and $N_{\text{RB}} = 5$.

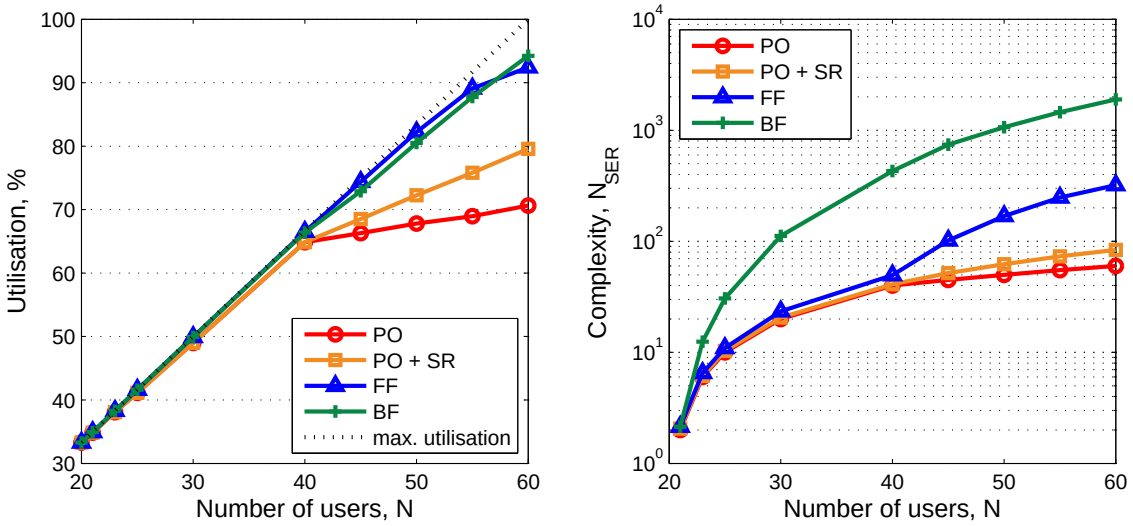

Figure 5.3: Performance of user selection with $N_{\text{BS}} = 3$ and $N_{\text{RB}} = 20$.

Both Figure 5.2 and Figure 5.3 show that utilisations of all algorithms start to deviate from the maximum utilisation only when the number of users is greater than 10 and 40 respectively. This is because 10 and 40 corresponds to the maximum number of users where each resource only need to be shared $N_{\text{BS}} - 1$ times, and it is easier to find independent signal paths if the spatial dimension of the channel matrix is not fully utilised. When the resources are being utilised at the maximum dimension, such as between $N = 10 \sim 15$ for $N_{\text{RB}} = 5$, and $N = 40 \sim 60$ for $N_{\text{RB}} = 20$; the user groups become more crowded. This increases the likelihood of users not meeting the link quality requirement.

In Figure 5.2 and Figure 5.3, the utilisation performances of both the PO and PO+SR algorithms start to significantly deviate from the maximum utilisation when $N > 10$ for

$N_{\mathrm{RB}} = 5$, and $N > 40$ for $N_{\mathrm{RB}} = 20$. This indicates that statistically, it is likely that the N_{BS}-th users who share the same resource with others do not meet the SER threshold, or cause a degradation in link quality to other previously allocated users. In particular, PO has worse utilisation than PO+SR because it employs a more aggressive user removal strategy. In the PO algorithm, if the primary user fails the SER threshold, it removes the allocation of all secondary users to preserve the link quality of the primary user. In general, FF and BF have better utilisation performance than PO and PO+SR because they check other user combinations, and choose only users that meet the SER threshold. When the system is fully loaded, the utilisations of FF and BF are 10% lower than the maximum utilisation, showing that when the system is in full user loading, it becomes much more challenging to find compatible users for all user groups. It is also worthy of noting that FF and BF have very similar utilisation performance, in some cases the utilisation of FF is slightly better than the BF. This suggest that the selecting the best-fit user from the unallocated user pool may not be the best strategy for the overall system performance.

5.1.2 Large BSG Size: 7 BSs

We also investigated the performance of the algorithms in a larger macrodiversity system. Here, we choose a BSG with 7 BSs because it is sufficiently larger than the 3 BSs system, and it is also a network layout proposed in the LTE CoMP system [3]. Figure 5.4 shows the network layout of the BSG with users randomly located in a uniform distribution.

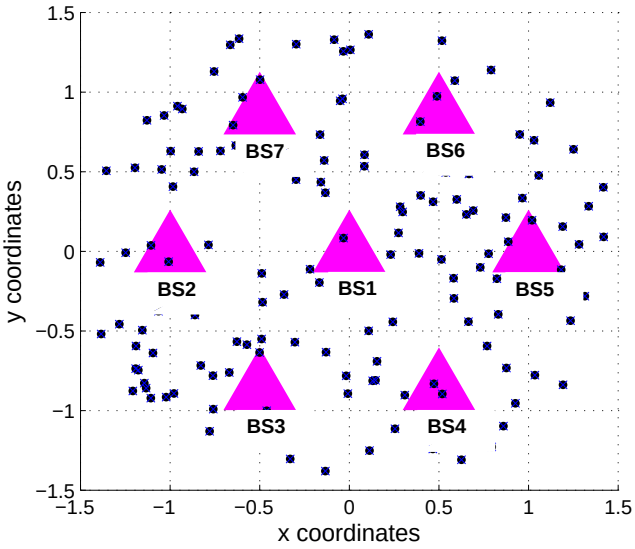

Figure 5.4: BSG layout with 7 BSs. $N = 200$.

Figure 5.5 and Figure 5.6 show the system performance of different resource allocation algorithms in the BSG, with $N_{\mathrm{RB}} = 5$ and $N_{\mathrm{RB}} = 20$ respectively. Because the BSG now has more BSs, the system can now support more users for the same number of resources. In this case, the spatial dimension of the channel matrix is 7. The system allows more users to share the same resource, but as in the 3 BSs system, when the system is in high user

loading, it also experiences a degradation in utilisation. For the PO algorithms, utilisations start to deviate from the maximum when user loading is above 65%. Beyond 85% user loading, the utilisation of the PO algorithm drops significantly. This shows that at this point, the number of users removed from the system is greater than the number of users added into the system. This is because for the 7 BSs system, there are more secondary users sharing resources with the primary users. When one primary user fails the SER threshold, all 6 other users who share the same resource are removed from the resource schedule. For the PO+SR, FF and BF algorithms, the increment in utilisation starts to tail off around 85% user loading. This corresponds to $N = 30$, which is the maximum number of users for $N_{\text{BS}} - 1$ resource-sharing for $N_{\text{RB}} = 5$.

In terms of complexity, the 7 BSs system in general has a higher complexity than the 3BSs system. This is because with a higher user capacity, the scheduler needs to check through more user combinations, resulting in a general increase in the user selection complexity. However, if the number of users and resources in the system is the same, the complexity of both 3 BSs and 7 BSs systems are of a similar order of magnitude. Table 5.2 shows a comparison of user selection complexity between the two systems, when both have the same number of users and resources. For most cases, the 7 BSs system still has a slightly higher complexity compared to the 3 BSs system, but they are of the same order of magnitude. It is worth noting that the complexity of the ES algorithm is beyond comparison for these algorithms. For the system dimension in Figure 5.5, with 100% user loading, the complexity of ES would be in the order of 10^{36} (2.2).

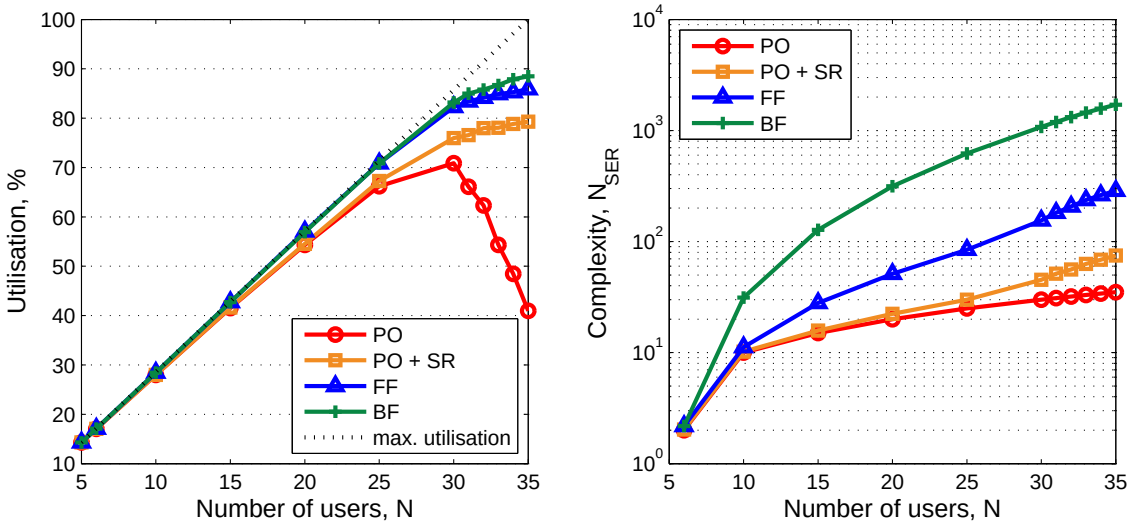

Figure 5.5: Performance of user selection with $N_{\text{BS}} = 7$ and $N_{\text{RB}} = 5$.

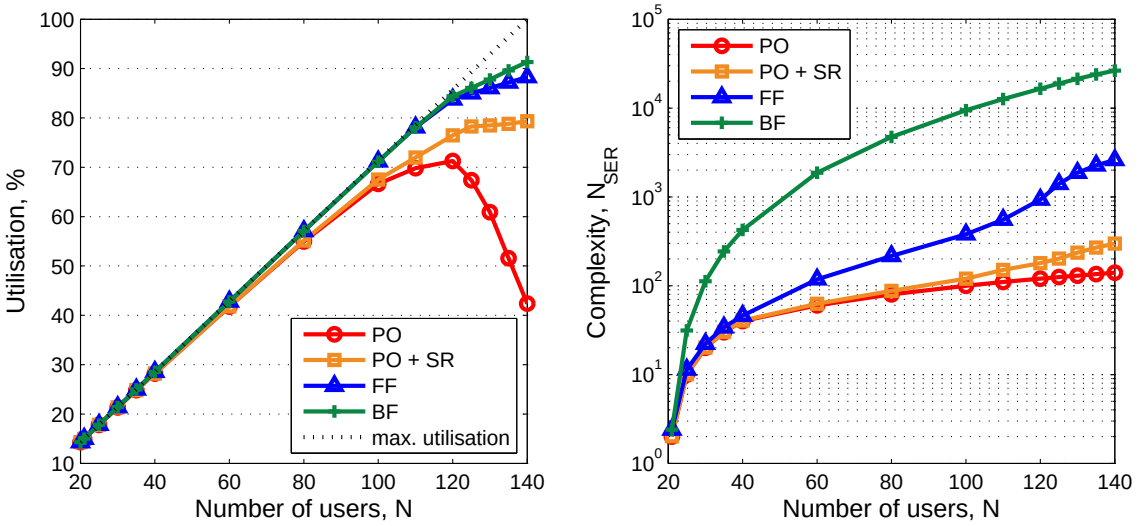

Figure 5.6: Performance of user selection with $N_{\text{BS}} = 7$ and $N_{\text{RB}} = 20$.

	$N_{\text{RB}} = 5,\ N = 15$				$N_{\text{RB}} = 20,\ N = 60$			
	PO	PO + SR	FF	BF	PO	PO + SR	FF	BF
3 BSs	15	20	40	130	60	84	320	1894
7 BSs	15	22	51	315	60	63	118	1868

Table 5.2: A cross-comparison of complexity (N_{SER}) between BSGs with the same number of users (N) and resources (N_{RB}) but different number of BSs (N_{BS}).

5.1.3 User Partitions

One strategy for reducing the complexity is by assigning users and resources into smaller partitions, and making scheduling decisions within each partition. The goal of user partitions is for systems with a large number of resources and users to achieve similar complexity to that of a smaller system. To emphasise the effect of complexity reduction, N_{RB} in the BSGs in Section 5.1.1 and Section 5.1.2 is increased to 20. With more resources, the user capacity for the 3 BSs system is increased to 60; the user capacity for the 7 BSs system is increased to 140. We use these systems as a platform for evaluating the effectiveness of complexity reduction by user partitions.

Figure 5.7 and Figure 5.8 show the performance of the PO, PO+SR, FF, and BF algorithms with user partitions in different macrodiversity systems. For the PO and PO+SR algorithms, there is no change in utilisation and complexity because all users are allocated in a fixed manner (according to the user priority order); there is only one user combination. For the FF algorithm, there is no change in utilisation and complexity when the user loading is low. The results with user partitions start to deviate from those without user partitions when

the user loading is high: For the 3 BSs system, it is $N \geq N_{\text{RB}} \times (N_{\text{BS}} - 1)$. For the 7 BSs system, it is $N = N_{\text{RB}} \times (N_{\text{BS}} - 1)$. Because the complexity for the FF algorithm remains the same with low user loading, it also suggests that it is easy to pass UCC when the dimension of the channel matrix is not fully utilised. The FF algorithm tends to accept the first candidate user available. For the BF algorithm, the reduction in complexity has a linear relationship with the number of partitions. It is also worth noting that although user partitions can reduce the complexity of the BF algorithm, the complexity of the FF algorithm is still lower than BF. With users and resources grouped into smaller partitions, the selection diversity decreases. We therefore observe a slight degradation in the utilisation for both the FF and the BF algorithm.

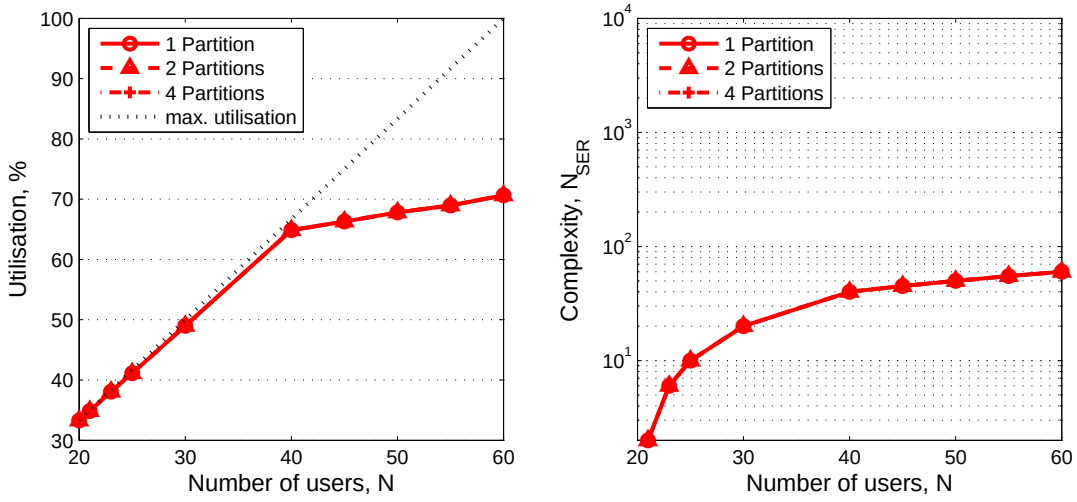

(a)

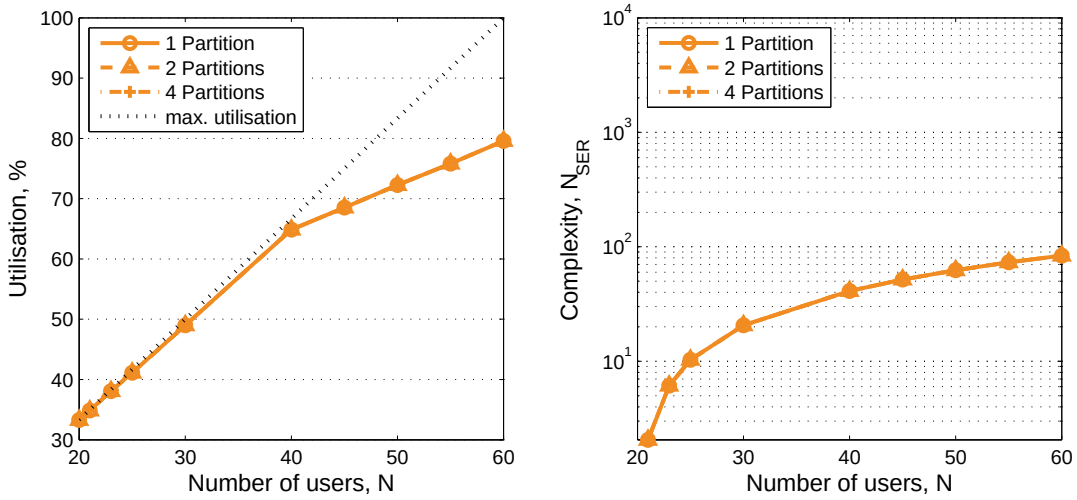

(b)

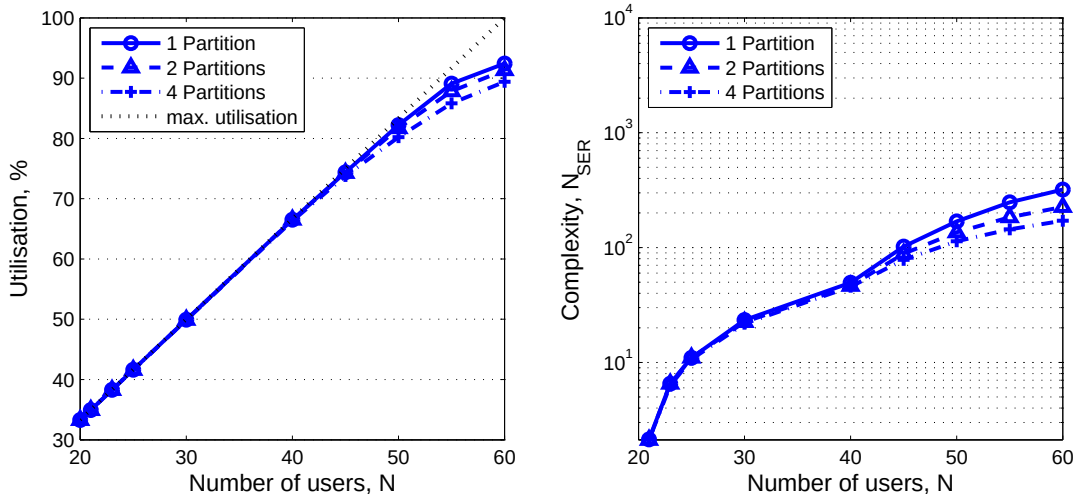

(c)

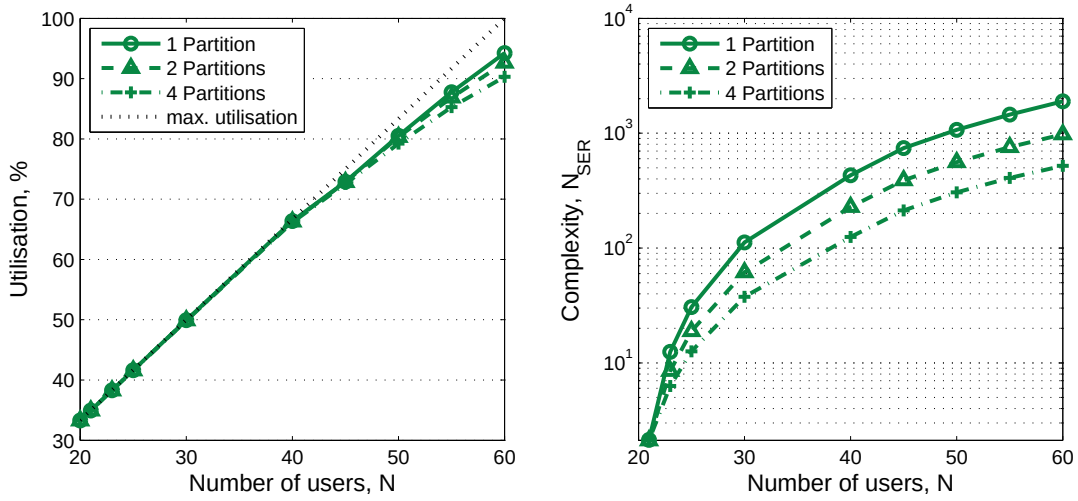

(d)

Figure 5.7: Performance of user selection with partitioning. $N_{\mathrm{BS}} = 3$ and $N_{\mathrm{P}} = 1, 2, 4$. (a) PO (b) PO + SR (c) FF (d) BF.

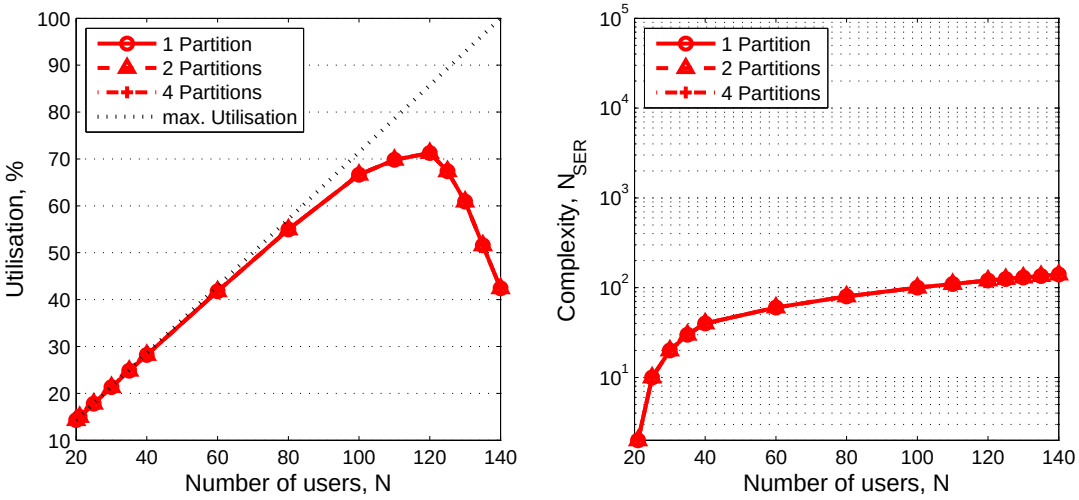
1 Partition
2 Partitions
4 Partitions
max. Utilisation
Utilisation, %
Number of users, N
Complexity, N_{SER}

(a)

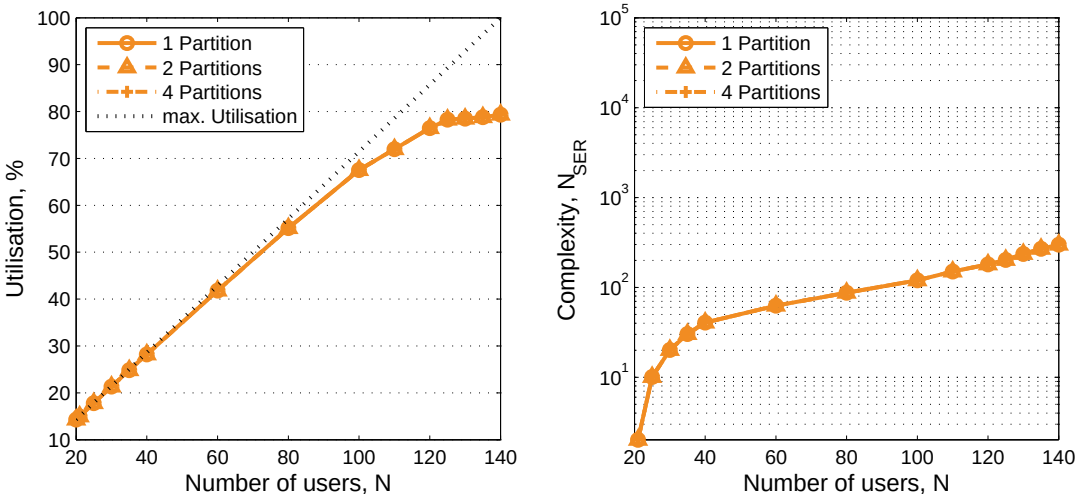
1 Partition
2 Partitions
4 Partitions
max. Utilisation
Utilisation, %
Number of users, N
Complexity, N_{SER}

(b)

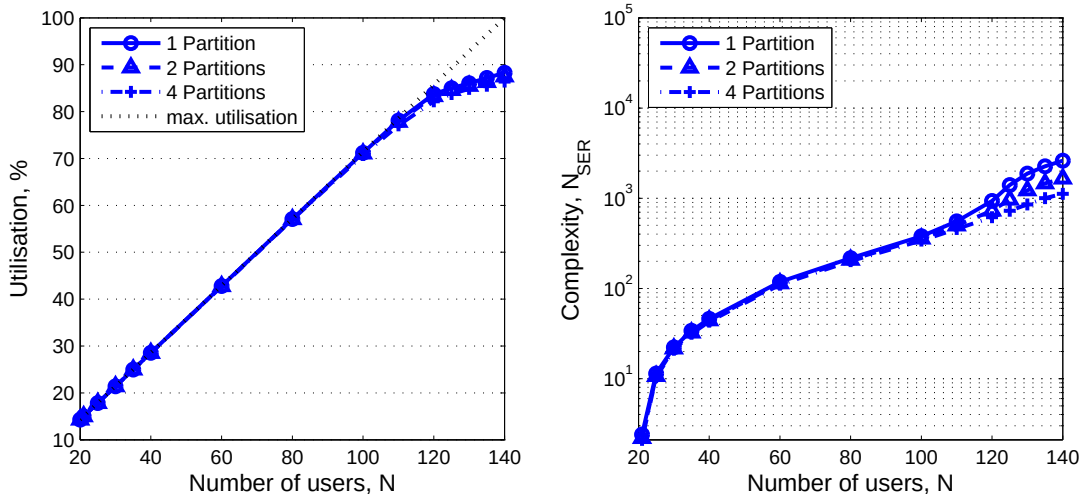

(c)

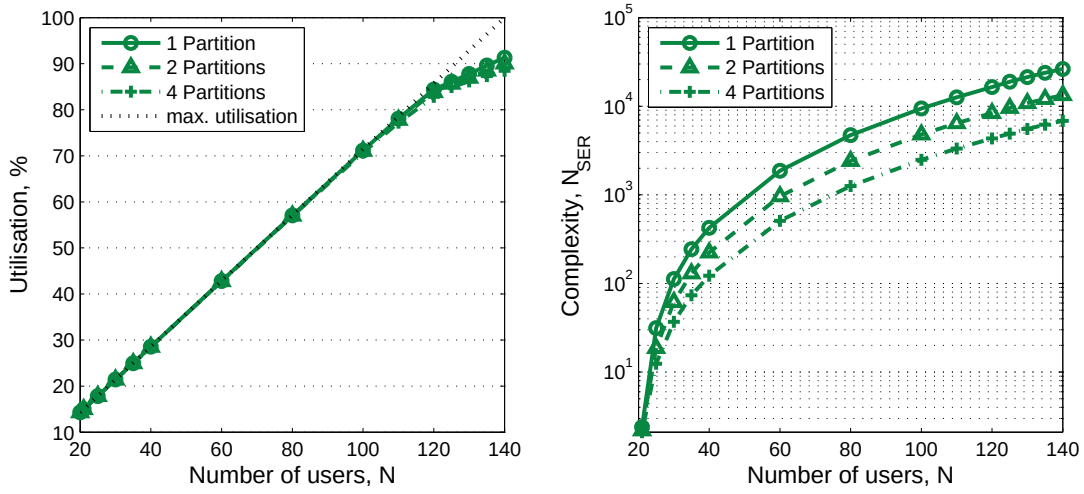

(d)

Figure 5.8: Performance of user selection with partitioning. $N_{\mathrm{BS}} = 7$ and $N_{\mathrm{P}} = 1, 2, 4$. (a) PO (b) PO + SR (c) FF (d) BF.

Power Ranking:

In Section 4.2, we suggested that degradation in link quality occurs mostly in situations where user channels are non-orthogonal, particularly when one user has similar channel characteristics to the other, but at a much higher power level. We proposed a very simple method of minimising the occurrence of one user dominating the channel over other resource-sharing users by ranking users according to their combined power, Figure 5.9 shows the performance comparison of a partitioned system without power ranking, and with power ranking. Contrary to the expectations, from these results, we cannot observe any significant differences in performance between user partitions with power ranking and user partitions without power ranking. One possible explanation is that the user selection algorithms inherently select the compatible users and reject the incompatible users, hence the occurrence of incompatible users being in the same group has already been minimised. The result suggests that power ranking is not an effective strategy for improving user compatibility.

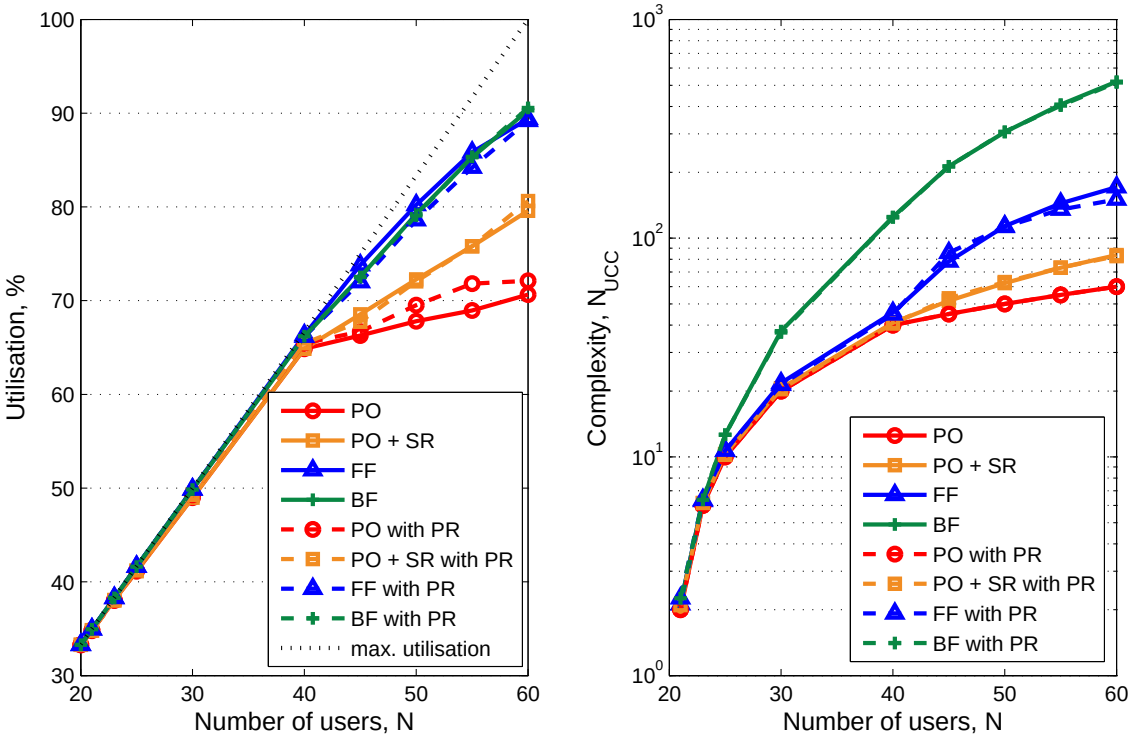

Figure 5.9: Performance of user selection algorithms with partitioning and power ranking: $N_{\mathrm{BS}} = 3$, $N_{\mathrm{RB}} = 20$, and $N_{\mathrm{P}} = 4$.

5.1.4 Discussion

With larger system dimensions, user capacity increases, but complexity also increases. The increased capacity translates to real benefits only if it can be effectively utilised. In general,

utilisation is close to maximum if the system is not heavily loaded. In a lightly loaded system, when the spatial dimensions of the channel matrix (N_{BS}, as defined in Section 3.3.2) is greater than the number of resource-sharing users, it is easier to find semi-orthogonal paths in which users can transmit with limited interference from others; in a heavily loaded system, performance in utilisation varies between different algorithms.

From the results, the ES algorithm provides the best utilisation of user capacity, however, the complexity of the algorithm prohibits its deployment in any large systems. For the PO and PO+SR algorithms, utilisations start to deviate when user loading is high ($> 60\%$). Due to the aggressive user removal strategy in the PO algorithm, utilisation drops significantly in a high user loading environment. This is because for the PO algorithm, in order to preserve the primary users, a lot of secondary users are removed even if they have good link quality. In this worst-case scenario, when the system is experiencing full user loading, utilisation drops from 70% to 40%. The PO+SR algorithm has consistently shown better performance in utilisation than the PO algorithm, with a relatively small increase in complexity. This is because the PO+SR algorithm removes users one by one, checking SER of remaining users in the group each time a user is removed. User removal stops as soon as all remaining users meet the SER threshold. Therefore, unless minimum complexity is absolutely critical, PO+SR would be considered as the more effective solution than PO. FF and BF algorithms have similar performance in terms of utilisation. However, the complexity of the FF algorithm is much lower than that of the BF algorithm. Therefore, in general, FF would be considered as a more effective solution than BF.

Assigning users into smaller partitions reduces the complexity of the FF and BF algorithms but not the PO and PO+SR algorithms. For PO and PO+SR algorithms, complexity does not change with user partitions because users are allocated in a fixed manner, according to their priority order; there is only one user combination. For FF, complexity reduction becomes noticeable only when the user loading is high, particularly when $N \geq N_{\text{RB}} \times (N_{\text{BS}} - 1)$. For BF, a significant complexity reduction is observed across all user loadings. This is because the BF algorithm checks all users in the user selection pool before making the user selection decisions. When user loading is high, the complexity of both FF and BF has a linear relationship with the number of partitions; it reduces linearly according to the number of partitions. In general FF has a better utilisation performance than the PO+SR algorithm, but also has a higher complexity, even with user partitions.

In general, complexity increases as the number of users in the system increases. Some complexity reduction can be obtained by assigning users into smaller partitions, but mostly it depends on the user selection algorithms. This section has shown that the PO+SR and FF algorithms can achieve reasonable performance with relatively low complexity. Selecting between these algorithms will depend on the utilisation requirement and system processing power of the particular implementation envisaged. We have also observed that there is a strategically advantageous point when $N = N_{\text{RB}} \times (N_{\text{BS}} - 1)$. If user loading is less or equal to this point, most user selection algorithms return utilisation performance close to the maximum utilisation.

5.2 Clustered User Distributions

The simulations in the previous section assume a uniform distribution of all users. In real life, users do not always follow a uniform distribution. In spaces such as shopping malls, train stations, or conference centres, people tend to cluster at one particular spot. With users clustered at one spot, the power profile of users is different, and as a consequence, the system performance may change. This section investigates the system performance of macrodiversity systems with user clustering. The user cluster is modelled by a 2-dimensional Gaussian distribution as defined in Chapter 3. In the figures, we plot 500 users on the map to give readers a stronger sense of user distribution. In the simulation, we consider only small systems with 15 users, to keep the simulation manageable. Two sample scenarios are investigated: the user cluster at the centre of the BSG, and the user cluster away from the centre of the BSG, at one of the cooperative BSs. Table 5.3 shows the environment settings for the simulations.

Table 5.3: The environment settings for clustered user distributions.

System Parameters	**Symbol**	**Value**
Number of BSs	N_{BS}	3
Number of Resources	N_{RB}	5
Number of Partitions	N_{P}	1
Number of Users	N	$0 \sim 100\%$ User Capacity
User Distribution	-	Gaussian: $\mathcal{N}(0, 0.375^2)$
Modulation Scheme	-	QPSK
SER Threshold	-	10^{-2}
Path Loss Exponent	γ	3.5
Shadow Fading s.d.	σ_{SF}	8
Power Scaling Factor	A	Adaptive

5.2.1 Cluster at the Centre of the BSG

Figure 5.10 shows the user cluster at the centre of the BSG, the density of the distribution decreases with the radius away from the centre. Figure 5.11 shows the corresponding system performance of the cluster under different user loadings. From the figure, the performance is slightly better compared to similar results for users in a uniform distribution (Figure 5.2). For the PO and PO+SR algorithms, the improvement in utilisation compared to a uniform distribution is about 10%; for the FF and the BF algorithms, the improvement is about 5%. In terms of the complexity, PO and BF have the same complexity as in scenarios where users are in a uniform distribution. PO+SR and FF have slightly lower

complexity in high user loading, compared to the uniform distribution.

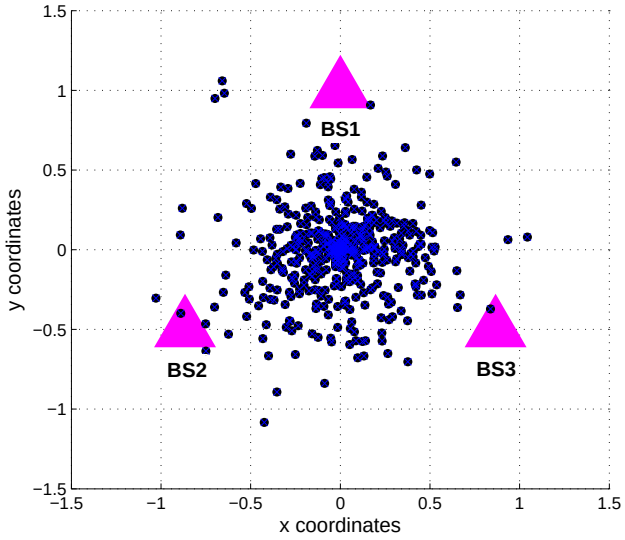

Figure 5.10: An example of a user cluster at the center of the BSG. The center of the cluster is at coordinates $(x, y) = (0, 0)$. The position of users is modelled by a 2D Gaussian distribution with standard deviation = 0.375. N=500.

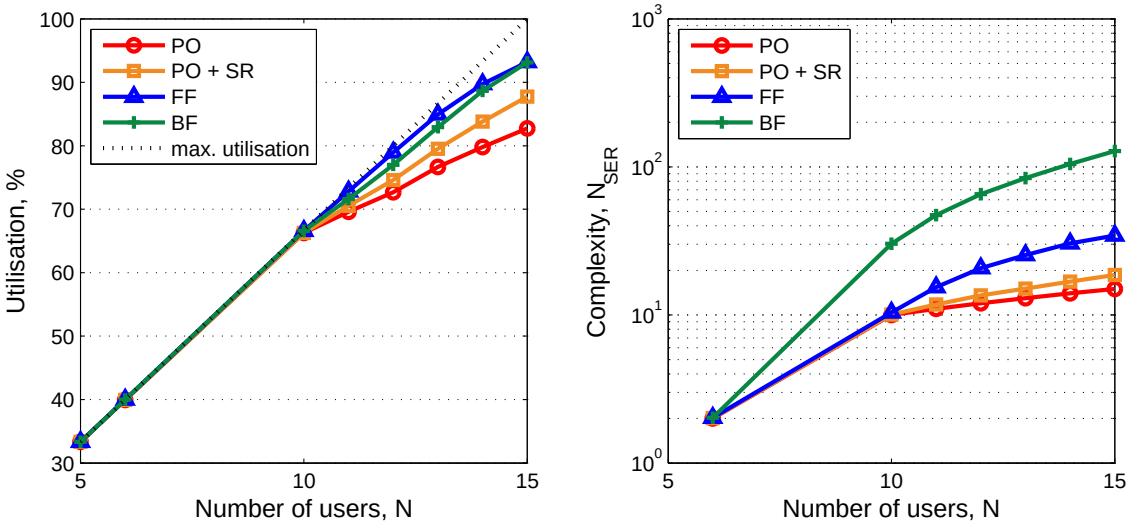

Figure 5.11: System performance with $N_{\text{BS}} = 3$ and $N_{\text{RB}} = 5$.

5.2.2 Cluster away from the Centre of the BSG

Figure 5.12 shows the user cluster away from the centre of the BSG. In this case, the user cluster is centred around BS3, having the same Gaussian distribution as in Figure 5.10. Figure 5.13 shows the corresponding system performance of the cluster under different user loadings. Under heavy user loading, the utilisation of the PO+SR, FF and BF algorithms degrades by about 15% when compared to the uniform user distribution, and for the PO

algorithm by about 25%. The PO algorithm has its peak utilisation performance at 65% of user loading, for the heavier user loading, the utilisation performance starts to degrade. In terms of the complexity, for the PO and BF algorithms, the complexity remains fixed. For the PO+SR and FF algorithms, complexity has also risen compared to Figure 5.11. This indicates that in this environment, it is more difficult to find compatible candidate users, meaning that it takes more iterations to find the appropriate solutions.

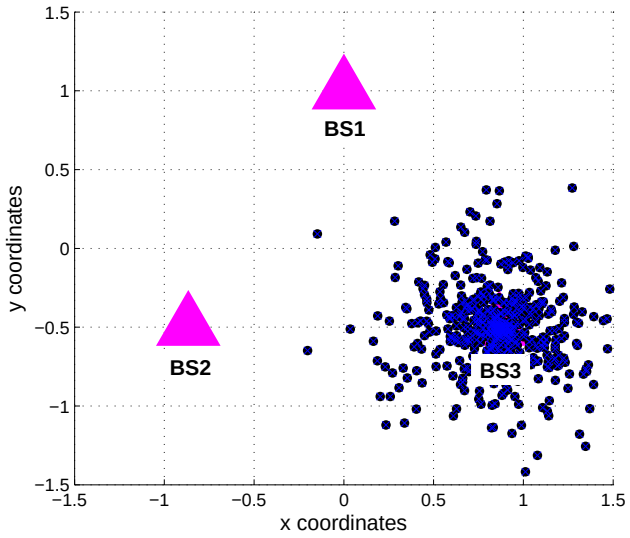

Figure 5.12: An example of a user cluster away from the centre of the BSG. The center of the cluster is at BS3 $(x, y) = (0.866, 0.5)$. The position of users is modelled by a 2D Gaussian distribution with standard deviation = 0.375. N=500.

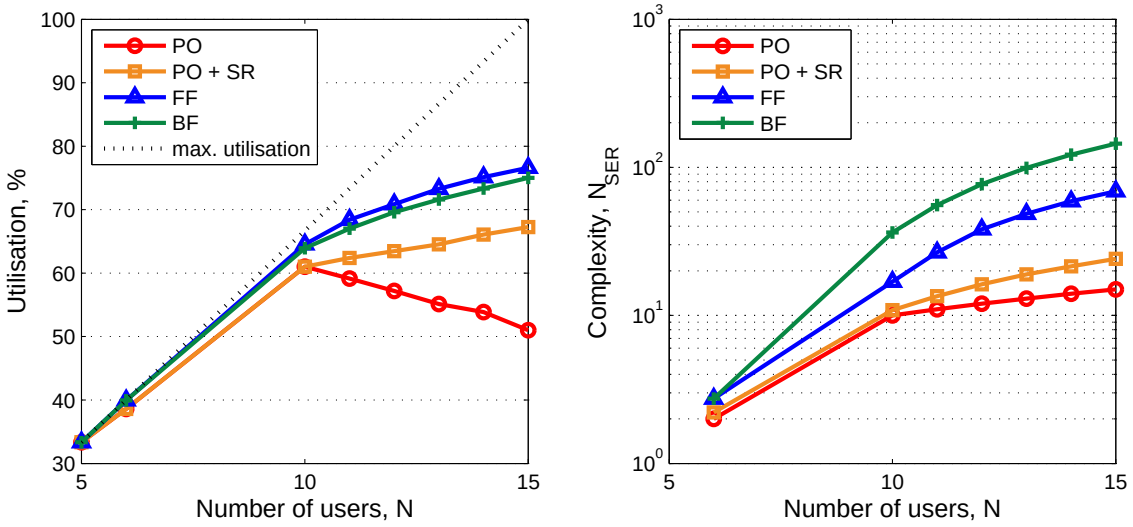

Figure 5.13: System performance with $N_{\text{BS}} = 3$ and $N_{\text{RB}} = 20$. The cluster is off-centred.

5.2.3 Discussion

When users are clustered at the centre of the BSG, we observed a slight increase in the system utilisation. This can be attributed to the more equal distribution of the received powers by all BSs: In general, signals received by BSs become weaker as users get further away. When users are at the centre of a BSG, although each BS only receives moderate power on average from the users, the transmitted signals tend to be more equally supported by all BSs. This allows the channel to operate at a higher spatial diversity, hence increasing the chance of users to co-exist with each other, sharing the same resource.

On the other hand, when users are clustered at one of the BSs near the edge of the BSG, we see a significant degradation in system utilisation. In the example studied, BS3 receives strong signals from the users but signals received by BS1 and BS2 are weak. Spatial diversity provided by BS1 and BS2 diminishes because of the weak power received by the BSs, and the BSG behaves like a single cell system where available resources are overloaded by multiple users. The performance of the PO algorithm is sensitive to the channel condition. As in the previous section, the utilisation performance peaks at $N = N_{\text{RB}} \times (N_{\text{BS}} - 1)$, and starts deteriorating with higher user loadings.

In terms of the complexity, the PO and BF algorithms have fixed complexity, regardless of the channel condition. For the PO+SR and FF algorithms, the complexity is lower in environments where it is easier to find compatible users (i.e. cluster at the centre of the BSG). The complexity is higher in environments where it is more difficult to find compatible users (i.e. cluster away from the centre of the BSG), as compared to users in a uniform distribution.

The results also show that the utilisation performance is mostly affected by how well the users are being equally support by all BSs in the BSG, rather than by the user clustering itself. The system achieves good utilisation performance when the cluster is at the centre of the BSG. It may be advantageous to construct the BSG dynamically, according to the location of the user cluster, hence maximising the system capacity [82].

5.3 Propagation Parameters

Depending on the physical environments in which the system is operating (rural, suburban, or urban), the wireless channel has different propagation characteristics. Having an understanding of how the propagation parameters affect system performance can help us in designing systems that are appropriate to the environments, or in predicting the likelihood of an outage.

In this section, we investigate the performance of the macrodiversity system under different propagation parameters. Since SER is calculated using long-term power, we look at only those factors that affect long-term power, such as path loss and shadow fading.

The effects of different propagation parameters are also investigated under different user distributions. Table 5.4 shows the environment settings used in the simulation. The values used for the path loss exponent (γ), and the shadow fading standard deviation (σ_{SF}), are commonly quoted in the literature [23, 83]. Standard power scaling is applied in the simulations.

Table 5.4: The environment settings for different propagation parameters.

System Parameters	**Symbol**	**Value**
Number of BSs	N_{BS}	3
Number of Resources	N_{RB}	5
Number of Partitions	N_{P}	1
Number of Users	N	$0 \sim 100\%$ User Capacity
User Distribution	-	Uniform, Gaussian
Modulation Scheme	-	QPSK
SER Threshold	-	10^{-2}
Path Loss Exponent	γ	2, 4
Shadow Fading s.d.	σ_{SF}	6, 12
Power Scaling Factor	A	Adaptive

5.3.1 Effects of Path Loss

Figure 5.14 and Figure 5.15 show the performance comparison of a standard 3 BS macro-diversity system under different path loss exponents. The minimum path loss exponent usually considered in a wireless system is $\gamma = 2$, which is the path loss in free space. The typical path loss exponent for urban environment is $\gamma = 4$, which includes signal attenuation through building structures. For the FF and BF algorithms, the performance variation due to γ change is almost unnoticeable. For the PO and PO+SR algorithms with $\gamma = 2$, utilisation has increased by about 5%, compared to the standard PLE factor where $\gamma = 3.5$ and with $\gamma = 4$, the change is almost unnoticeable. This is because the effects of path loss are normalised due to the adaptive power-scaling scheme applied in the system.

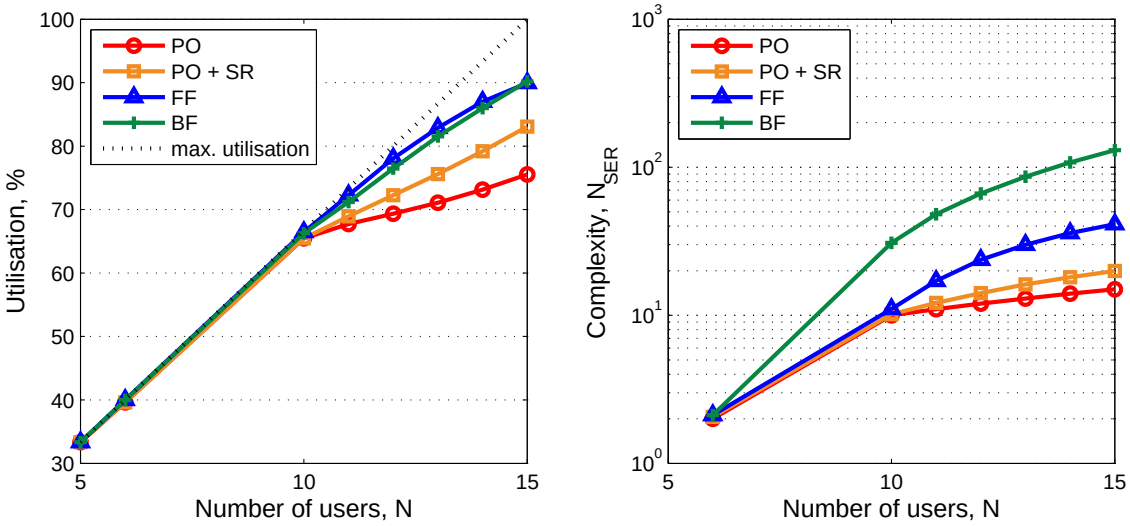

Figure 5.14: System performance with $\gamma = 2$ and $\sigma_{\text{SF}} = 8$.

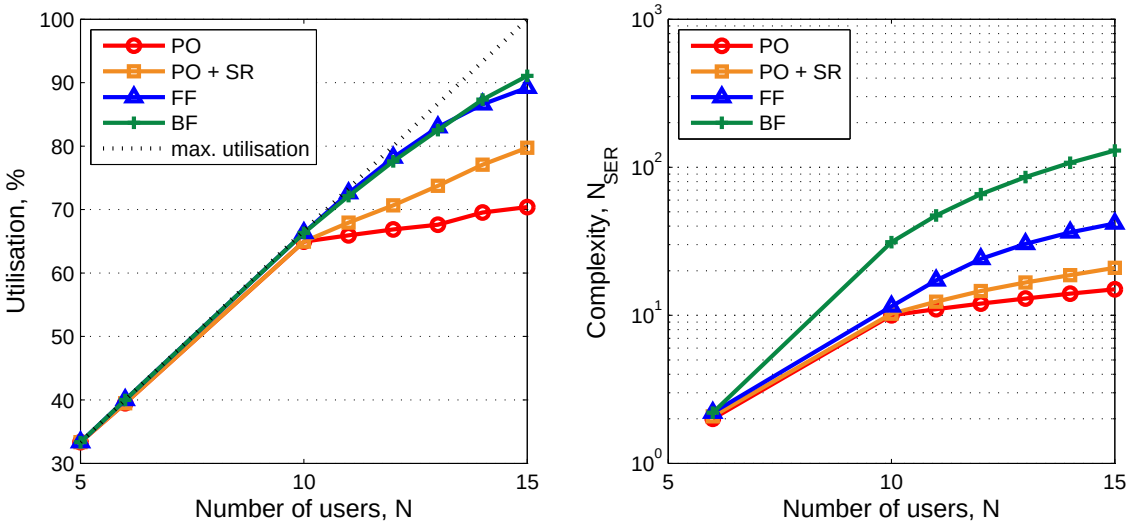

Figure 5.15: System performance with $\gamma = 4$ and $\sigma_{\text{SF}} = 8$.

User Cluster at the centre of the BSG:

Figure 5.16 and Figure 5.17 show the effect of path loss where users are clustering at the centre of the BSG. Compared to Figure 5.14 and Figure 5.15, we see a general improvement in utilisation for the same reasons explained in Section 5.2. Between Figure 5.16 and Figure 5.17, the utilisation results are very similar.

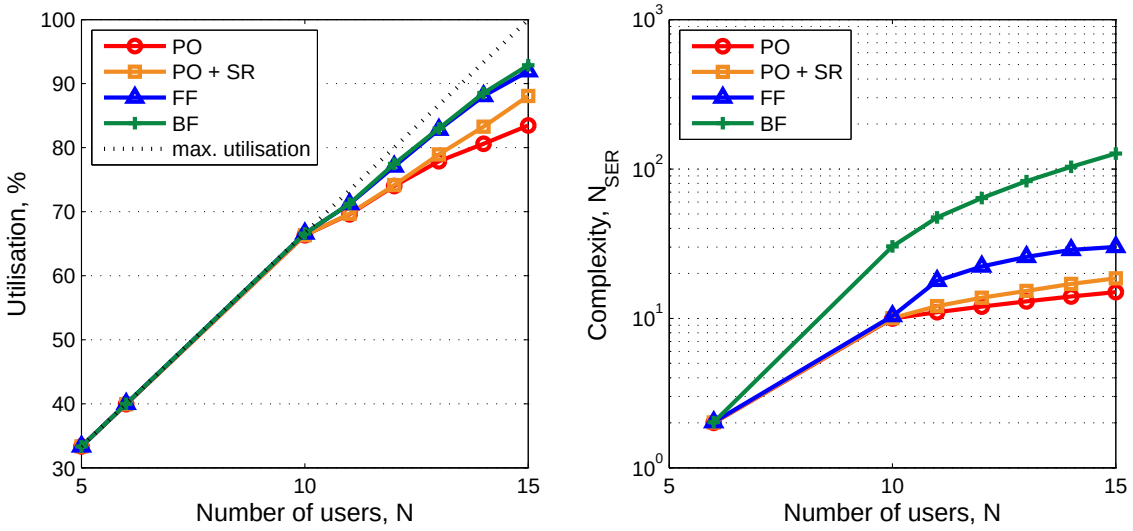

Figure 5.16: User cluster at the centre of the BSG with $\gamma = 2$ and $\sigma_{\text{SF}} = 8$.

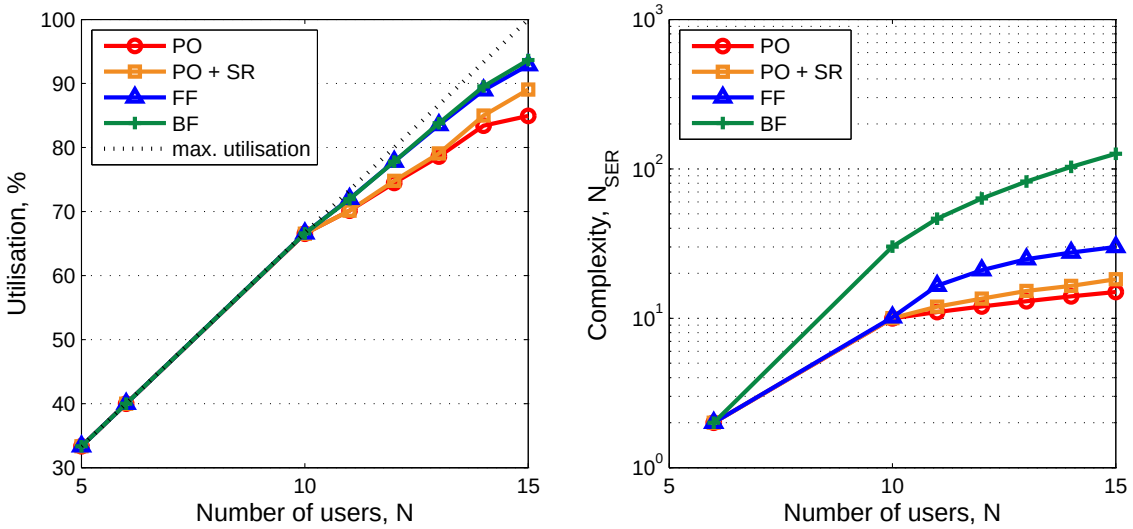

Figure 5.17: User cluster at the centre of the BSG with $\gamma = 4$ and $\sigma_{\text{SF}} = 8$.

5.3.2 Effects of Shadow Fading

Figure 5.18 and Figure 5.19 show the performance comparison of a standard 3 BS system under different shadow fading factors with a uniform user distribution. Compared to the standard settings in Figure 5.2, the change in performance is very small. The utilisations for

PO and PO+SR algorithms have dropped by 2% when $\sigma_{SF} = 6$, and increased by 3% when $\sigma_{SF} = 12$. For the FF and BF algorithms, there is little to no change in the performance.

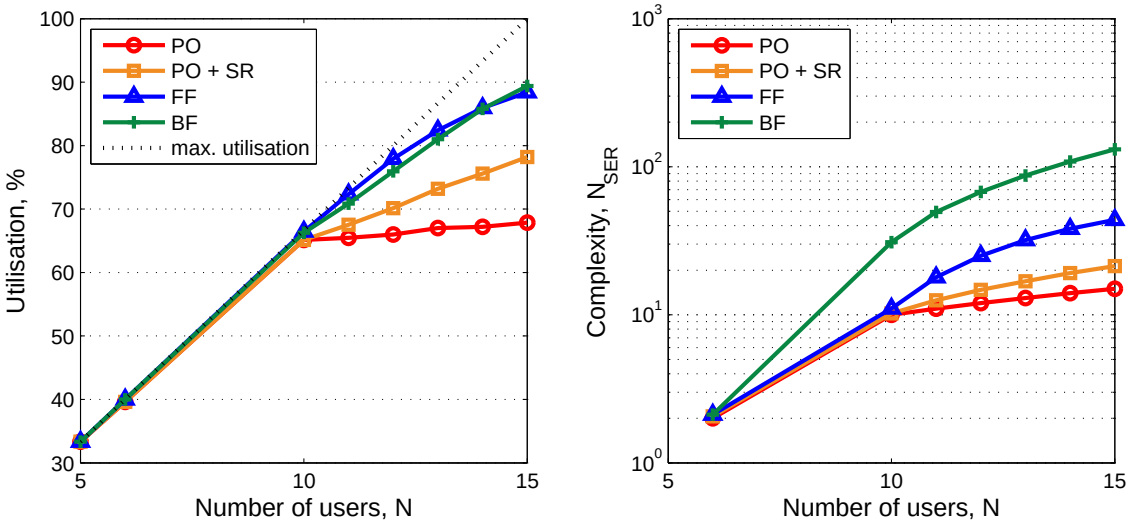

Figure 5.18: System performance with $\gamma = 3.5$, and $\sigma_{SF} = 6$.

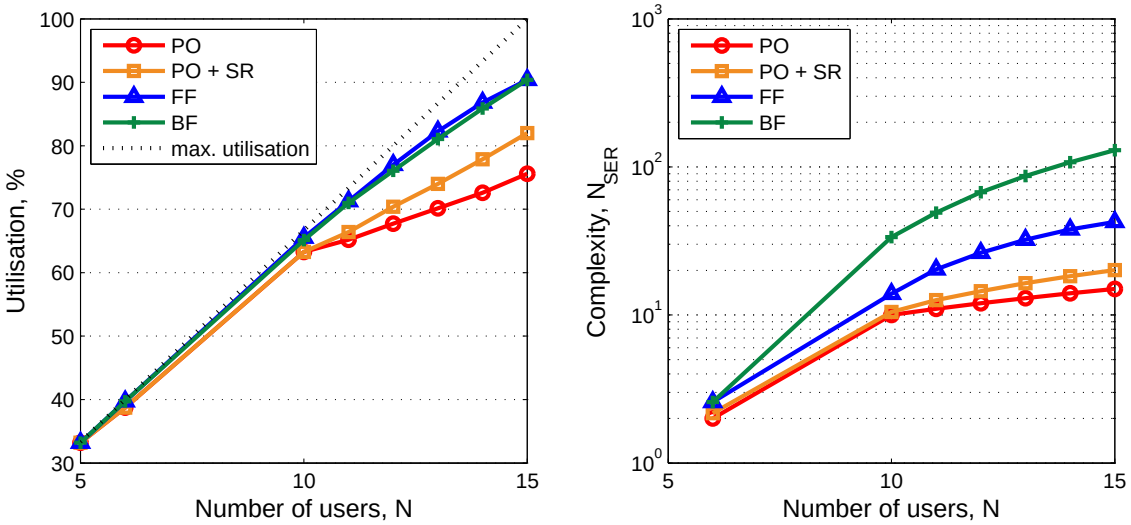

Figure 5.19: System performance with $\gamma = 3.5$, and $\sigma_{SF} = 12$.

User Cluster at the centre of the BSG:

Figure 5.20 and Figure 5.21 show the effect of shadow fading when users are clustered at the centre of the BSG. Compared to Figure 5.18 and Figure 5.19, we see an overall improvement in utilisation for $\sigma_{SF} = 6$, and a minor improvement in utilisation for PO and PO+SR algorithms for $\sigma_{SF} = 12$. With an increase in shadow fading, signal variation also increases. Hence, from the perspective of the BSG, users are seen as more randomly distributed than clustered. Hence, we see a similar utilisation as for users in a uniform distribution.

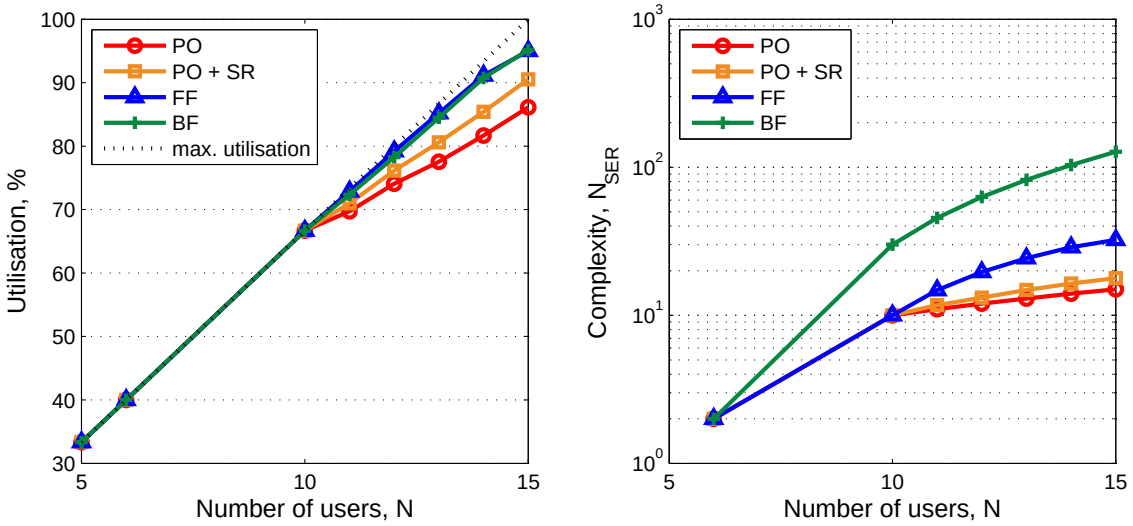

Figure 5.20: User cluster at the centre of the BSG, $\sigma_{\text{SF}} = 6$.

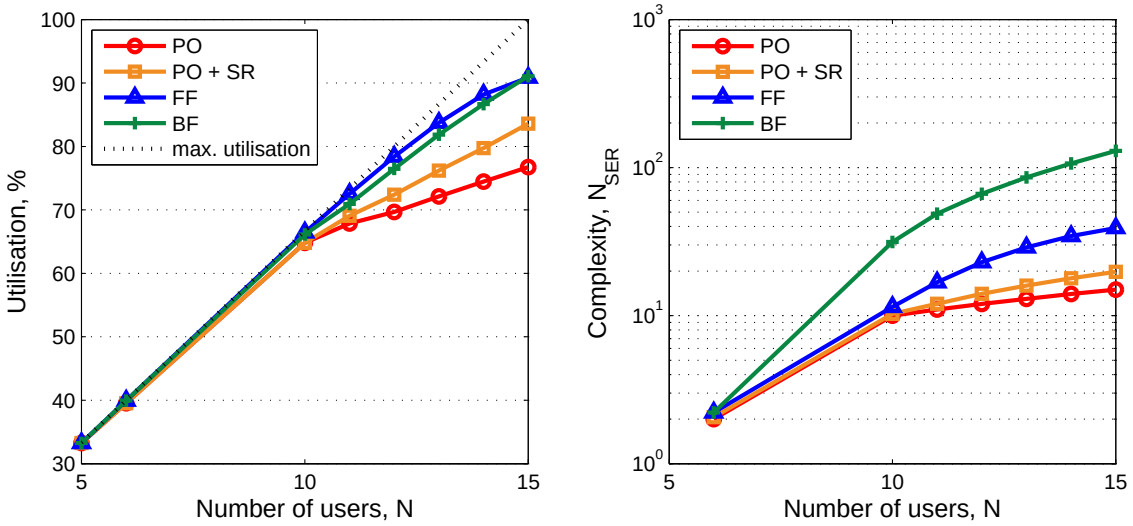

Figure 5.21: User cluster at the centre of the BSG, $\sigma_{\text{SF}} = 12$.

5.3.3 Discussion

For different path-loss exponents, we do not see much performance variation, either in the uniform distribution, or in the cluster distribution. This is due to the adaptive power-scaling in the system. For different shadow fading factors, there is little to no change in utilisation for users in a uniform distribution. However, for users in a cluster distribution, shadow fading has an equivalent effect of randomising the user distributions.

When users are clustered at the centre of the BSG, with $\sigma_{\text{SF}} = 6$, we see an improvement in the utilisation performance; with $\sigma_{\text{SF}} = 12$, we see the utilisation performance becomes

similar to users in a uniform distribution. This is because higher shadow fading averages out the effect of user clustering, making the power profile of users seem more varied. If the environment has higher shadow fading, we can expect a more consistent system performance, which is close to that of a uniform user distribution, regardless of the actual user distribution.

5.4 A Higher Link Quality Requirement

There are situations where a higher link quality is required: One way of achieving this is by appropriate scaling of the transmission power, but there may be cases such that the power is limited, or the system is interference limited. In these cases, we can ensure a higher link quality by changing the SER threshold in the UCC. Table 5.5 shows the environment settings used in the simulation. Here, the usual power scaling is applied to the system (i.e. 95% of users meet the SER threshold of 10^{-2} in single-cell systems), but the SER threshold for the UCC is reduced to 10^{-3}. Having a more stringent SER threshold also implies that the system can transmit at higher data rates (if an adaptive MCS is employed).

Table 5.5: The environment settings for a higher QoS requirement.

System Parameters	Symbol	Value
Number of BSs	N_{BS}	3
Number of Resources	N_{RB}	5
Number of Partitions	N_{P}	1
Number of Users	N	$0 \sim 100\%$ User Capacity
User Distribution	-	Uniform
Modulation Scheme	-	QPSK
SER Threshold	-	10^{-3}
Path Loss Exponent	γ	3.5
Shadow Fading s.d.	σ_{SF}	8
Power Scaling Factor	A	Adjust to SER $= 10^{-2}$

5.4.1 Changing the SER Threshold

Figure 5.22 and Figure 5.23 show the utilisation performance for 3 BSs and 7 BSs systems. With the SER threshold is reduced to 10^{-3}, we observe a reduction in utilisation, particularly when the system is under a heavy user loading. In Figure 5.22, utilisation of the PO algorithm reaches a peak at 58% when the system is at 66% user loading. The utilisation is reduced to 40% when the system is at the maximum user loading. For the PO+SR, FF and

BF algorithms, utilisations are 60%, 70%, and 70% at the maximum user loading, respectively. This is about 10% degradation from the utilisation seen in the equivalent scenario where the SER threshold was 10^{-2} (Figure 5.2). Similar results are observed in the 7 BSs system: In Figure 5.23, utilisation of the PO algorithm reaches a peak at 58% when the system is at 70% user loading. This is reduced to 18% at the maximum user loading. For the PO+SR, FF and BF algorithms, utilisations are 65%, 77%, and 82% at the maximum user loading. These results are about 15%, 10%, and 5% degradation respectively from the utilisation in the equivalent scenario where the SER threshold was 10^{-2} (Figure 5.5).

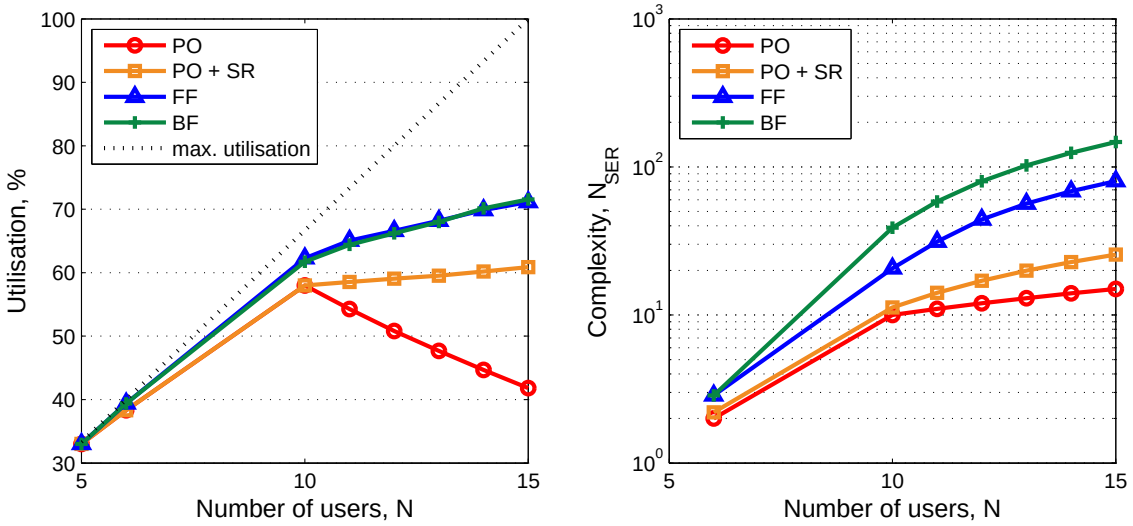

Figure 5.22: System performance with $N_{\text{BS}} = 3$ and SER Threshold = 10^{-3}.

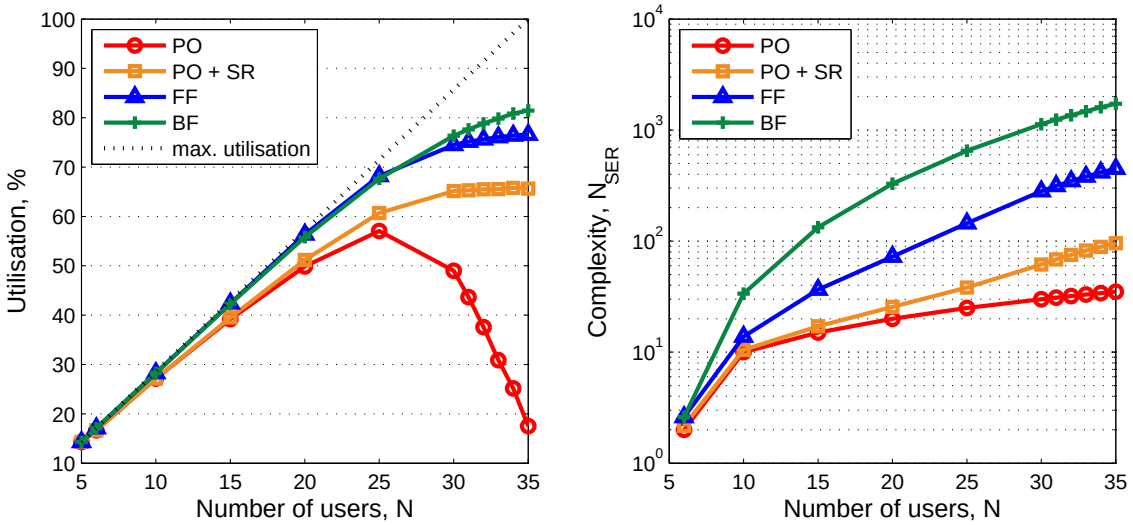

Figure 5.23: System performance with $N_{\text{BS}} = 7$ and SER Threshold = 10^{-3}.

In Figure 5.24, the power is scaled so that 95% of users meet the new SER threshold of 10^{-3}. In this case, we observed good utilisation performance for all algorithms.

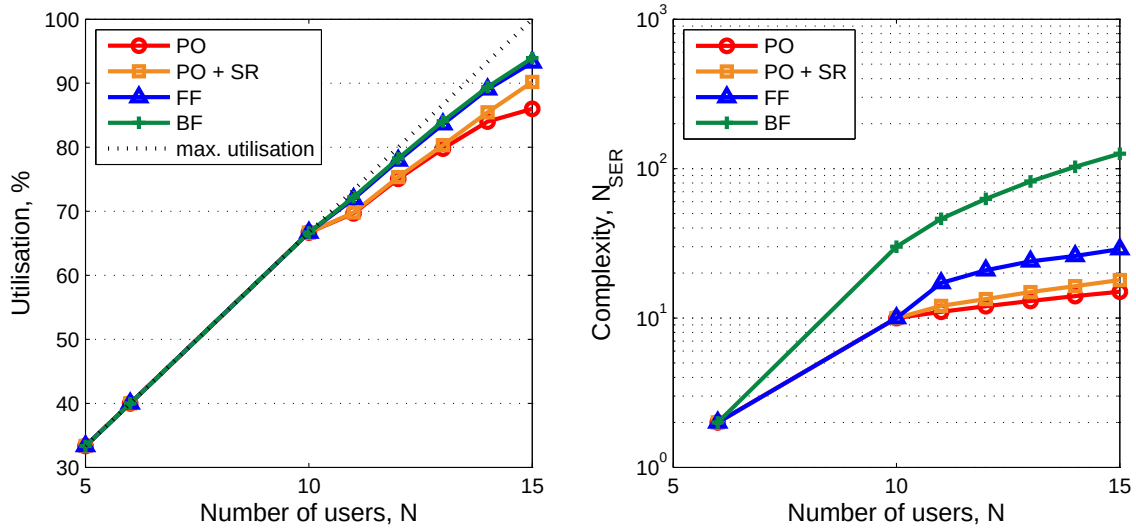

Figure 5.24: System performance with $N_{\text{BS}} = 3$ and SER Threshold = 10^{-3}. Power is scaled to SER Threshold = 10^{-3}.

5.4.2 Discussion

From the results, a general degradation in utilisation is observed when the SER threshold is reduced to 10^{-3}. Particularly for the PO algorithm, with 3 BSs, the utilisation peaked at 58% when the system was between $65\% \sim 70\%$ user loading. For the PO+SR, FF, and BF algorithms, at the maximum user loading, the utilisation performance dropped by about 10% in both the 3 BSs and 7 BSs systems.

In general, we observe that the user link quality is highly dependent on the overall power level received by the BSG. To achieve a lower SER threshold with the same power setting, utilisation performance suffers. If the power is scaled appropriately according to the SER threshold, then the utilisation performance returns to normal levels. In other words, for the PO+SR, FF, and BF algorithms, the utilisation performance is close to the maximum utilisation, if the system is not fully loaded. The performance "sweet-spot" is around $N = N_{\text{RB}} \times (N_{\text{BS}} - 1)$, as was already established in Section 5.1.

5.5 Summary

This chapter shows the trade-offs between utilisation and complexity for all the algorithms proposed in Chapter 4. The simulation results show that the ES algorithm is highly complex, even for a small system dimension. Although it has the best utilisation performance, in practice, it is not an efficient solution for most systems. Amongst the PO, PO+SR, FF, and BF algorithms, PO+SR and FF have a good balance between utilisation performance and complexity. The FF algorithm has a better utilisation performance than the PO+SR algorithm, but it is also more complex when the system is under heavy user loading. The

final choice of algorithm will depend on the processing power of the particular system.

When the number of BSs increases, the user capacity of the system increases because of the increase in the spatial dimension of the system. However, the complexity of user selection also increases. For the FF and BF algorithms, where resources are dynamically allocated, user partitions is a reasonable method of reducing the complexity; the degree of complexity reduction is proportional to the number of user partitions. For the PO and PO+SR algorithms, since the resources are allocated in a fixed manner, user partitions does not affect the complexity. In the simulations, PO and PO+SR have much lower complexity even without user partitions. The simulation results also show that power ranking does not make any meaningful improvement to system performance, either in utilisation, or in complexity.

In our investigation of user distributions, we observed that utilisation is strongly affected by the ability of all BSs to simultaneously support the users. In the scenario where users are clustered at the centre of the BSG, all users are equally supported by all BSs, and utilisation is better than that for users in a uniform distribution. In the scenario where users are clustered near the edge of the BSG, users are strongly supported by one BS, and poorly supported by the other BSs. Here, the utilisation is lower. Utilisation does not vary greatly with path loss. This is because in our simulations, we assumed that the system power is scaled according to the path loss of the environment. Shadow fading has the effect of randomising the power profile of the users. In an environment with high random shadow fading, users with a clustered distribution have a similar utilisation performance to that users randomly located in a uniform distribution.

We have also looked at system performance where user selection is based on a higher link quality requirement. As we increased the link quality requirement by lowering the SER threshold of the UCC, we observed a significant drop in utilisation of all the algorithms. For the PO algorithm, we started seeing degradation in utilisation when the user loading exceeded 60%. For the PO+SR, FF, and BF algorithms, we saw that utilisation started to plateau when $N > N_{\text{RB}} \times (N_{\text{BS}} - 1)$. If we set the system power with the higher link quality requirement, then we saw similar performance to systems with higher SER threshold (lower link quality requirement). Based on this observation, it is clear that utilisation performance is highly dependent on the overall power level of the system.

In the simulations, we also observed a strategic region of user loading, which offers a good trade-off between utilisation and complexity. In general, when the number of users is less than $N = N_{\text{RB}} \times (N_{\text{BS}} - 1)$, we see that utilisation generally trends towards the maximum utilisation. When the number of users is greater than $N = N_{\text{RB}} \times (N_{\text{BS}} - 1)$, we start to see utilisation deviating from the maximum utilisation. It may be an advantage to limit the user loading so the number of users is always below this threshold. This way, we are likely to achieve good utilisation performance even with very simple and low-complexity algorithms.

Chapter 6

Conclusion

Macrodiversity systems have many promising features that can improve system performance from a network perspective, such as improving the weak signals of users affected by shadow fading, or users at the cell-edge. They also allow multiple users to share the same resource in time and frequency, improving the overall user capacity. As a result, it has been adopted as a part of the LTE standard since Release 11. However, there are still many challenges remaining in the implementation of such systems. The issue of multi-user resource allocation is one such challenge. Traditionally, evaluating link quality of the resource-sharing users requires instantaneous channel state information (CSI), and users are selected based on performance measures such as sum capacity, or symbol error rate (SER). This becomes a challenging task in macrodiversity systems. For macrodiversity systems, instantaneous CSI could be passed to the backhaul processing unit (BPU) through the network backhaul. This creates a delay in the signal, and makes instantaneous CSI a less accurate reflection of the channel environment at the time. Passing instantaneous CSI of all users also creates a significant amount of network overheads, reducing the overall efficiency of the network. Since the system can cover a larger geographical area and more users compared to multi-user MIMO (MU-MIMO) in single-cell systems, the number of user selection combinations can become extremely large, making scheduling decisions in real time an even more challenging task. These problems limit the realisation of the user capacity potential of macrodiversity systems.

One approach to the problem is using long-term power for resource allocation decisions. Using long-term power bypasses the issue of channel estimation error introduced by the network delay, and it also reduces the communication overhead on the network backhaul. In this research, we implemented a method of finding approximate SER of users in a macrodiversity system using long-term power. This method is much more efficient than the alternative Monte Carlo methods, which find SER by repetitively sending a dummy symbol over a simulated channel; it allows us to evaluate link quality of many users in a relatively short time frame. This is particularly useful in resource allocation problems where we need to evaluate the performance of multiple user combinations before reaching an acceptable

solution. Compared to the Monte Carlo method, the proposed method overestimates SER in low SNR scenarios. In this research, we consider it an acceptable defect, because for the link quality, it is better to overestimate SER than underestimate SER, and the improvement in computation efficiency outweights the gain in accuracy. For these reasons, the approximate SER is used as the default metric for evaluating link quality. We have also considered alternative metrics for evaluating link quality, however, none of them are effective.

Our contribution in this research is developing a resource allocation method for macro-diversity systems using long-term power. This method uses the approximate SER as a prediction for link quality, and we define a UCC such that it allows resource-sharing only if all users in the user group meet the SER threshold. As a part of the resource allocation method, four different heuristic user selection algorithms were proposed, from very low complexity to moderate complexity. We developed a framework for evaluating the performance of the user selection algorithms. In this framework, we measure performance in terms of utilisation and complexity. Utilisation refers to the percentage of allocated users over the theoretical user capacity. Complexity refers to the number of SER calculations required to find a resource allocation solution. Using the framework, resource allocation is simulated in four different aspects: system dimension, user distribution, propagation parameters, and a higher link quality requirement. The key points are the following:

- *Complexity reduction with the heuristic user selection algorithms.*
  Compared to the ES algorithm, the proposed heuristic user selection algorithms have much less complexity. For a small system as in Figure 5.2, the difference in complexity is the order of 10^8 dropping to 10^2. However, even for the heuristic algorithms, the complexity can become quite significant for larger system dimensions. In Figure 5.6, the complexity of the BF algorithm is greater than 10^4. To keep user selection complexity manageable, we partitioned users and resources into smaller subsets, in the hope that this would minimise complexity for larger system dimensions. This is effective for the BF algorithm, because the complexity of the algorithm has a linear relationship with the number of users in the system. For the PO, PO+SR, and FF algorithms, the complexity varies depending on the channel condition, so the benefits are less obvious. We also ranked users according to their combined power before user selection takes place. However, we cannot observe any noticeable improvement in utilisation or complexity based on this idea. Overall, FF and PO+SR algorithms are the preferred choices because they offer good trade-offs between utilisation and complexity.

- *Utilisation is optimised if all users are equally supported by all BSs.*
  From Chapter 5, we observed that the performance is best if all users are equally supported by all BSs with strong power. In Section 5.2, if users are clustered at the centre of the BSG, the signals transmitted by all users are received by the BSs at a similar level. In this scenario, the spatial diversity of the system is maximised. On the other hand, if users are clustered around only one BS, there is low spatial diversity, so the utilisation performance is poor. This observation suggests that if there is a tendency

of users clustering at one particular spot, we could optimise the system performance by aligning the centre of the BSG with the centre of the cluster. If, on the other hand, there is a tendency for users to cluster, but in different locations at different times, we could optimise the system performance by having dynamic formations of the BSG according to the user cluster. Where users follow more a uniform distribution, we would not see much difference in performance. If the shadow fading of the environment is high, this causes a higher variance in received signal powers, making the users appear more distributed. This suggests that in urban environments where shadow fading is high, assuming random shadow fading, we can expect the received channel power has an equivalent effect of users in a uniform distribution.

- *Higher allocation rate if the spatial dimensions of the channel matrix are not fully utilised.* In the simulations, we observed across a range of environments, all algorithms have utilisation performance close to the maximum utilisation as long as the user loading is less than $N = N_{\text{RB}} \times (N_{\text{BS}} - 1)$. For this system model, the spatial dimension of the system is defined by the number of BSs, N_{BS}. This observed phenomenon suggests that as long as the spatial dimension of the channel is not fully utilised, most users can co-exist with one another regardless of their power profiles. From user's perspective, this means they have a higher allocation rate when they demand a resource from the network. In designing macrodiversity systems, we may be able to utilise this feature to minimise the user selection complexity.

From the key points, utilisation is close to maximum as long as the number of users in a user group is less than the maximum spatial dimension. When designing a macrodiversity system, we could first decide the maximum number of users which the system is intended to cater for, then have one additional BS so the maximum user capacity is always greater than the expected number of users. With this system size, we can use a low-complexity user selection algorithm, such as PO+SR or FF, and still achieve utilisation close to the maximum utilisation. Although the user capacity is not fulfilled, we can be almost certain that all users will be allocated in these very low-complexity systems, therefore the allocation rate is high. The following shows the steps for implementing a low-complexity macrodiversity system:

1. Decide on the maximum number of users (N_{max}) which the system intends to support.
2. Have BSs in the system so that $N_{\text{max}} \leq (N_{\text{BS}} - 1) \times N_{\text{RB}}$.
3. If users have the tendency to cluster at one area. Plan the system so that the BSG is centred at the user cluster.
4. Choose a user selection algorithm, so the system meets the complexity and allocation rate goals.

As an example, consider we have 20 resources available, and we want to deploy a macrodiversity system that can cater for up to 120 users. If we design the macrodiversity system so that it has 7 BSs, then according to Figure 5.6, we can achieve 76.4% utilisation with the PO+SR algorithm, and 83.8% utilisation with the FF algorithm. For the allocation rate as defined in (3.18), that equates to, respectively, an 89.1% and 97.7% guarantee of service, with complexity of about 180 and 930 SER calculations. If there are only 6 BSs in the system, at the full user loading ($N = 120$), we can expect utilisation to be about 80% and 90% respectively, and the allocation rate would be 80% and 90% as well. The complexity is higher because lower allocation rate also means the likelihood of the first candidate user meeting the UCC is lower (240 and 1820 SER calculations for the PO+SR and FF algorithms respectively).

6.1 Future Work

Some of the assumptions made in this research may not accurately reflect the real-life environments where macrodiversity systems are deployed. The following represents a short list of potential directions for research to take:

- *Resource Allocation with multiple BSGs, including the effect of inter-group interference (IGI).*
  In this research we did not consider the scenario where there are multiple BSG coexisting with one another. If there are multiple BSGs, all using different resources, it would be very inefficient in terms of the overall spectral efficiency. However, if the BSGs all use the same resources, then IGI is likely to occur. How to model IGI while integrating resource allocation for the broader picture that encompasses multiple BSGs, would be an important study for the deployment of macrodiversity systems on a large scale.

- *Dynamic BS grouping strategies.*
  As shown in Section 5.2, utilisation is maximised if a user cluster is at the centre of the BSG. On the contrary, utilisation is very poor if the user cluster is at the edge of the BSG. This depends on the number of BSs that could simultaneously support users in the system. If the formation of the BSGs can be adaptive to the user distribution at the time, then it is possible to achieve an even higher system performance and spectral efficiency.

- *Data aggregation at the network backhaul.*
  In this research we assume that once a resource is allocated to a user, and a connection between the user and the BSG is established, the signal received by the BSG will behave as it would in MIMO systems with co-located antennas. In reality, the signal received by all BSs will pass through the network backhaul before it is centrally combined and detected at the BPU. How to aggregate the data flows and to operate the network in the most effective manner, is an important study of its own.

6.2 Final Remarks

The big picture in this thesis is multi-user resource allocation in macrodiversity systems using long-term power. The goal is to increase user capacity with minimum complexity and network overhead.

Without resource-sharing, user capacity is limited to the number of available resources. With resource-sharing, user capacity within the BSG can increase greatly, based on the number of BSs. For a macrodiversity system with 3BSs, we see nearly a 100% increase in utilisation even with the simplest user selection algorithm. With more complex algorithms, utilisation can increase up to 200%. Alternatively, we can design the system so it does not use the full capacity, but the additional spatial diversity allows most users to have guaranteed services. In this thesis, we have identified that using the PO+SR, or the FF algorithm for user selection can achieve good utilisation with relatively low complexity. The final choice of the algorithm will depend on the processing power of the particular system.

Based on the framework presented here, decisions about how to construct a macrodiversity network can now be made in a way that takes account of the needs of each particular situation. These networks are a promising resource, and as we move forward, it is hoped that the research conducted here will allow us to take advantage of the best points of balance between speed and reliability of service delivery.

Appendix A

SER Calculation using Long-Term Power

A.1 Derivation of exact SER in Macrodiversity Scenarios with No Resource-Sharing

This section describes the derivation of exact SER for the single user macrodiversity scenario assuming *Quadrature Phase Shift Keying (QPSK)* is used for the base-band modulation scheme. Equation numbers listed in reference to integrals are taken from the 7th edition of *Table of Integrals, Series and Products* by Gradshteyn and Ryzhik [79].

Consider the received signal from a single source given by

$$\mathbf{r} = \mathbf{h}s + \mathbf{n}, \tag{A.1}$$

where $\mathbf{r}$ is the signal received at the BS array, $\mathbf{h}$ is the channel matrix with dimension $[N_{\mathrm{R}} \times 1]$, where N_{R} is the number of receive antennas; for the case of BSs with a single antenna, N_{R} is the number of BSs. s is the transmit symbol, in the form of a scalar complex number. We assume $\mathrm{E}|s|^2 = 1$ for the following derivation. $\mathbf{n}$ is the noise added at the receiver where each element, n_j, of $\mathbf{n}$ satisfies $n_j \sim \mathcal{CN}(0, \sigma^2)$.

As explained in Section 3.3, the channel matrix $\mathbf{h}$ has the structure:

$$\mathbf{h} = \begin{bmatrix} h_{1,1} \\ h_{2,1} \\ \vdots \\ h_{N_{\mathrm{R}},1} \end{bmatrix} = \begin{bmatrix} \sqrt{P_{1,1}}u_{1,1} \\ \sqrt{P_{2,1}}u_{2,1} \\ \vdots \\ \sqrt{P_{N_{\mathrm{R}},1}}u_{N_{\mathrm{R}},1} \end{bmatrix}, \tag{A.2}$$

where $h_{i,1}$ is the channel coefficient between the user and the BS_i, The $h_{i,1}$ term can be

represented by the long-term power component, $P_{i,1}$, and the fast fading component, $u_{i,1}$. Here $h_{i,1} \sim \mathcal{CN}(0, P_{i,1})$ and $u_{i,1} \sim \mathcal{CN}(0, 1)$.

The transmit symbol can be detected by applying a decoding matrix, $\mathbf{w}$, to the received signal, $\mathbf{r}$, giving

$$\widehat{\mathbf{r}} = \mathbf{w}\mathbf{r}, \tag{A.3}$$

where $\widehat{\mathbf{r}}$ is the output of the receive combiner. $\widehat{\mathbf{r}} = s + \widehat{\mathbf{n}}$.

In the single user scenario, maximum ratio combining (MRC) and zero-forcing (ZF) detection schemes have the same decoding matrix where

$$\mathbf{w} = \frac{\mathbf{h}^\dagger}{\mathbf{h}^\dagger\mathbf{h}}. \tag{A.4}$$

The combiner output $\widehat{\mathbf{r}}$, is therefore

$$\begin{aligned}
\widehat{\mathbf{r}} &= \frac{\mathbf{h}^\dagger}{\mathbf{h}^\dagger\mathbf{h}}\mathbf{r} \\
&= \frac{\mathbf{h}^\dagger}{\mathbf{h}^\dagger\mathbf{h}}\mathbf{h}s + \frac{\mathbf{h}^\dagger}{\mathbf{h}^\dagger\mathbf{h}}\mathbf{n} \\
&= s + \frac{\mathbf{h}^\dagger}{\mathbf{h}^\dagger\mathbf{h}}\mathbf{n} \\
&= s + \widehat{\mathbf{n}},
\end{aligned} \tag{A.5}$$

where $\widehat{\mathbf{n}}$ is the adjusted noise after receive combining.

The signal-to-noise ratio (SNR) is

$$\begin{aligned}
\text{SNR} &= \frac{E[|s|^2]}{E[|\widehat{\mathbf{n}}|^2]} \\
&= \frac{1}{E\left[(\mathbf{w}\mathbf{n})(\mathbf{w}\mathbf{n})^\dagger\right]} \\
&= \frac{1}{E\left[\mathbf{w}\mathbf{n}\mathbf{n}^\dagger\mathbf{w}^\dagger\right]} \\
&= \frac{1}{E\left[\frac{\mathbf{h}^\dagger}{\mathbf{h}^\dagger\mathbf{h}}\mathbf{n}\mathbf{n}^\dagger\frac{\mathbf{h}}{\mathbf{h}\mathbf{h}^\dagger}\right]} \\
&= \frac{1}{\sigma^2(\mathbf{h}\mathbf{h}^\dagger)^{-1}} \\
&= \frac{1}{\sigma^2(\mathbf{h}^{\dagger-1}\mathbf{h}^{-1})} \\
&= \frac{\mathbf{h}^\dagger\mathbf{h}}{\sigma^2}.
\end{aligned} \tag{A.6}$$

Hence, if MRC or ZF is used for signal detection, the output signal power is $\mathbf{h}^\dagger\mathbf{h}$:

$$\begin{aligned}\mathbf{h}^\dagger\mathbf{h} &= [{h_{1,1}}^* \dots {h_{N_\mathrm{R},1}}^*] \begin{bmatrix} h_{1,1} \\ \vdots \\ h_{N_\mathrm{R},1} \end{bmatrix} \\ &= \sum_{i=1}^{N_\mathrm{R}} |h_{i,1}|^2 \\ &= \sum_{i=1}^{N_\mathrm{R}} P_{i,1}|u_{i,1}|^2.\end{aligned} \tag{A.7}$$

To compute the SER, we need to first find the *probability density function* (PDF) of $\mathbf{h}^\dagger\mathbf{h}$. We can describe $\mathbf{h}^\dagger\mathbf{h}$ in (A.7) as a sum of multiple random variables having Chi-Square distributions:

$$\begin{aligned}\mathbf{h}^\dagger\mathbf{h} &= \sum_{i=1}^{N_\mathrm{R}} P_{i,1}|u_{i,1}|^2 \\ &= \sum_{i=1}^{N_\mathrm{R}} \frac{P_{i,1}}{2} \times 2|u_{i,1}|^2 \\ &= \sum_{i=1}^{N_\mathrm{R}} \frac{P_{i,1}}{2} {\mathcal{X}_2}^2(i),\end{aligned} \tag{A.8}$$

where $\mathcal{X}_2^2(i)$ is the ith fast fading component normalised to a standard Chi-Square distribution with two degrees of freedom. Hence, $\mathbf{h}^\dagger\mathbf{h}$ is a weighted sum of $\mathcal{X}_2^2$ variables.

Now, from [84], it is known that the PDF of $\mathbf{h}^\dagger\mathbf{h}$ in (A.8) is given by

$$P_x(x) = \frac{1}{2} \sum_{i=1}^{N_\mathrm{R}} \frac{b_{i,1}}{\beta_{i,1}} e^{-\frac{x}{2\beta_{i,1}}}, \tag{A.9}$$

where

$$\begin{aligned}\beta_{i,1} &= \frac{P_{i,1}}{2}, \\ b_{i,1} &= {\beta_{i,1}}^{N_\mathrm{R}-1} \prod_{i \neq j}^{N_\mathrm{R}} (\beta_{i,1} - \beta_{j,1})^{-1}.\end{aligned} \tag{A.10}$$

Figure A.1 describes a standard constellation map for the QPSK modulation scheme with symbol amplitude normalised to 1. SER is calculated based on the tail error probability of the symbol moving out of the constellation boundaries.

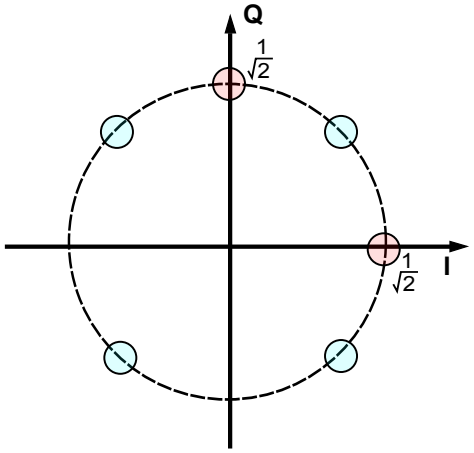

Figure A.1: QPSK constellation plane. Blue dots are designated signal points, red dots are closest signal boundaries in reference to the upper right blue dot where an error occurs.

From Figure A.1, assuming $s = \frac{1}{\sqrt{2}} + j\frac{1}{\sqrt{2}}$, SER can be expressed as

$$\begin{aligned}
SER &= 1 - P\left(\frac{1}{\sqrt{2}} + \frac{\mathbf{n_I}}{\sqrt{\mathbf{h}^\dagger\mathbf{h}}} > 0\right) P\left(\frac{1}{\sqrt{2}} + \frac{\mathbf{n_Q}}{\sqrt{\mathbf{h}^\dagger\mathbf{h}}} > 0\right) \\
&= 1 - \mathbf{E}\left[P\left(\mathbf{n_I} > -\sqrt{\frac{\mathbf{h}^\dagger\mathbf{h}}{2}}\right)^2\right] \\
&= 1 - \mathbf{E}\left[\left(1 - P\left(\mathbf{n_I} > \sqrt{\frac{\mathbf{h}^\dagger\mathbf{h}}{2}}\right)\right)^2\right], \text{Since } \mathbf{n_I} = -\mathbf{n_I}, \\
&= 1 - \mathbf{E}\left[\left(1 - P\left(\tilde{\mathbf{n}} > \sqrt{\frac{\mathbf{h}^\dagger\mathbf{h}}{2\frac{\sigma^2}{2}}}\right)\right)^2\right] \\
&= 1 - \mathbf{E}\left[\left(1 - Q\left(\sqrt{\frac{\mathbf{h}^\dagger\mathbf{h}}{\sigma^2}}\right)\right)^2\right] \\
&= 1 - \mathbf{E}\left[1 - 2Q\left(\sqrt{\frac{\mathbf{h}^\dagger\mathbf{h}}{\sigma^2}}\right) + Q^2\left(\sqrt{\frac{\mathbf{h}^\dagger\mathbf{h}}{\sigma^2}}\right)\right] \\
&= 2\mathbf{E}\left[Q\left(\sqrt{\frac{\mathbf{h}^\dagger\mathbf{h}}{\sigma^2}}\right)\right] - \mathbf{E}\left[Q^2\left(\sqrt{\frac{\mathbf{h}^\dagger\mathbf{h}}{\sigma^2}}\right)\right].
\end{aligned} \tag{A.11}$$

In (A.11), $\mathbf{n_I}$ and $\mathbf{n_Q}$ are the in-phase and quadrature components of the noise, $\mathbf{n}$, where each element in $\mathbf{n_I}$ and $\mathbf{n_Q} \sim \mathcal{CN}(0, \frac{\sigma^2}{2})$. $\tilde{\mathbf{n}}$ is a real noise component with variance normalized to 1. The Q-function is the tail probability of the standard Gaussian channel.

Substituting (A.9) in (A.11), gives

$$\begin{aligned} SER = &\sum_{i=1}^{N_R} \left(\frac{b_{i,1}}{\beta_{i,1}}\right) \int_0^\infty Q\left(\sqrt{\frac{x}{\sigma^2}}\right) e^{-\frac{x}{2\beta_{i,1}}} dx - \\ &\frac{1}{2} \sum_{i=1}^{N_R} \left(\frac{b_{i,1}}{\beta_{i,1}}\right) \int_0^\infty Q^2\left(\sqrt{\frac{x}{\sigma^2}}\right) e^{-\frac{x}{2\beta_{i,1}}} dx. \end{aligned} \tag{A.12}$$

From (A.12), we see that integrals of the form of $\int_0^\infty Q(\sqrt{bx})e^{-ax}dx$ and $\int_0^\infty Q^2(\sqrt{bx})e^{-ax}dx$ are required to compute the SER. These integrals are derived in A.1.1 and A.1.2 below.

A.1.1 Computation of $\int_0^\infty Q(\sqrt{bx})e^{-ax}dx$:

The Q-function can be expressed in terms of the error function as

$$Q(x) = \frac{1}{2} - \frac{1}{2}\text{erf}\left(\frac{x}{\sqrt{2}}\right). \tag{A.13}$$

The expression, $\int_0^\infty Q(\sqrt{bx})e^{-ax}dx$, then becomes

$$\begin{aligned} \int_0^\infty Q(\sqrt{bx})e^{-ax}dx &= \int_0^\infty \left(\frac{1}{2} - \frac{1}{2}\text{erf}\left(\sqrt{\frac{bx}{2}}\right)\right) e^{-ax}dx \\ &= \left[-\frac{e^{-ax}}{2a}\right]_0^\infty - \frac{1}{2}\int_0^\infty \text{erf}\left(\sqrt{\frac{bx}{2}}\right) e^{-ax}dx \\ &= \frac{1}{2a} - \frac{1}{2}\int_0^\infty \text{erf}\left(\sqrt{\frac{bx}{2}}\right) e^{-ax}dx. \end{aligned} \tag{A.14}$$

In Gradshteyn and Ryzhik (*eqn.6.283.2*) [79],

$$\int_0^\infty \text{erf}(\sqrt{qt})e^{-pt}dt = \frac{\sqrt{q}}{p}\frac{1}{\sqrt{p+q}}. \tag{A.15}$$

Applying (A.15) in (A.14) gives

$$\begin{aligned} \int_0^\infty Q(\sqrt{bx})e^{-ax}dx &= \frac{1}{2a} - \frac{1}{2}\left(\frac{1}{a}\sqrt{\frac{b}{2}}\frac{1}{\sqrt{a+b/2}}\right) \\ &= \frac{1}{2a}\left(1 - \frac{1}{\sqrt{\frac{2a}{b}+1}}\right). \end{aligned} \tag{A.16}$$

A.1.2 Computation of $\int_0^\infty Q^2(\sqrt{bx})e^{-ax}dx$:

Using integration by parts, the expression $\int_0^\infty Q^2(\sqrt{bx})e^{-ax}dx$ becomes

$$\int_0^\infty Q^2(\sqrt{bx})e^{-ax}dx = \left[Q^2(\sqrt{bx})\left(\frac{e^{-ax}}{-a}\right)\right]_0^\infty - \int_0^\infty 2Q(\sqrt{bx})\left(\frac{d}{dx}Q(\sqrt{bx})\right)\left(\frac{e^{-ax}}{-a}\right)dx. \tag{A.17}$$

For the Q-function, the derivative in (A.17) is expanded as below:

$$Q(x) = \frac{1}{\sqrt{2\pi}}\int_x^\infty e^{-\frac{u^2}{2}}du, \tag{A.18}$$

$$\frac{d}{dx}Q(x) = -\frac{1}{\sqrt{2\pi}}e^{-\frac{x^2}{2}}, \tag{A.19}$$

$$\frac{d}{dx}Q(y) = \left[\frac{d}{dy}Q(y)\right]\frac{dy}{dx},\ y = \sqrt{bx},\ \frac{dy}{dx} = \frac{\sqrt{b}}{2}x^{-\frac{1}{2}}, \tag{A.20}$$

$$\frac{d}{dx}Q(\sqrt{bx}) = -\frac{1}{\sqrt{2\pi}}e^{-\frac{bx}{2}}\frac{\sqrt{b}}{2}x^{-\frac{1}{2}}. \tag{A.21}$$

Applying (A.21) in (A.17) we have

$$\begin{aligned}\int_0^\infty Q^2(\sqrt{bx})e^{-ax}dx =& \frac{1}{4a} - \int_0^\infty 2Q(\sqrt{bx})\left(-\frac{1}{\sqrt{2\pi}}e^{-\frac{bx}{2}}\frac{\sqrt{b}}{2}x^{-\frac{1}{2}}\right)\left(\frac{e^{-ax}}{-a}\right)dx \\ =& \frac{1}{4a} - \frac{\sqrt{b}}{a\sqrt{2\pi}}\int_0^\infty Q(\sqrt{bx})x^{-\frac{1}{2}}e^{-(a+\frac{b}{2})x}dx.\end{aligned} \tag{A.22}$$

For $y = \sqrt{bx}$, $x = \frac{y^2}{b}$, $x^{-\frac{1}{2}} = \frac{\sqrt{b}}{y}$, $dx = \frac{2y}{b}dy$, (A.22) becomes

$$\begin{aligned}\int_0^\infty Q^2(\sqrt{bx})e^{-ax}dx =& \frac{1}{4a} - \frac{\sqrt{b}}{a\sqrt{2\pi}}\int_0^\infty Q(\sqrt{bx})x^{-\frac{1}{2}}e^{-(a+\frac{b}{2})x}dx \\ =& \frac{1}{4a} - \frac{\sqrt{b}}{a\sqrt{2\pi}}\int_0^\infty Q(y)\left(\frac{\sqrt{b}}{y}\right)\left(\frac{2y}{b}\right)e^{-(a+\frac{b}{2})\frac{y^2}{b}}dy \\ =& \frac{1}{4a} - \frac{2}{a\sqrt{2\pi}}\int_0^\infty Q(y)e^{-(\frac{a}{b}+\frac{1}{2})y^2}dy \\ =& \frac{1}{4a} - \frac{2}{a\sqrt{2\pi}}\int_0^\infty \left(\frac{1}{2} - \frac{1}{2}\mathrm{erf}\left(\frac{y}{\sqrt{2}}\right)\right)e^{-(\frac{a}{b}+\frac{1}{2})y^2}dy \\ =& \frac{1}{4a} - \frac{1}{a\sqrt{2\pi}}\int_0^\infty \left(1 - \mathrm{erf}\left(\frac{y}{\sqrt{2}}\right)\right)e^{-(\frac{a}{b}+\frac{1}{2})y^2}dy.\end{aligned} \tag{A.23}$$

For $v = \frac{y}{\sqrt{2}}$, $y = \sqrt{2}v$, $dy = \sqrt{2}dv$, (A.23) becomes

$$\begin{aligned}\int_0^\infty Q^2(\sqrt{bx})e^{-ax}dx =& \frac{1}{4a} - \frac{1}{a\sqrt{2\pi}}\int_0^\infty (1 - erf(v))\, e^{-(\frac{a}{b}+\frac{1}{2})2v^2}\sqrt{2}dv \\ =& \frac{1}{4a} - \frac{1}{a\sqrt{\pi}}\int_0^\infty (1 - erf(v))\, e^{-(\frac{2a}{b}+1)v^2}dv.\end{aligned} \tag{A.24}$$

In Gradshteyn and Ryzhik (*eqn.6.285.1*) [79],

$$\int_0^\infty [1 - \mathrm{erf}(v)]e^{-\mu^2 v^2}dv = \frac{\arctan(\mu)}{\sqrt{\pi}\mu}. \tag{A.25}$$

Hence, (A.24) becomes

$$\begin{aligned}\int_0^\infty Q^2(\sqrt{bx})e^{-ax}dx =& \frac{1}{4a} - \frac{1}{a\sqrt{\pi}}\left(\frac{\arctan(\mu)}{\sqrt{\pi}\mu}\right) \\ =& \frac{1}{4a} - \frac{1}{a\pi\sqrt{\frac{2a}{b}+1}}\arctan\left(\sqrt{\frac{2a}{b}+1}\right).\end{aligned} \tag{A.26}$$

Substituting (A.26) and (A.16) in (A.12) gives

$$\begin{aligned}SER =& \sum_{i=1}^{N_\mathrm{R}}\left(\frac{b_{i,1}}{\beta_{i,1}}\right)\frac{1}{2a}\left(1 - \sqrt{\frac{b}{2a+b}}\right) - \frac{1}{2}\sum_{i=1}^{N_\mathrm{R}}\left(\frac{b_{i,1}}{\beta_{i,1}}\right)\left(\frac{1}{4a} - \frac{1}{a\pi\sqrt{\frac{2a}{b}+1}}\arctan\left(\sqrt{\frac{2a}{b}+1}\right)\right) \\ =& \sum_{i=1}^{N_\mathrm{R}}\left(\frac{b_{i,1}}{\beta_{i,1}}\right)\frac{1}{2a}\left(\left(1 - \frac{1}{\sqrt{\frac{2a}{b}+1}}\right) - \left(\frac{1}{4} - \frac{1}{\pi\sqrt{\frac{2a}{b}+1}}\arctan\left(\sqrt{\frac{2a}{b}+1}\right)\right)\right) \\ =& \sum_{i=1}^{N_\mathrm{R}}\left(\frac{b_{i,1}}{\beta_{i,1}}\right)\frac{1}{2a}\left(\frac{3}{4} - \frac{1}{\sqrt{\frac{2a}{b}+1}}\left(1 - \frac{1}{\pi}\arctan\left(\sqrt{\frac{2a}{b}+1}\right)\right)\right).\end{aligned} \tag{A.27}$$

Substituting $a = \frac{1}{2\beta_{i,1}} = \frac{1}{P_{i,1}}$, $b = \frac{1}{\sigma^2}$, (A.27) becomes

$$SER = \sum_{i=1}^{N_\mathrm{R}} b_{i,1}\left(\frac{3}{4} - \frac{1}{\sqrt{\frac{2\sigma^2}{P_{i,1}}+1}}\left(1 - \frac{1}{\pi}\arctan\left(\sqrt{\frac{2\sigma^2}{P_{i,1}}+1}\right)\right),\right) \tag{A.28}$$

where $b_{i,1} = \frac{P_{i,1}}{2}^{(N_\mathrm{R}-1)}\prod_{i\neq j}^{N_\mathrm{R}} 2\left(P_{i,1} - P_{j,1}\right)^{-1}$. We now have a full expression for SER in terms of the noise variance, σ^2, and the long-term powers, $P_{i,1}$, given by

$$SER = \sum_{i=1}^{N_\mathrm{R}}\frac{P_{i,1}}{2}^{(N_\mathrm{R}-1)}\prod_{i\neq j}^{N_\mathrm{R}} 2\left(P_{i,1} - P_{j,1}\right)^{-1}\left(\frac{3}{4} - \frac{1}{\sqrt{\frac{2\sigma^2}{P_{i,1}}+1}}\left(1 - \frac{1}{\pi}\arctan\left(\sqrt{\frac{2\sigma^2}{P_{i,1}}+1}\right)\right)\right). \tag{A.29}$$

Appendix B

Results of Alternative Metrics for UCC

We are interested in finding alternative metrics M, that can effectively replace the existing SER calculation with lower complexity. In our investigation, we proposed three different metrics, and we compare their proximity to the analytical SER using a log-log scale plot.

We are primarily interested in modelling the SER for the resource-sharing scenarios. We use a small macrodiversity system to observe the relationship. The system has 3 BSs, 1 resource, and 3 users. All 3 users share the same resource. To maximise the dynamic range of our signals, we make the path loss exponent $\gamma = 5$, and shadow fading standard deviation $\sigma_{\text{SF}} = 12$. Table B.1 shows the environment settings used in the simulation.

Table B.1: Summary of the environment settings.

System Parameters	**Symbol**	**Value**
Number of BSs	N_{BS}	3
Number of Resources	N_{RB}	1
Number of Partitions	N_{P}	1
Number of Users	N	3
User Distribution	-	Uniform
Modulation Scheme	-	QPSK
SER Limit	-	10^{-2}
Path Loss Exponent	γ	5
Shadow Fading s.d.	σ_{SF}	12
Power Scaling Factor	A	Adaptive

To find out the relationship between the alternative metrics and the analytical SER in a stat-

istical sense, we simulate 1000 samples, each sample has users located in different places. Figure B.1 shows an example of the log-log scale plot. Here, M is the analytical SER itself. From the figure, we see the two parameters follow a linear relationship, from a very low SER (10^{-10}), to a very high SER ($\sim 10^{0}$). Ideally, we would like the alternative metric to follow a similar relationship.

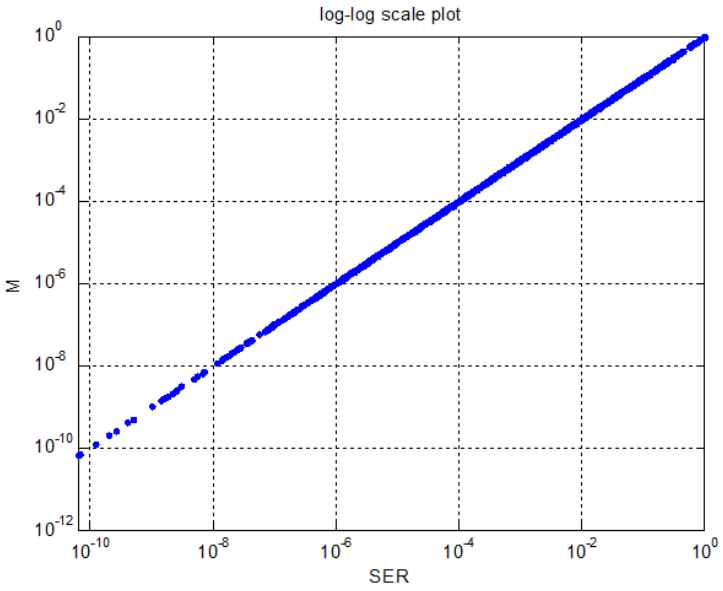

Figure B.1: Log-log plot of the analytical SER results with themselves.

Alternative metric with no resource-sharing:

This metric assumes that we can replace the analytical SER for resource-sharing scenarios by the exact SER for no resource-sharing scenarios. From the figure, we can see that for a given SER, the variation in M is of the order of 10^6, which is too wide for the purpose of the metric.

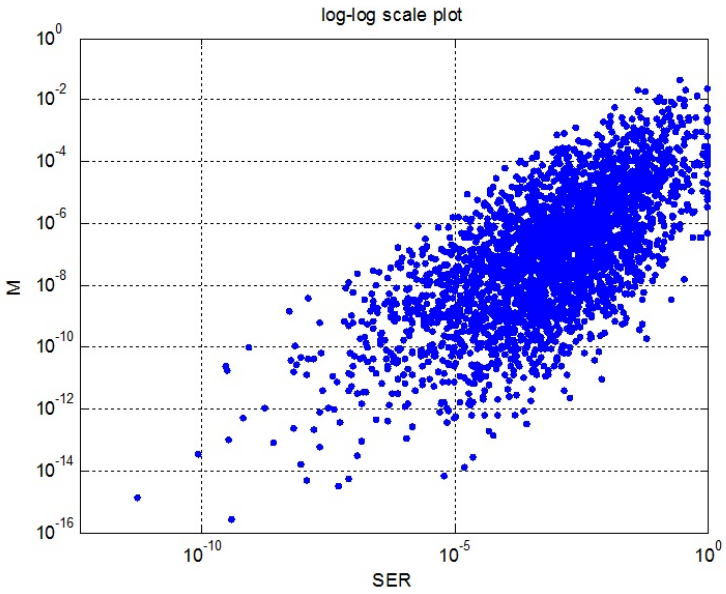

Figure B.2: Log-log plot of the analytical SER results v.s. the SER calculation for single-user scenario.

Alternative metric using part of equation (3.9):

Consider using part of $\tilde{K}_0$ as the simplified metric, where

$$M = \frac{\mathrm{Perm}(\mathbf{Q}_n)}{|\mathbf{P}_n|}. \tag{B.1}$$

We could not observe any meaningful correlation between M and SER.

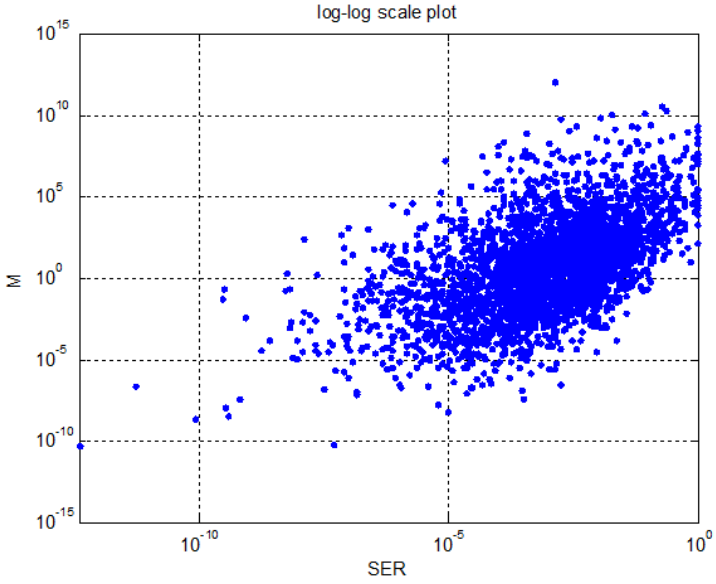

Figure B.3: Log-log plot of the analytical SER results v.s. $M = \frac{\mathrm{Perm}(\mathbf{Q}_n)}{|\mathbf{P}_n|}$.

From our investigation, we could not find any alternative metric that is a meaningful low-complexity replacement of the analytical SER calculation for the resource-sharing scenarios. Therefore, the only metric we used for determining the compatibility criteria of the UCC is the SER.

Bibliography

[1] D. A. Basnayaka, P. J. Smith, and P. A. Martin, "Performance analysis of macrodiversity MIMO Systems with MMSE and ZF Receivers in Flat Rayleigh Fading," *Wireless Communications, IEEE Transactions on*, vol. 12, no. 5, pp. 2240–2251, May 2013.

[2] M. Dohler, R. Heath, A. Lozano, C. B. Papadias, and R. A. Valenzuela, "Is the PHY layer dead?" *Communications Magazine, IEEE*, vol. 49, no. 4, pp. 159–165, 2011.

[3] 3GPP, "TR 36.819 Coordinated Multi-Point Operation for LTE physical layer aspects," ETSI, Tech. Rep. 36.819, 12 2011.

[4] M. Baker, "LTE-Advanced Physical Layer," 3GPP, Tech. Rep., 2009.

[5] M. K. Karakayali, G. J. Foschini, and R. A. Valenzuela, "Network coordination for spectrally efficient communications in cellular systems," *Wireless Communications, IEEE*, vol. 13, no. 4, pp. 56–61, 2006.

[6] D. Lee, H. Seo, B. Clerckx, E. Hardouin, D. Mazzarese, S. Nagata, and K. Sayana, "Coordinated multipoint transmission and reception in LTE-advanced: deployment scenarios and operational challenges," *Communications Magazine, IEEE*, vol. 50, no. 2, pp. 148–155, 2012.

[7] P. Marsch and G. P. Fettweis, *Coordinated Multi-Point in Mobile Communications: From Theory to Practice*. Cambridge University Press, 2011.

[8] Q. H. Spencer and A. L. Swindlehurst, "Channel allocation in multi-user MIMO wireless communications systems," in *Communications, 2004 IEEE International Conference on*, vol. 5. IEEE, 2004, pp. 3035–3039.

[9] T. F. Maciel and A. Klein, "On the Performance, Complexity, and Fairness of Suboptimal Resource Allocation for Multiuser MIMO–OFDMA Systems," *Vehicular Technology, IEEE Transactions on*, vol. 59, no. 1, pp. 406–419, 2010.

[10] D. Wang, X. Xu, X. Chen, and X. Tao, "Joint scheduling and resource allocation based on genetic algorithm for coordinated multi-point transmission using adaptive modulation," in *Personal Indoor and Mobile Radio Communications (PIMRC), 2012 IEEE 23rd International Symposium on*. IEEE, 2012, pp. 220–225.

[11] Q. H. Spencer, C. B. Peel, A. L. Swindlehurst, and M. Haardt, "An introduction to the multi-user MIMO downlink," *Communications Magazine, IEEE*, vol. 42, no. 10, pp. 60–67, 2004.

[12] N. Pau, *Optimal antenna and user clustering for implementation of macro-diversity in future cellular systems*. WRC, Jan. 2013.

[13] F. Shad, T. D. Todd, V. Kezys, and J. Litva, "Dynamic slot allocation (DSA) in indoor SDMA/TDMA using a smart antenna basestation," *Networking, IEEE/ACM Transactions on*, vol. 9, no. 1, pp. 69–81, 2001.

[14] M. Fuchs, G. Del Galdo, and M. Haardt, "A novel tree-based scheduling algorithm for the downlink of multi-user MIMO systems with ZF beamforming," in *Acoustics, Speech, and Signal Processing, 2005. Proceedings.(ICASSP'05). IEEE International Conference on*, vol. 3. IEEE, March 2005, pp. 1121–1124.

[15] T. F. Maciel and A. Klein, "A low-complexity SDMA grouping strategy for the downlink of Multi-User MIMO systems," in *Personal, Indoor and Mobile Radio Communications, 2006 IEEE 17th International Symposium on*. IEEE, 2006, pp. 1–5.

[16] S. Wesemann, W. Rave, and G. Fettweis, "Combinatorial advantages due to joint resource allocation in uplink CoMP systems," in *Wireless Communication Systems (ISWCS), 2011 8th International Symposium on*. IEEE, 2011, pp. 740–744.

[17] R. Irmer, H. Droste, P. Marsch, M. Grieger, G. Fettweis, S. Brueck, H.-P. Mayer, L. Thiele, and V. Jungnickel, "Coordinated multipoint: Concepts, performance, and field trial results," *Communications Magazine, IEEE*, vol. 49, no. 2, pp. 102–111, 2011.

[18] D. Basnayaka, "Macrodiversity MIMO Transceivers," Ph.D. dissertation, University of Canterbury, 2012.

[19] C. Jackson, "Dynamic sharing of radio spectrum: A brief history," in *New Frontiers in Dynamic Spectrum Access Networks, 2005. DySPAN 2005. 2005 First IEEE International Symposium on*. IEEE, 2005, pp. 445–466.

[20] *Radio Regulations*, ITU Appendix 13, part A2, 5, 2001.

[21] T. Ojanpera and R. Prasad, "An overview of air interface multiple access for IMT-2000/UMTS," *Communications Magazine, IEEE*, vol. 36, no. 9, pp. 82–86, 1998.

[22] S. Hara and R. Prasad, "Overview of multicarrier CDMA," *Communications Magazine, IEEE*, vol. 35, no. 12, pp. 126–133, 1997.

[23] T. S. Rappaport, *Wireless Communications: Principles and Practice*. Prentice Hall, 2002.

[24] N. Abramson, "THE ALOHA SYSTEM: another alternative for computer communications," in *Proceedings of the November 17-19, 1970, fall joint computer conference*. ACM, 1970, pp. 281–285.

[25] L. G. Roberts, "ALOHA packet system with and without slots and capture," *ACM SIGCOMM Computer Communication Review*, vol. 5, no. 2, pp. 28–42, 1975.

[26] C. Krishna, *Real-Time Systems*. Wiley Online Library, 1999.

[27] R. Knopp and P. A. Humblet, "Information capacity and power control in single-cell multiuser communications," in *Communications, 1995. ICC'95 Seattle,'Gateway to Globalization', 1995 IEEE International Conference on*, vol. 1. IEEE, 1995, pp. 331–335.

[28] W. Ajib and D. Haccoun, "An overview of scheduling algorithms in MIMO-based fourth-generation wireless systems," *Network, IEEE*, vol. 19, no. 5, pp. 43–48, 2005.

[29] L. Yang and M.-S. Alouini, "Performance analysis of multiuser selection diversity," *Vehicular Technology, IEEE Transactions on*, vol. 55, no. 6, pp. 1848–1861, 2006.

[30] A. Reichman, "An overview of multi-mode multi-user adaptation and scheduling techniques in MIMO-based fourth-generation wireless systems," in *Electrical and Electronics Engineers in Israel, 2008. IEEEI 2008. IEEE 25th Convention of*. IEEE, 2008, pp. 726–730.

[31] S. T. Chung and A. J. Goldsmith, "Degrees of freedom in adaptive modulation: a unified view," *Communications, IEEE Transactions on*, vol. 49, no. 9, pp. 1561–1571, 2001.

[32] E. Dahlman, S. Parkvall, and J. Skold, *4G: LTE/LTE-Advanced for Mobile Broadband: LTE/LTE-Advanced for Mobile Broadband*. Academic Press, 2011.

[33] V. Hassel, "Design Issues and Performance Analysis for Opportunitistic Scheduling Algorithms in Wireless Networks," Ph.D. dissertation, Norwegian University of Science and Technology, 2007.

[34] F. P. Kelly, A. K. Maulloo, and D. K. Tan, "Rate control for communication networks: shadow prices, proportional fairness and stability," *Journal of the Operational Research society*, vol. 49, no. 3, pp. 237–252, 1998.

[35] Y. Cao and V. O. Li, "Scheduling algorithms in broadband wireless networks," *Proceedings of the IEEE*, vol. 89, no. 1, pp. 76–87, 2001.

[36] X. Liu, E. K. Chong, and N. B. Shroff, "A framework for opportunistic scheduling in wireless networks," *Computer Networks*, vol. 41, no. 4, pp. 451–474, 2003.

[37] H. Kim, K. Kim, Y. Han, and S. Yun, "A proportional fair scheduling for multicarrier transmission systems," in *Vehicular Technology Conference, 2004. VTC2004-Fall. 2004 IEEE 60th*, vol. 1. IEEE, 2004, pp. 409–413.

[38] R. Kwan and C. Leung, "A survey of scheduling and interference mitigation in LTE," *Journal of Electrical and Computer Engineering*, 2010.

[39] E. Biglieri, *MIMO Wireless Communications*. Cambridge University Press, 2007.

[40] A. Tolli and M. Juntti, "Scheduling for multiuser MIMO downlink with linear processing," in *Personal, Indoor and Mobile Radio Communications, 2005. PIMRC 2005. IEEE 16th International Symposium on*, vol. 1. IEEE, 2005, pp. 156–160.

[41] D. Choi, D. Lee, and J. H. Lee, "Resource allocation for CoMP with multiuser MIMO-OFDMA," *Vehicular Technology, IEEE Transactions on*, vol. 60, no. 9, pp. 4626–4632, 2011.

[42] T. F. Maciel and A. Klein, "A convex quadratic SDMA grouping algorithm based on spatial correlation," in *Communications, 2007. ICC'07. IEEE International Conference on*. IEEE, 2007, pp. 5342–5347.

[43] B. Bandemer and S. Visuri, "Capacity-based uplink scheduling using long-term channel knowledge," in *Communications, 2007. ICC'07. IEEE International Conference on*. IEEE, 2007, pp. 785–790.

[44] D. Basnayaka, P. Smith, and P. Martin, "Ergodic sum capacity of macrodiversity MIMO systems in flat Rayleigh fading," in *Information Theory Proceedings (ISIT), 2012 IEEE International Symposium on*. IEEE, 2012, pp. 2171–2175.

[45] D. Basnayaka, P. Smith, and P. Martin, "Symbol error rate performance for macrodiversity maximal ratio combining in flat Rayleigh fading," in *Communications Theory Workshop (AusCTW), 2012 Australian*. IEEE, 2012, pp. 25–30.

[46] Y. J. Zhang and K. B. Letaief, "An efficient resource-allocation scheme for spatial multiuser access in MIMO/OFDM systems," *Communications, IEEE Transactions on*, vol. 53, no. 1, pp. 107–116, 2005.

[47] T. F. Maciel and A. Klein, "A resource allocation strategy for SDMA/OFDMA systems," in *Mobile and Wireless Communications Summit, 2007. 16th IST*. IEEE, 2007, pp. 1–5.

[48] J. Sharony, "Introduction to Wireless MIMO–Theory and Applications," *IEEE Long Island Sect.*, vol. 15, November 2006.

[49] A. Panajotovic, M. Stefanovic, and D. Draca, "Effect of microdiversity and macrodiversity on average bit error probability in shadowed fading channels in the presence of interference," *ETRI Journal*, vol. 31, no. 5, 2009.

[50] L. Juho, H. Jin-Kyu *et al.*, "MIMO technologies in 3GPP LTE and LTE-advanced," *EURASIP Journal on Wireless Communications and Networking*, vol. 2009, 2009.

[51] Bell Labs Research Project, "Network MIMO: Coherently-Coordinated Base Stations," Alcatel-Lucent, Tech. Rep., 2008.

[52] H. Huh, A. Tulino, and G. Caire, "Network MIMO With Linear Zero-Forcing Beamforming: Large System Analysis, Impact of Channel Estimation, and Reduced-Complexity Scheduling," *Information Theory, IEEE Transactions on*, vol. 58, no. 5, pp. 2911–2934, 2012.

[53] C. Mihailescu, X. Lagrange, and P. Godlewski, "Soft handover analysis in downlink UMTS WCDMA system," in *Mobile Multimedia Communications, 1999.(MoMuC'99) 1999 IEEE International Workshop on*. IEEE, 1999, pp. 279–285.

[54] R. Rummler, I. Ashraf, and A. Aghvami, "On the capacity of different channel selection strategies for multicast transmissions in WCDMA," *Vehicular Technology, IEEE Transactions on*, vol. 56, no. 4, pp. 2180–2193, 2007.

[55] B. Marchent and M. McTiffin, "Handover and macro diversity for 3rd generation mobile systems within atm fixed networks," in *Global Telecommunications Conference, 1996. GLOBECOM'96.'Communications: The Key to Global Prosperity*, vol. 2. IEEE, 1996, pp. 1151–1155.

[56] C. Lee and R. Steele, "Effect of soft and softer handoffs on CDMA system capacity," *Vehicular Technology, IEEE Transactions on*, vol. 47, no. 3, pp. 830–841, 1998.

[57] L. Xiao, J. Yang, L. Hui, and W. Zhang, "Handover algorithm in WiMAX system," in *Communications and Mobile Computing (CMC), 2011 Third International Conference on*. IEEE, 2011, pp. 393–396.

[58] Z. Becvar and J. Zelenka, "Handovers in the Mobile WiMAX," *Research in Telecommunication Technology*, vol. 1, pp. 147–50, 2006.

[59] M. Alatise, M. Mzyece, and A. Kurien, "A Handover Scheme for Mobile WiMAX Using Signal Strength and Distance," 2011.

[60] O. Milet, "Technical overview of Single Frequency Network (SFN)," ENENSYS, Tech. Rep., 2005.

[61] H. Zhang, L. Venturino, N. Prasad, P. Li, S. Rangarajan, and X. Wang, "Weighted sum-rate maximization in multi-cell networks via coordinated scheduling and discrete power control," *Selected Areas in Communications, IEEE Journal on*, vol. 29, no. 6, pp. 1214–1224, 2011.

[62] S. A. Ramprashad and G. Caire, "Cellular vs. network MIMO: A comparison including the channel state information overhead," in *Personal, Indoor and Mobile Radio Communications, 2009 IEEE 20th International Symposium on*. IEEE, 2009, pp. 878–884.

[63] G. Caire, S. Ramprashad, and H. Papadopoulos, "Rethinking network MIMO: cost of CSIT, performance analysis, and architecture comparisons," in *Information Theory and Applications Workshop (ITA), 2010*. IEEE, 2010, pp. 1–10.

[64] F. Diehm and G. Fettweis, "On the impact of signaling delays on the performance of centralized scheduling for joint detection cooperative cellular systems," in *Wireless Communications and Networking Conference (WCNC), 2011 IEEE*. IEEE, 2011, pp. 1897–1902.

[65] D. Basnayaka, P. Smith, and P. Martin, "The effect of macrodiversity on the performance of Maximal Ratio Combining in Flat Rayleigh Fading," *Communications, IEEE Transactions on*, vol. 61, no. 4, pp. 1384–1392, April 2012.

[66] D. Basnayaka, P. Smith, and P. Martin, "Exact dual-user macrodiversity performance with linear receivers in flat Rayleigh fading," *IEEE ICC, Ottawa, Canada*, 2012.

[67] D. Basnayaka, P. Smith, and P. Martin, "Performance analysis of dual-user macrodiversity MIMO systems with linear receivers in Flat Rayleigh Fading," *Wireless Communications, IEEE Transactions on*, vol. 11, no. 12, pp. 4394–4404, December 2012.

[68] P. Smith and D. Basnayaka, "Scheduling metrics for Macrodiversity MIMO Systems with linear Receivers in Flat Rayleigh Fading," *WRC Report*, 2012.

[69] 3GPP, "TR 36-814 Further advancements for EUTRA physical layer aspects," ETSI, Tech. Rep. 36.814, 2010.

[70] 3GPP, "TS 36-213 EUTRA Physical layer propcedures," ETSI, Tech. Rep. 36.213, 2012.

[71] 3GPP, "Radio Resource Control (RRC) Protocol specification," ETSI, Tech. Rep. 25.331, 2012.

[72] A. Sanderovich, O. Somekh, H. Poor, and S. Shamai, "Uplink macro diversity of limited backhaul cellular network," *Information Theory, IEEE Transactions on*, vol. 55, no. 8, pp. 3457–3478, 2009.

[73] O. Simeone, O. Somekh, H. Poor, and S. Shamai, "Downlink macro-diversity with limited backhaul capacity," *EURASIP J Wirel Commun Netw*, 2009.

[74] Y. Okumura, E. Ohmori, T. Kawano, and K. Fukuda, "Field strength and its variability in VHF and UHF land-mobile radio service," *Rev. Elec. Commun. Lab*, vol. 16, no. 9, pp. 825–73, 1968.

[75] M. Hata, "Empirical formula for propagation loss in land mobile radio services," *Vehicular Technology, IEEE Transactions on*, vol. 29, no. 3, pp. 317–325, 1980.

[76] *Prediction methods for the terrestrial land mobile service in the VHF and UHF bands*, ITU ITU-R Recommendation P. 529-2, 1995, Okumura-Hata propagation prediction model for UHF range.

[77] B. Sklar, "Rayleigh fading channels in mobile digital communication systems. I. Characterization," *Communications Magazine, IEEE*, vol. 35, no. 7, pp. 90–100, 1997.

[78] H. Minc, *Permanents*. Cambridge University Press, 1984, vol. 6.

[79] I. Gradshteyn and I. Ryzhik, *Table of Integrals, Series, and Products*. Academic Press, 2007.

[80] L. G. Valiant, "The complexity of computing the permanent," *Theoretical computer science*, vol. 8, no. 2, pp. 189–201, 1979.

[81] R. A. Brualdi and H. J. Ryser, *Combinatorial matrix theory*. Cambridge University Press, 1991, vol. 39.

[82] N. Pau, *Macro-Diversity: Base Station Grouping Development Summary*. WRC, July 2013.

[83] H. L. Bertoni, *Radio Propagation for Modern Wireless Systems*. Pearson Education, 1999.

[84] N. L. Johnson, S. Kotz, and N. Balakrishnan, *Continuous univariate distributions, vol. 2*. John Wiley & Sons, 1994.